

# MIRIAM



## Comparison of Rolling Resistance Measuring Equipment - Pilot Study



Anneleen Bergiers, BRRRC  
Luc Goubert, BRRRC  
Fabienne Anfosso-Lédée, IFSTTAR  
Niels Dujardin, DRI  
Jerzy A. Ejsmont, TUG  
Ulf Sandberg, VTI  
Marek Zöller, BAST

MIRIAM, SP1 Deliverable No. 3  
Final version 2011-12-31

# Table of contents

Table of contents.....	1
Foreword .....	4
Acknowledgements .....	5
Abbreviations and acronyms .....	6
1. Introduction.....	8
2. Purpose of the study .....	9
3. Measurement devices .....	10
3.1 Trailers used in measurements on site .....	10
3.2 Drum measurements in laboratories .....	12
4 Test location and surfaces .....	15
4.1 Test track.....	15
4.2 Test track surfaces .....	15
4.3 Texture of the test sections .....	19
4.3.1 Texture spectra.....	19
4.3.2 Mean Profile Depth.....	21
4.3.3 Homogeneity .....	22
4.3.3.1 Transversal .....	22
4.3.3.2 Longitudinal .....	23
4.3.4 Intercorrelation of one-third-octave band texture levels .....	23
5 Tyres .....	25
5.1 Characteristics.....	25
5.2 Tyre pressure and load .....	26
5.3 Wheels .....	26
6 Measurement program .....	27
6.1 Comparison tests of the three measuring devices .....	27
6.1.1 BAST .....	27
6.1.2 BRRC .....	27
6.1.3 TUG .....	28
6.2 Additional tests to explore certain features.....	28
6.2.1 Tyres (TUG/ BAST) .....	28
6.2.2 Speed influence (TUG).....	28
6.2.3 Warm-up (BRRC) .....	28
6.2.4 Influence of wheel adjustment (BRRC) .....	29
6.2.5 Cement concrete (BRRC).....	29
7 Measurement procedure .....	30
8 Measurement results.....	31
8.1 Wind .....	31
8.2 Temperature correction .....	31
8.3 Repeatability of the RR devices .....	32
8.3.1 BAST .....	32
8.3.1.1 Short term repeatability .....	32
8.3.1.2 Day-to-day repeatability .....	33
8.3.2 BRRC .....	35
8.3.2.1 Short term repeatability .....	35
8.3.2.2 Day-to-day repeatability .....	36
8.3.3 TUG .....	36
8.3.3.1 Short term repeatability .....	36
8.3.3.2 Day-to-day repeatability .....	37
8.4 Reproducibility of the RR devices .....	37
8.4.1 BAST – TUG.....	38
8.4.1.1 All measurements.....	38
8.4.1.2 Relation between BAST and TUG ES16 tyre measurements.....	39

8.4.1.3	Relation between BAST and TUG SRTT tyre measurements .....	41
8.4.1.4	Relation between BAST and TUG AAV4 tyre measurements .....	42
8.4.2	BRRC – TUG .....	44
8.4.2.1	All measurements .....	44
8.4.2.2	Relation between BRRC and TUG ES14 tyre measurements .....	45
8.4.3	BAST - BRRC .....	47
8.4.3.1	All measurements .....	47
8.4.3.2	Relation between ES16/BAST and ES14/BRRC tyre measurements .....	48
9	Additional tests .....	50
9.1	Tyres .....	50
9.1.1	Measurements .....	50
9.1.2	Tyre related corrections .....	51
9.1.3	Trailer related differences .....	58
9.2	Speed influence .....	61
9.3	Warm-up .....	63
9.4	Influence of side forces .....	65
9.5	Cement concrete .....	67
10	Drum measurements .....	68
10.1	BAST .....	68
10.2	TUG .....	68
10.3	BAST – TUG .....	71
10.4	Data from Michelin .....	71
11	Texture influence on rolling resistance .....	72
11.1	Texture measurement devices .....	72
11.1.1	BRRC .....	72
11.1.2	IFSTTAR / CETE of Lyon .....	72
11.1.3	Comparison texture measurements performed by IFSTTAR and BRRC on test track .....	73
11.2	One-third-octave band texture levels .....	74
11.2.1	Without enveloping .....	74
11.2.2	With enveloping .....	75
11.3	MPD .....	76
11.3.1	Without enveloping .....	76
11.3.2	With enveloping .....	77
11.4	Band-limited macrotexture and megatexture levels .....	79
11.4.1	Macrotexture .....	79
11.4.1.1	Without enveloping .....	79
11.4.1.2	With enveloping .....	81
11.4.2	Megatexture .....	82
11.4.2.1	Without enveloping .....	82
11.4.2.2	With enveloping .....	84
11.5	MPD, macrotexture and megatexture .....	85
11.5.1	Correlations .....	85
11.5.1.1	Without enveloping .....	85
11.5.1.2	With enveloping .....	86
11.5.2	Slope coefficients .....	87
11.5.2.1	Without enveloping .....	87
11.5.2.2	With enveloping .....	90
11.6	IRI .....	92
12	Conclusions .....	95
13	References .....	97
	Annexes .....	98
A.	Texture spectra measured in middle, right and left wheel track direction east .....	98
B.	Correlation between MPD and $C_r$ for various tyres measured by different participants – without enveloping .....	102

C. Correlation between MPD and $C_r$ for various tyres measured by different participants – with enveloping .....	105
D. Correlation between macrotexture and $C_r$ for various tyres measured by different participants – without enveloping .....	108
E. Correlation between macrotexture and $C_r$ for various tyres measured by different participants – with enveloping .....	111
F. Correlation between megatexture and $C_r$ for various tyres measured by different participants – without enveloping .....	114
G. Correlation between megatexture and $C_r$ for various tyres measured by different participants – with enveloping .....	117
H. Correlation between IRI and $C_r$ for various tyres and different participants .....	120

## Foreword

The order of co-authors on the front page, following main author Bergiers and second author Goubert, is by alphabetical order and has nothing to do with the extent or importance of the contributions.

MIRIAM, an acronym for "Models for rolling resistance In Road Infrastructure Asset Management systems", is a project started and funded by twelve partners from Europe and USA. The managing partner is the Danish Road Institute.

The overall purpose of MIRIAM is to provide information useful for achieving a sustainable and environmentally friendly road infrastructure. In this project, the focus is on reducing the energy consumption due to the tyre/road interaction, by selection of pavements with lower rolling resistance – and hence lowering CO<sub>2</sub> emissions and increasing energy efficiency.

A first phase of the project will contribute with investigation of pavement characteristics, energy efficiency, modelling, and raising awareness of the project in order to secure economical and political support for a second phase. The second phase will focus on development and implementation of CO<sub>2</sub> controlling models into the road infrastructure asset management systems.

The website of MIRIAM is <http://www.miriam-co2.net/> where comprehensive project information can be found.

MIRIAM has been divided into five sub-projects (SP), of which SP 1 is "Measurement methods and surface properties model".

This report is part of task 15 within SP 1 and is the fourth Deliverable of SP 1. The Deliverables of Phase 1 are the following:

Deliverable 1:

"Rolling Resistance – Basic Information and State-of-the-Art on Measurement methods"

Deliverable 2:

"Rolling Resistance – Measurement Methods for Studies of Road Surface Effects"

Deliverable 3:

"Comparison of Rolling Resistance Measuring Equipment - Pilot Study"

Deliverable 4:

"Road surface influence on tyre/road rolling resistance"

These are all represented by written reports. See the MIRIAM website to download the reports, or to check where the reports may be downloaded.

## **Acknowledgements**

The authors would like to thank IFSTTAR for their hospitality and for opening up the test tracks in Nantes for the round robin test. Thanks are especially in order for Mrs. Fabienne Anfosso-Lédée and Mr. Patrice Bernier.

MIRIAM is funded by contributions by the participating organizations, mainly to cover their own work, as well as pooled funding for which contributions have been obtained collectively by some of the participating organizations and which may be used for special purposes. The work presented in this report has been funded both by the participating organizations themselves (see list of authors) and by the pooled funding.

## Abbreviations and acronyms

Abbreviation /acronym	Explanation	Comment
AAV4	Test tyre Avon AV4	Specified in section 5.1
BAST	Bundesanstalt für Straßenwesen	Federal Highway Research Institute, in English
BRRC	Belgian Road Research Centre	
$C_r$	Rolling Resistance Coefficient	Also abbreviated “RRC”
CT	Symbol indicating a tyre having a corrupted tread	
ES14	Michelin Energy Saver 14” tyre	Specified in section 5.1
ES16	Michelin Energy Saver 16” tyre	Specified in section 5.1
IFSTTAR	l’Institut Français des Sciences et Technologies des Transports, de l’Aménagement et des Réseaux	French institute of sciences and technology for transport, development and networks
IRI	International Roughness Index	Standardized in ASTM E1926 - 08
L <sub>Ma</sub>	Macrotexture level: special case of logarithmic texture profile level with the profile passing through a band-pass filter encompassing all one-third-octave bands within the macrotexture range (0.63 mm to 50 mm of centre wavelengths) [1]. Unit: dB vs 1 $\mu$ m rms.	
L <sub>Me</sub>	Megatexture level: special case of logarithmic texture profile level with the profile passing through a band-pass filter encompassing all one-third-octave bands within the megatexture range (63 mm to 500 mm of centre wavelengths) [1]. Unit: dB vs 1 $\mu$ m rms.	
MPD	Mean Profile Depth, a measure representing pavement texture depth	Standardized in ISO 13473-1
$R^2$	Correlation coefficient R squared	This is a measure of the variance explained by the tested regression
RR	Sometimes used as an abbreviation for Rolling Resistance	
RRC	In this report the symbol $C_r$ is used for the Rolling Resistance Coefficient	

RRT	Sometimes used as an abbreviation for Round Robin Test	Extensive test comparing a number of measuring devices or subjects; in this case rolling resistance trailers
SRTT	Standard Reference Test Tyre	Specified in section 5.1
TUG	Technical University of Gdansk, Poland	
VTI	Swedish National Road and Transport Research Institute	
XXXX/YYYY	Tyre type XXXX, owned by institute YYYY, measured by institute YYYY (unless specified otherwise)	
XXXX/YYYY_ZZZZ	Tyre type XXXX, owned by institute YYYY, measured by institute ZZZZ	
XXXX/YYYY_50	Tyre type XXXX, owned by institute YYYY, measured at 50 km/h	
XXXX/YYYY_80	Tyre type XXXX, owned by institute YYYY, measured at 80 km/h	



# 1. Introduction

This research is part of the MIRIAM project (Models for rolling resistance In Road Infrastructure Asset Management systems), which aims at developing methods for improved control of road transport carbon dioxide (CO<sub>2</sub>) emissions in order to obtain sustainable and environmental friendly road infrastructure.

As a first part of MIRIAM, a “Phase 1” was conducted in 2010-2011. It is planned to start a “Phase 2” in 2012.

MIRIAM is divided into five sub-projects. Sub-project number 1 (SP 1) is designated “Measurement methods and surface properties model”, and lead by Ulf Sandberg, VTI. Within SP 1, one of the major tasks is to study various measurement methods and the performance of available measurement equipment for rolling resistance, with a focus on measuring the pavement properties. As part of this task, in 2011 an international experiment was conducted to compare the measurement devices available within the MIRIAM project. This comparison experiment was popularly called “Round Robin Test” (RRT), which is the name used in this report.

The RRT was organized from 6 to 10 June 2011 on the test track owned by IFSTTAR in Nantes, France. Three institutes participated with their rolling resistance trailers: BAST, BRRC, and TUG. The practical organization was coordinated by IFSTTAR and the technical organization by BRRC. Texture measurements were performed by BRRC to verify the homogeneity of the test sections. Measurements on drums in laboratories were performed by BAST and TUG with the same tyres as used in the RRT.

At a later stage also truck rolling resistance measurements were carried out on a smaller selection of surfaces on the test track in Nantes. However, when this report was written these measurement results were not yet available<sup>1</sup>.

This experiment was, as far as the authors are aware, the first time when this type of devices was compared.

This report presents the RRT in terms of how it was carried out and the results obtained.

---

<sup>1</sup> The results of this test are planned to be presented in January 2012 at BAST.

## **2. Purpose of the study**

The main purposes of the study were:

- To assess the repeatability of the individual devices
- To evaluate how well the results of the trailers correlate with each other
- To assess the influence of the texture, expressed in terms of third of octave texture levels, broad band texture levels and the Mean Profile Depth, on the rolling resistance
- To measure the influence of the tyres on the rolling resistance and how they classify the pavements

### 3. Measurement devices

#### 3.1 Trailers used in measurements on site

The following organizations provided rolling resistance measuring devices in the form of towed trailers for comparison on the test track of IFSTTAR:

Belgian Road Research Centre (BRRC)

- Staff: Anneleen Bergiers and Philippe Debroux

Bundesanstalt für Straßenwesen (BASt)

- Staff: Marek Zöller and Jens Steinheuer

Technical University of Gdansk (TUG)

- Staff: Jerzy Ejsmont and Grzegorz Ronowski

The devices are described and compared in Table 3.1 below. The trailers are further described in [2]. Photos are shown in Figure 3.1 to Figure 3.4.

**Table 3.1: Essential features of trailers used during the round robin test in Nantes**

Owner organization	BASt	BRRC	TUG
Test tyre size	14"-16"	14"	14"-16"
Wind shield	yes	no	yes
Force/angle measurement	force	angle	angle
Number of supporting tyres	2	0 (test tyre is supporting tyre)	2
Number of test tyres	1	1	1
Self-supporting construction	no	no	yes
Tyre load	4000 N	2000 N	4000 N
Tyre pressure	200 kPa	200 kPa	210 kPa
Exterior/Interior tyre temperature measurement	exterior	exterior/interior	exterior
Corrections made during measurement or afterwards?	afterwards	afterwards	during measurement
Measurement in wheel track or middle track?	middle track	middle track	middle track



**Figure 3.1: Trailer BAST**



**Figure 3.2: Trailer BRRC**





**Figure 3.3: Trailer TUG**



**Figure 3.4: All participating trailers on test track**

### **3.2 Drum measurements in laboratories**

The following organizations provided rolling resistance measurements on laboratory drums, as a supplement to the field measurements by trailers:

Bundesanstalt für Straßenwesen (BAST)

- Staff: Marek Zöller and Jens Steinheuer

Technical University of Gdansk (TUG)

- Staff: Jerzy Ejsmont and Grzegorz Ronowski

The devices are described and compared in Table 3.2 below for the MIRIAM test conditions. The drum facilities are further described in [2]. Photos are shown in Figure 3.5 and Figure 3.6.

**Table 3.2: Essential features of drums used for this research**

Owner organization	BAST	TUG
Drum diameter	5.5 m inner diameter	1.7 m

Drum surface	Sandpaper "Safety Walk" and Steel drum	Sandpaper "Safety Walk" and APS
Tyre load	4000 N	4000 N
Tyre pressure	200 kPa	200 kPa
Measuring principle	direct force measurement (see [2] section 9.1.3)	TUG standard (see [2] section 9.3.2)
Correction for flat surface	no	yes



**Figure 3.5: Drum BASt**

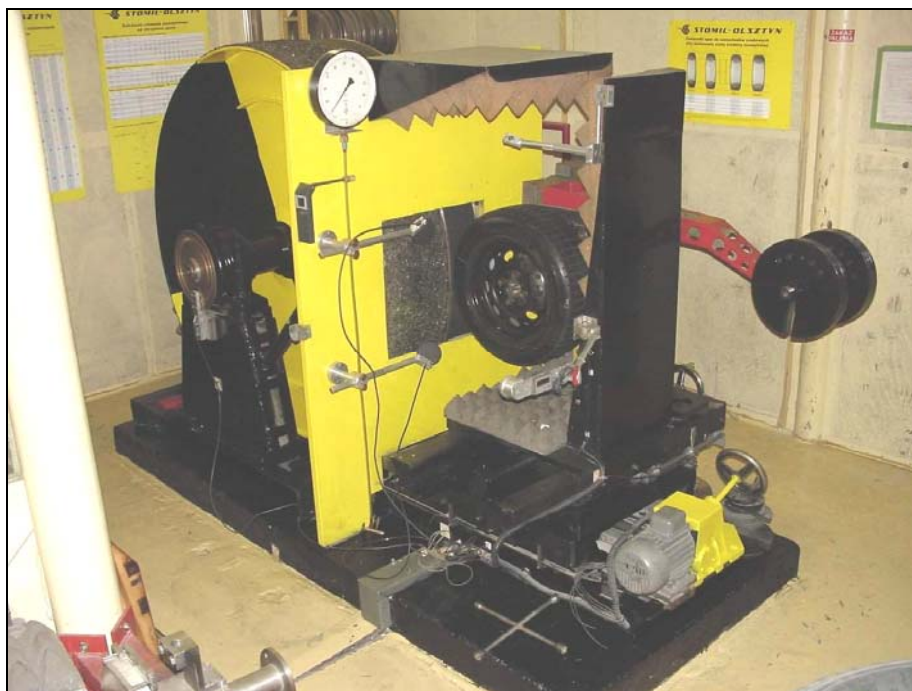


**Figure 3.6: Drum TUG**

Photos of drum surfaces that were used for MIRIAM, are shown in Figure 3.7 - Figure 3.9.

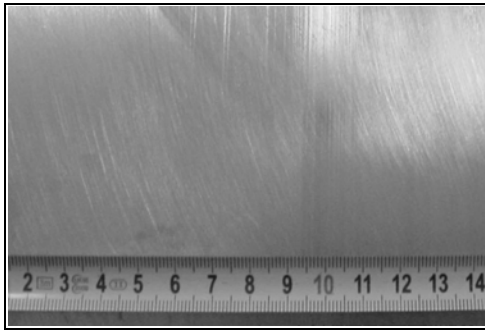


**Figure 3.7: Steel surface used on TUG drum**

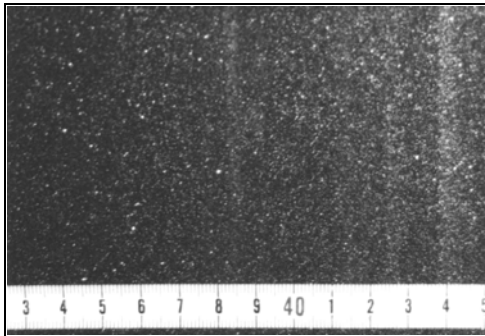


**Figure 3.8: Safety Walk surface used on TUG drum**



**Figure 3.9: APS 4 surface used on TUG drum**

## 4 Test location and surfaces

### 4.1 Test track

The test track is situated adjacent to the IFSTTAR offices in Nantes, France. It consists of a large half circle followed by test sections with different road surfaces.

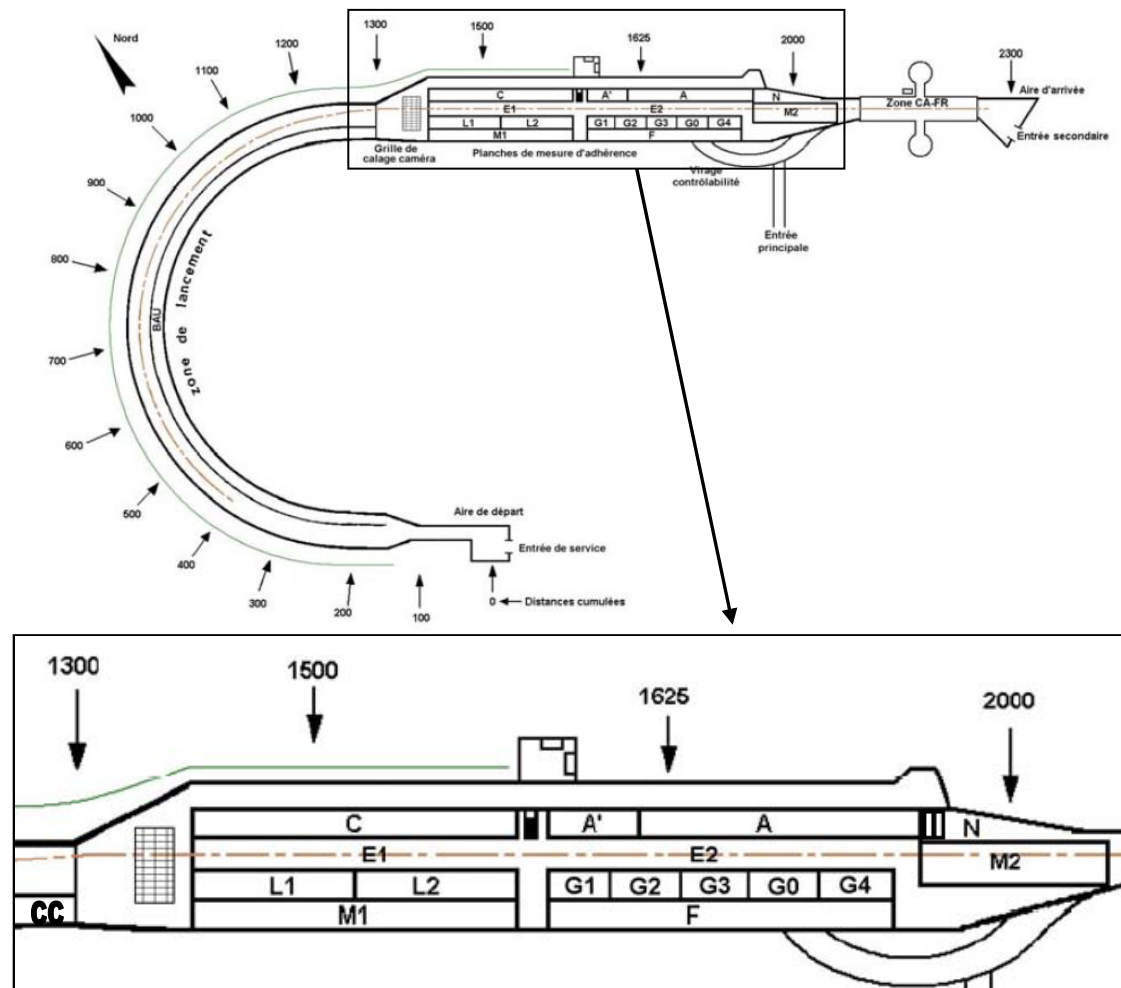


Figure 4.1: The IFSTTAR test track, with the test sections expanded below

### 4.2 Test track surfaces

An overview of all test sections is shown in Table 4.1 and a more detailed description with pictures may be found in Table 4.2.




Table 4.1: Summary of test sections





Pavement designation	Description
M1	Very Thin Asphalt Concrete 0/10, class 1
F	Colgrip: Surface Dressing 1/3 bauxite (high skid resistance)
L1	Epoxy Resin (smooth section)








L2	Sand Asphalt 0/4
E1	Dense Asphalt Concrete 0/10 (new)
E2	Dense Asphalt Concrete (old)
M2	Very Thin Asphalt Concrete 0/6, class 2
C	Surface Dressing 0.8/1.5
A'	Surface Dressing 8/10
A	Porous Asphalt Concrete 0/6
N	Porous Cement Concrete
CC	(Dense) Cement Concrete

**Table 4.2: Description of test sections (the coin in the pictures has a diameter of 23 mm)**

Section	Pavement	Photo	Length	Remarks
M1	Very Thin Asphalt Concrete 0/10, class 1		244 m	Grinded in middle, steel plate at km point 1550
F	Colgrip: Surface Dressing 1/3 bauxite (high skid resistance)		250 m	
L1	Epoxy Resin (smooth section)		128 m	Peeling

L2	Sand Asphalt 0/4		116 m	
E1	Dense Asphalt Concrete 0/10 (new)		252 m	Road markings in middle, crack
E2	Dense Asphalt Concrete (old)		250 m	Disposed and existing road markings in middle, disposed road markings at east end
M2	Very Thin Asphalt Concrete 0/6, class 2		150 m	

C	Surface Dressing 0.8/1.5		244 m	Transversal uneven, disposed zebra crossing at west end, cracks, repaired cracks, surface shortly interrupted at east end
A'	Surface Dressing 8/10		50 m	
A	Porous Asphalt Concrete 0/6		220 m	
N	Porous Cement Concrete		185 m	Interrupted at west end by concrete plates
CC	(Dense) Cement Concrete		90 m	Plates



## 4.3 Texture of the test sections

### 4.3.1 Texture spectra

The texture of the test tracks was measured with the BRRC dynamic laser profilometer (for a description of this device see section 11.1.1). Several runs were carried out with a step size of 0.2 mm at a speed of 30 km/h and over the full length of the test track. The texture profile was measured between the wheel tracks of the vehicle, more or less at the axle of the test track. For each profile the one-third-octave band texture spectrum was calculated. Texture spectra corresponding to six runs on track L2 are shown in Figure 4.2. The repeatability appears to be fair with a standard deviation which is the largest in the megatexture area, but even there it is not higher than 0.5 dB(A).

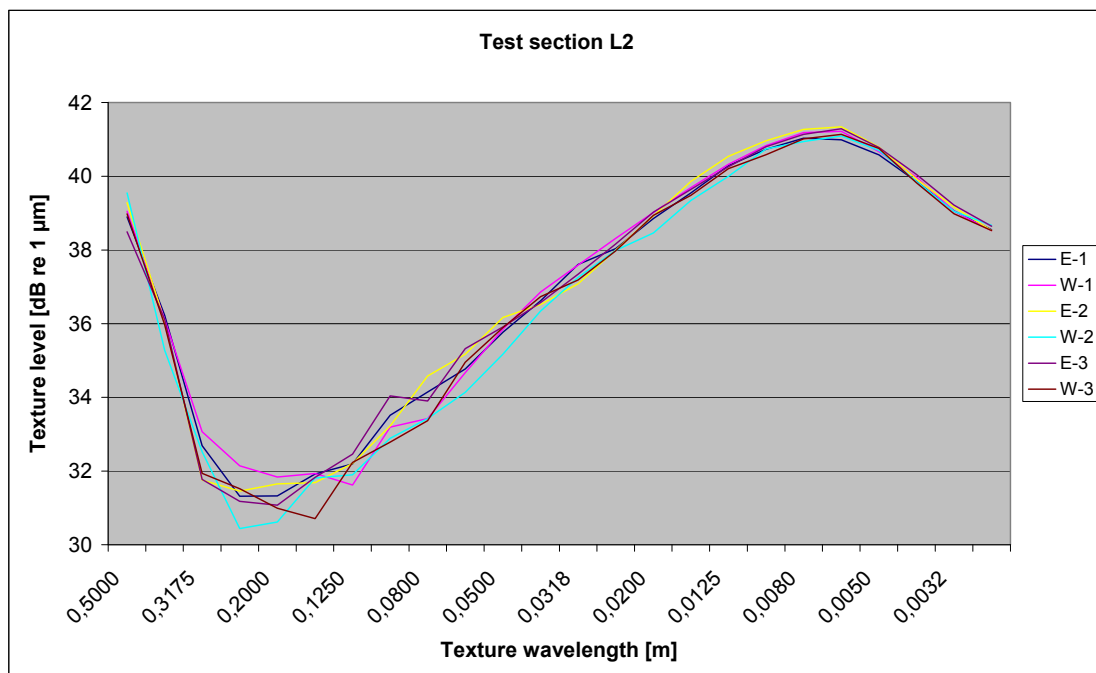


**Figure 4.2: Texture spectra corresponding to several runs (three in eastern and three in western direction) on test track L2**

Figure 4.3 shows the average texture spectra of the twelve IFSTTAR test tracks. Note the special shape of the spectrum of test track L1, the extremely smooth epoxy surface. On this surface, the part of the spectrum with texture wavelength below 3 cm is determined by the internal noise of the laser profilometer, rather than that it reflects a real texture.

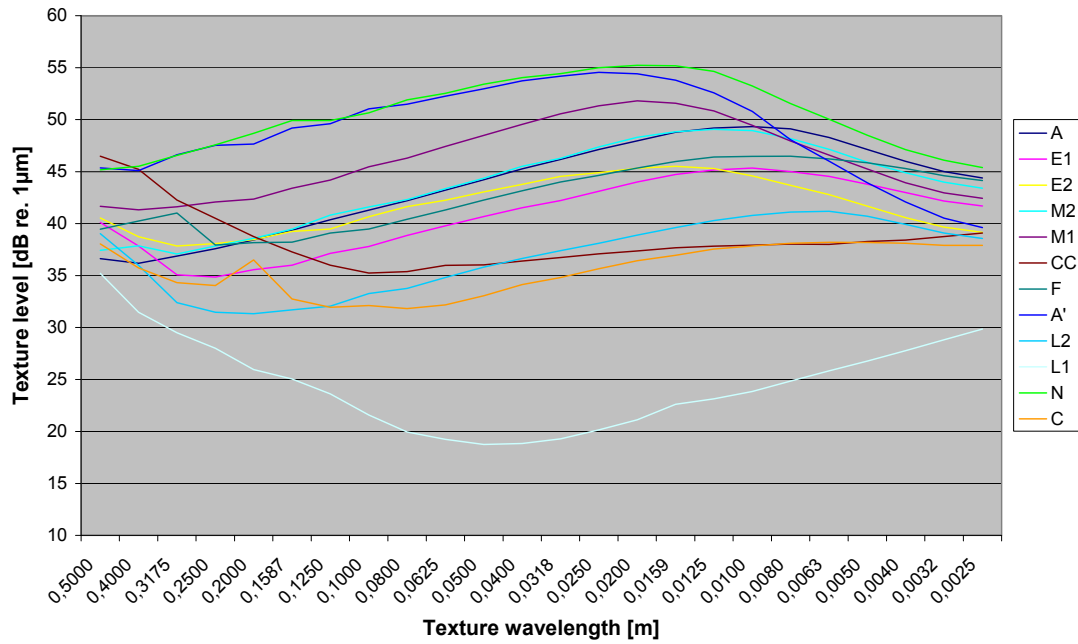


**Figure 4.3: Average texture spectra of the IFSTTAR test tracks**

Due to the stiffness of the rubber, a tyre tread can not protrude very deep in the texture profile. The rubber envelopes only a part of the texture. This is called enveloping. To reach a more realistic result all data were additionally analyzed with enveloping following a method described by [3] with value  $d^* = 0.0025 \text{ mm}^{-1}$ . This value was chosen quite arbitrarily, believing that it will be reasonably representative of passenger tyres, but this has not been studied closely. More information about the enveloping procedure can be found in [4].

The average texture spectra analysed after first applying the enveloping function on the profiles are shown in Figure 4.4.

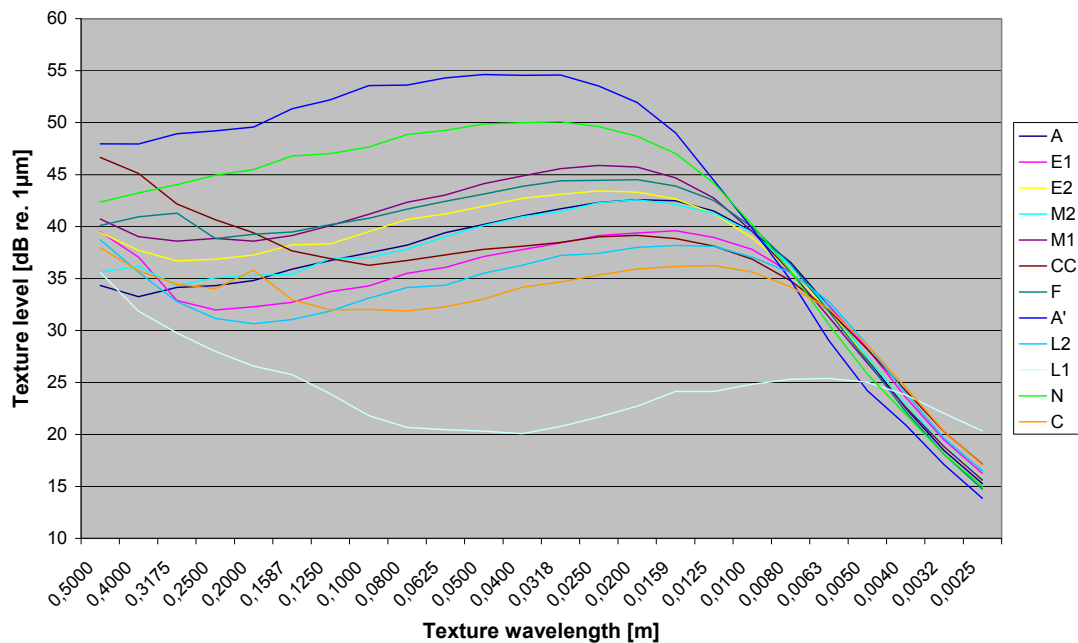


**Figure 4.4: Average texture spectra of the IFSTTAR test tracks – with enveloping applied on the profiles before spectrum analysis**

The impact of applying enveloping on the texture spectra can be seen in Figure 4.5 for test sections L2 (which is rather smooth) and A' (which is rough).

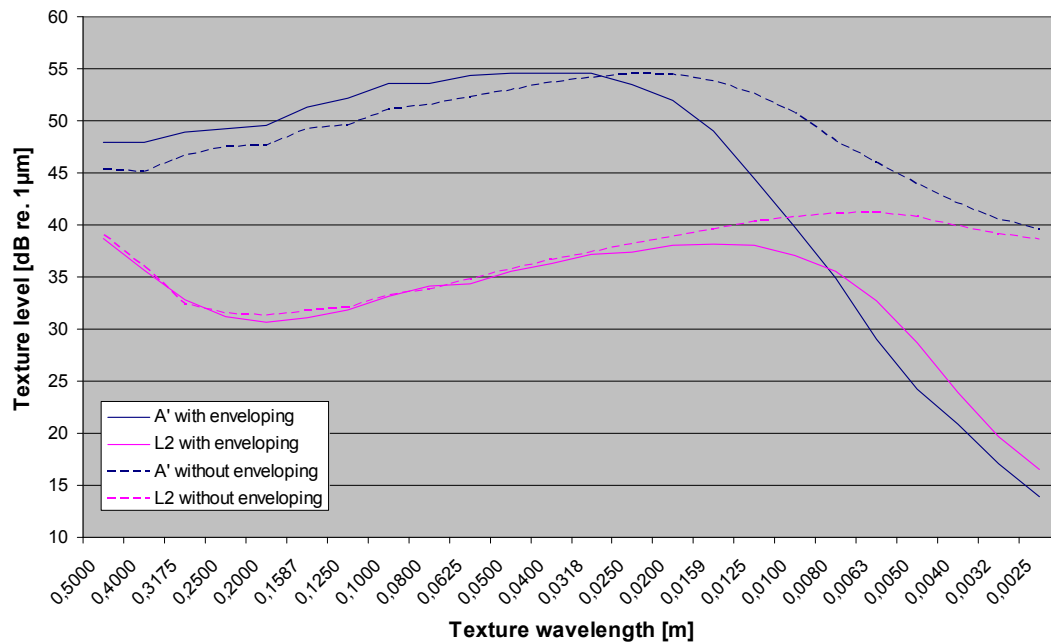


**Figure 4.5: Average texture spectra of test section A' and L2 with and without enveloping**

### 4.3.2 Mean Profile Depth

Test section C has been excluded out of the analyses of the correlation between  $C_r$  and texture because of too many irregularities of the surface (see Table 4.2).

The values of the Mean Profile Depth without and with enveloping applied on the profile before calculating the MPD (averages over the whole test track lengths) are shown in Table 4.3.

**Table 4.3: MPD values of the IFSTTAR test sections used in this experiment**

Test section	MPD [mm] without enveloping	MPD [mm] with enveloping
M1	1.14	0.63
F	1.00	0.82
L1	0.08	0.09
L2	0.42	0.36
E1	0.59	0.38
E2	0.82	0.64
M2	0.86	0.48
A	0.93	0.50
CC	0.44	0.50
A'	2.77	2.24
N	1.92	1.02
C	0.35	0.34

### 4.3.3 Homogeneity

#### 4.3.3.1 Transversal

The width of the test sections ranged between 2.5 and 3.9 m, meaning that trailers might not measure in the same wheel track (see Table 4.4). All trailers measure the rolling resistance in the middle track of the vehicle. However, a slight difference in positioning of the measuring vehicle may cause different results. For example: N is ground in the middle and not in the right and left wheel tracks, E1 and E2 have road markings in the middle track. M2 is a wider test section, meaning that probably not all teams measured in exactly the same track. Therefore, transversal homogeneity was checked. Texture measurements were performed in the middle, left and right wheel track of the test sections with step size 0.2 mm. Due to spatial limitations on-site, in some cases only the left or right wheel tracks could be measured.

**Table 4.4: Width of the test sections**

Test section	Width [m]
M1	3.00
F	3.00
L1	3.00
L2	2.50
E1	3.45
E2	3.45
M2	3.90
A	3.00
CC	-
A'	3.00
N	2.60
C	3.00

The results of test section C are shown in Figure 4.6:. The graphs of all other test sections can be found in Annex A. The graph of test section N shows a slight difference between middle and right wheel track (see Figure A.3). Also the graph of test section L1 reveals some difference between middle and right wheel track, which is unexpected (see Figure A.6). No significant influence of road markings can be seen on the graphs of test sections E1 and E2 (see Figure A.4 and Figure A.5).

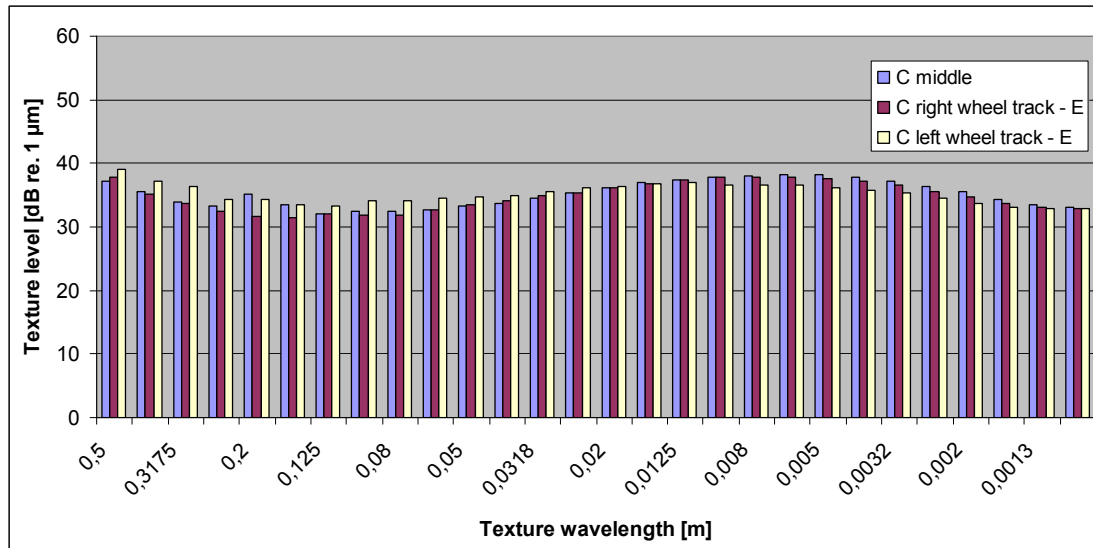


**Figure 4.6: Texture spectra of test section C measured in middle, right and left wheel track direction east (E)**

### 4.3.3.2 Longitudinal

Texture has been analyzed per 20 m. The standard deviation of the 20 m sections in percentage (standard deviation in dB divided by the average level in dB) has been calculated for the various wavelengths. The results are shown in Figure 4.7.

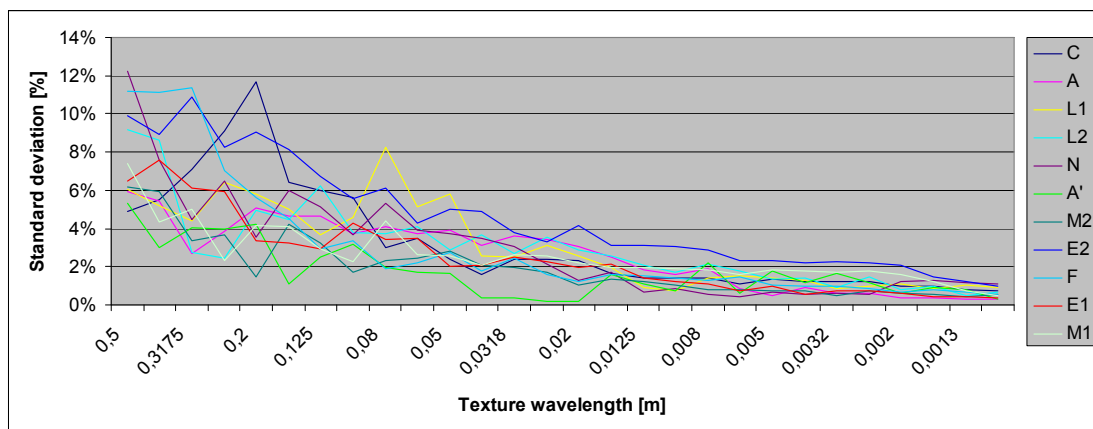


**Figure 4.7: Standard deviation (in percentage) of the 20 m sections for various wavelengths and test tracks**

The calculated standard deviation may be used to give an idea about the longitudinal homogeneity of the test tracks. E2 can be considered as the least homogeneous test track for most wavelengths, which may be due to the road markings. F is the least homogeneous test track for the largest wavelengths. L1, N and C are less homogeneous in the megatexture area.

### 4.3.4 Intercorrelation of one-third-octave band texture levels

In order to study the influence of the texture on the rolling resistance, it is ideal to use a set of test tracks for which the texture levels in any of the one-third-octave bands



are not correlated with the levels in any other band. Suppose e.g. that the rolling resistance is strongly correlated with the texture levels belonging to texture wavelengths 0.5 m and 0.01 m. If the texture levels of these two bands are strongly correlated with each other, then it is unclear to which texture wavelength band the rolling resistance is correlated to.

Therefore it was checked how well the texture levels of the different one-third-octave bands of the sample of test tracks correlate with each other. Table 4.5 shows the correlations for the relevant one-third-octave bands.

**Table 4.5: Correlations ( $R^2$ ) among the texture levels measured in the various one-third-octave bands; where **high correlation  $> 0.7$**  is indicated in red, **medium correlation  $> 0.4$  but  $\leq 0.7$**  is indicated in yellow and **low correlation  $\leq 0.4$**  is indicated in green.**

	0.5	0.4	0.3175	0.25	0.2	0.1587	0.125	0.1	0.08	0.0625	0.05	0.04	0.0318	0.025	0.02	0.0159	0.0125	0.01	0.008	0.0063	0.005	0.004	0.0032	0.0025
0.5	1.0	0.9	0.7	0.6	0.5	0.5	0.4	0.4	0.4	0.3	0.3	0.3	0.3	0.3	0.3	0.2	0.2	0.2	0.1	0.1	0.1	0.1	0.1	0.1
0.4	0.9	1.0	0.9	0.8	0.7	0.7	0.6	0.6	0.6	0.6	0.5	0.5	0.5	0.5	0.5	0.4	0.4	0.4	0.3	0.3	0.3	0.3	0.3	0.3
0.3175	0.7	0.9	1.0	1.0	0.9	0.9	0.8	0.7	0.7	0.7	0.7	0.7	0.6	0.6	0.6	0.6	0.6	0.5	0.5	0.4	0.4	0.4	0.4	0.4
0.25	0.7	0.8	1.0	1.0	1.0	0.9	0.9	0.9	0.8	0.8	0.8	0.8	0.7	0.7	0.7	0.7	0.7	0.6	0.5	0.5	0.4	0.4	0.4	0.4
0.2	0.6	0.7	0.9	1.0	1.0	1.0	0.9	0.9	0.9	0.9	0.8	0.8	0.8	0.8	0.8	0.8	0.7	0.7	0.6	0.6	0.6	0.5	0.5	0.5
0.1587	0.5	0.7	0.9	0.9	1.0	1.0	1.0	1.0	1.0	0.9	0.9	0.9	0.9	0.9	0.9	0.9	0.8	0.8	0.7	0.7	0.6	0.6	0.5	0.5
0.125	0.4	0.6	0.8	0.9	0.9	1.0	1.0	1.0	1.0	1.0	1.0	1.0	0.9	0.9	0.9	0.9	0.9	0.9	0.8	0.7	0.7	0.7	0.6	0.6
0.1	0.4	0.6	0.7	0.9	0.9	1.0	1.0	1.0	1.0	1.0	1.0	1.0	1.0	1.0	1.0	1.0	0.9	0.9	0.8	0.8	0.7	0.7	0.6	0.6
0.08	0.4	0.6	0.7	0.8	0.9	1.0	1.0	1.0	1.0	1.0	1.0	1.0	1.0	1.0	1.0	1.0	0.9	0.9	0.9	0.8	0.8	0.7	0.7	0.6
0.0625	0.3	0.6	0.7	0.8	0.9	0.9	1.0	1.0	1.0	1.0	1.0	1.0	1.0	1.0	1.0	1.0	1.0	0.9	0.9	0.8	0.8	0.8	0.7	0.7
0.05	0.3	0.5	0.7	0.8	0.8	0.9	1.0	1.0	1.0	1.0	1.0	1.0	1.0	1.0	1.0	1.0	1.0	0.9	0.9	0.9	0.8	0.8	0.7	0.7
0.04	0.3	0.5	0.7	0.8	0.8	0.9	1.0	1.0	1.0	1.0	1.0	1.0	1.0	1.0	1.0	1.0	1.0	1.0	0.9	0.9	0.8	0.8	0.7	0.7
0.0318	0.3	0.5	0.6	0.7	0.8	0.9	0.9	1.0	1.0	1.0	1.0	1.0	1.0	1.0	1.0	1.0	1.0	1.0	0.9	0.9	0.8	0.8	0.7	0.7
0.025	0.3	0.5	0.6	0.7	0.8	0.9	0.9	1.0	1.0	1.0	1.0	1.0	1.0	1.0	1.0	1.0	1.0	1.0	0.9	0.9	0.9	0.8	0.8	0.7
0.02	0.3	0.5	0.6	0.7	0.8	0.9	0.9	1.0	1.0	1.0	1.0	1.0	1.0	1.0	1.0	1.0	1.0	1.0	0.9	0.9	0.9	0.8	0.8	0.7
0.0159	0.2	0.4	0.6	0.7	0.8	0.9	0.9	1.0	1.0	1.0	1.0	1.0	1.0	1.0	1.0	1.0	1.0	1.0	1.0	0.9	0.9	0.8	0.8	0.8
0.0125	0.2	0.4	0.6	0.7	0.8	0.9	0.9	0.9	0.9	1.0	1.0	1.0	1.0	1.0	1.0	1.0	1.0	1.0	1.0	0.9	0.9	0.8	0.8	0.8
0.01	0.2	0.4	0.5	0.6	0.7	0.8	0.9	0.9	0.9	0.9	0.9	1.0	1.0	1.0	1.0	1.0	1.0	1.0	1.0	1.0	0.9	0.9	0.8	0.8
0.008	0.1	0.3	0.5	0.5	0.6	0.7	0.8	0.8	0.9	0.9	0.9	0.9	0.9	0.9	0.9	1.0	1.0	1.0	1.0	1.0	1.0	0.9	0.9	0.9
0.0063	0.1	0.3	0.4	0.5	0.6	0.7	0.7	0.8	0.8	0.8	0.9	0.9	0.9	0.9	0.9	0.9	1.0	1.0	1.0	1.0	1.0	1.0	0.9	0.9
0.005	0.1	0.3	0.4	0.4	0.6	0.6	0.7	0.7	0.8	0.8	0.8	0.8	0.8	0.9	0.9	0.9	0.9	1.0	1.0	1.0	1.0	1.0	1.0	0.9
0.004	0.1	0.3	0.4	0.4	0.5	0.6	0.7	0.7	0.8	0.8	0.8	0.8	0.8	0.8	0.8	0.8	0.9	0.9	1.0	1.0	1.0	1.0	1.0	1.0
0.0032	0.1	0.3	0.4	0.4	0.5	0.5	0.6	0.6	0.7	0.7	0.7	0.7	0.7	0.8	0.8	0.8	0.8	0.9	0.9	0.9	1.0	1.0	1.0	1.0
0.0025	0.1	0.3	0.4	0.4	0.5	0.5	0.6	0.6	0.6	0.7	0.7	0.7	0.7	0.7	0.7	0.8	0.8	0.8	0.9	0.9	0.9	1.0	1.0	1.0

It is clear from Table 4.5 that the texture levels of the different one-third-octave bands are strongly correlated over rather wide texture wavelength ranges, making it impossible to identify a narrow area of the texture wavelength range as responsible for the rolling resistance, if that would be the case. In section 12, therefore, also the correlation of the rolling resistance with wide band descriptors, as MPD (Mean Profile Depth), LMe (global texture level of the megatexture range) and LMa (global texture level over the macrotexture range) are calculated.

## 5 Tyres

### 5.1 Characteristics

An attempt was made to find tyres from the same batch (as identified by the DOT marking on the tyre) for all teams in order to minimize differences that are due to a variation in tyre properties. Only the SRTT tyres came from different batches. Each team used his own set of tyres. Moreover TUG performed measurements with all sets of tyres to detect possible variations per tyre type.

In Table 5.1 more details may be found about the tyres that were used on the test track. Shore hardness of all tyres was measured in the TUG laboratory.

**Table 5.1: Overview of tyres used during RRT**

Symbol	Producent	Tyre tread	Tyre size	Index	DOT	Hard-ness
AAV4/BASt	Avon	Supervan AV4	195 R14 C	106/104N	ATJ8 PC2810	64 Sh
AAV4/TUG	Avon	Supervan AV4	195 R14 C	106/104N	ATJ8 PC2810	62 Sh
AAV4_CT/TUG	Avon	Supervan AV4	195 R14 C	106/104N	-	64 Sh
ES16/BASt	Michelin	Energy Saver	225/60 R16	98V	HC 3V 00KX1511	66 Sh
ES16/TUG	Michelin	Energy Saver	225/60 R16	98V	HC 3V 00KX1511	63 Sh
ES14/BRR C	Michelin	Energy Saver	195/70 R14	91T	F1 J9 681X3010	66 Sh
ES14/TUG	Michelin	Energy Saver	195/70 R14	91T	F1 J9 681X3010	63 Sh
SRTT/BASt	Uniroyal	Tiger paw M+S	P225/60 R16	97S	ANX0 EVUU4608	68 Sh
SRTT/TUG	Uniroyal	Tiger paw M+S	P225/60 R16	97S	...0404	65 Sh

All tyre types used for the RRT are shown in Figure 5.1 and Figure 5.2.

For use as a reference tyre in the RRT, three samples of an Avon AV4 tyre were purchased by VTI. These were sent to IFSTTAR, BASt and TUG. It appeared that one of them had a tread pattern which was different from the "normal" one. This tyre type is chosen as a second reference tyre for CPX measurements of noise and the experience of this is that the tread pattern normally has a rather poor alignment between the left and right halves of the tread; implying that the tread blocks and grooves in the middle have a slightly distorted shape. This seems to be "normal" for this tyre so it has been accepted. However, the deviating tyre AAV4/TUG\_CT purchased for this project had the two halves of the tread pattern substantially more displaced and misaligned, making the appearance of the tread weird (see Figure 5.1 middle and right picture). In this project, this tyre has been described as having a "corrupted tread".

Strange enough, it appeared in the tests that the  $C_r$  of this tyre sample did not differ significantly from the samples having a "normal" tread. This is shown later in this report.



**Figure 5.1:** SRTT (left), AAV4 (middle) and AAV4\_CT (right)



**Figure 5.2:** ES14 (left) and ES16 (right)

## **5.2 Tyre pressure and load**

Tyre inflation pressure was 2.0 bar (200 kPa) for BAST and BRRC and 2.1 bar (210 kPa) for TUG. The tyres were filled up with nitrogen. The process to fill the tyre was repeated 3 times in order to make sure that all air was gone.

Before the experiments it had been decided to use 200 kPa as the standard in all measurements. However, this was violated by one of the institutions (TUG) which bias the comparisons.

Later, attempts will be made to determine what effect the differences in inflation might have had. In the Artesis project the influence of tire inflation was looked into [5]. In the Artesis project a difference of 0.1 bar (10 kPa) was found to correspond with a  $C_r$  difference of 1.6 %.

The loads were 4000 N in all cases except for the BRRC trailer where the load was 2000 N because of a limitation of the trailer suspension.

## **5.3 Wheels**

The wheels that were used for SRTT and ES16 have a wheel width of 6.5". The wheels that were used for ES14 and for AAV4 have a wheel width of 6 and 5.5" respectively. Wheel width may influence rolling resistance.

## 6 Measurement program

The number of runs that were performed in east (E) and west (W) direction per team is specified in the tables hereunder.

### 6.1 Comparison tests of the three measuring devices

The number of test runs performed per speed and direction by all institutes can be found in Table 6.1 to Table 6.3.

#### 6.1.1 BAST

**Table 6.1: Number of runs performed by BAST in east (E) and west (W) direction**

Pavement	AAV4		SRTT		ES16		ES14	
	50 km/h E-W	80 km/h E-W	50 km/h E-W	80 km/h E-W	50 km/h E-W	80 km/h E-W	50 km/h E-W	80 km/h E-W
M1	4 - 4	4 - 4	4 - 4	6 - 6	4 - 4	4 - 4	-	-
F	1 - 1	1 - 1	2 - 2	2 - 2	1 - 1	1 - 2	-	-
L1	1 - 1	1 - 2	2 - 2	3 - 3	1 - 1	1 - 1	-	-
L2	4 - 4	4 - 4	6 - 5	6 - 6	2 - 3	4 - 4	-	-
E1	1 - 1	1 - 1	2 - 3	2 - 2	1 - 1	0 - 2	-	-
E2	-	-	-	-	-	-	-	-
M2	1 - 1	1 - 0	1 - 1	2 - 0	1 - 1	1 - 0	-	-
C	1 - 2	1 - 2	2 - 2	2 - 2	1 - 1	1 - 1	-	-
A'	1 - 1	-	2 - 2	3 - 2	1 - 1	-	-	-
A	2 - 1	1 - 1	3 - 2	2 - 2	1 - 2	0 - 1	-	-
N	2 - 2	4 - 0	5 - 5	4 - 0	1 - 1	1 - 0	-	-
CC	-	-	-	-	-	-	-	-

#### 6.1.2 BRRC

**Table 6.2: Number of runs performed by BRRC in east (E) and west (W) direction**

Pavement	AAV4		SRTT		ES16		ES14	
	50 km/h E-W	80 km/h E-W	50 km/h E-W	80 km/h E-W	50 km/h E-W	80 km/h E-W	50 km/h E-W	80 km/h E-W
M1	-	-	-	-	-	-	10 - 10	10 - 11
F	-	-	-	-	-	-	10 - 10	10 - 11
L1	-	-	-	-	-	-	10 - 11	10 - 10
L2	-	-	-	-	-	-	10 - 11	10 - 10
E1	-	-	-	-	-	-	4 - 4	4 - 4
E2	-	-	-	-	-	-	4 - 4	4 - 4
M2	-	-	-	-	-	-	4 - 4	4 - 4
C	-	-	-	-	-	-	11 - 11	11 - 9
A'	-	-	-	-	-	-	16 - 16	15 - 14

A	-	-	-	-	-	-	11 - 11	10 - 9
N	-	-	-	-	-	-	10 - 11	12 - 10
CC	-	-	-	-	-	-	4 - 4	4 - 5

### 6.1.3 TUG

**Table 6.3: Number of runs performed by TUG in east (E) and west (W) direction**

Pavement	AAV4		SRTT		ES16		ES14	
	50 km/h E-W	80 km/h E-W	50 km/h E-W	80 km/h E-W	50 km/h E-W	80 km/h E-W	50 km/h E-W	80 km/h E-W
M1	2 - 2	2 - 2	8 - 2	6 - 1	2 - 2	2 - 2	2 - 2	2 - 2
F	2 - 2	2 - 2	8 - 2	6 - 1	2 - 2	2 - 2	2 - 2	2 - 2
L1	2 - 4	2 - 2	9 - 3	2 - 2	2 - 2	2 - 2	2 - 2	4 - 3
L2	2 - 4	2 - 2	9 - 3	2 - 2	2 - 2	2 - 2	2 - 2	4 - 3
E1	2 - 2	2 - 2	2 - 7	2 - 2	2 - 2	2 - 2	2 - 2	2 - 2
E2	2 - 2	2 - 2	2 - 7	2 - 2	2 - 2	2 - 2	2 - 2	2 - 2
M2	4 - 6	2 - 2	17 - 5	2 - 2	4 - 4	2 - 6	4 - 6	6 - 4
C	2 - 2	2 - 2	2 - 8	2 - 2	2 - 2	2 - 2	2 - 2	2 - 2
A'	2 - 2	2 - 2	2 - 8	2 - 2	2 - 2	2 - 2	2 - 2	2 - 2
A	2 - 2	2 - 2	2 - 8	2 - 2	2 - 2	2 - 2	2 - 2	2 - 2
N	0	0	0	0	0	0	0	0
CC	0	0	0	0	0	0	0	0

## 6.2 Additional tests to explore certain features

### 6.2.1 Tyres (TUG/ BAST)

All tyres were tested on the test track to have an idea of differences between tyres of the same type. Also measurements with various trailers (BAST and TUG) with exactly the same tyre can be compared to show trailer related differences. Additionally afterwards all tyres were tested on the TUG drum and three tyres on the BAST drum in laboratory conditions.

### 6.2.2 Speed influence (TUG)

Test sections L1 and L2 were measured at high speed in order to determine the influence of speed.

### 6.2.3 Warm-up (BRRC)

To determine the influence of warm-up, measurements have been performed on the highway. The exterior temperature at the tyre shoulder and the interior temperature inside the tyre were registered continuously while driving 45 minutes at 80 km/h. Tyre pressure was measured each 15 minutes during a short standstill. This test was done with air and with nitrogen in the tyre. The process to fill the tyre with air and nitrogen respectively was repeated 3 times.

#### **6.2.4 Influence of wheel adjustment (BRRC)**

To simulate the effect of wheel adjustment, measurements have been performed in a shallow curb on dense asphalt 0/10 at various speeds: 30, 50 and 70 km/h. However there was some doubt whether this really would give a similar result.

#### **6.2.5 Cement concrete (BRRC)**

Some measurements have been performed on cement concrete on the test track. However there is some uncertainty about the results.

## **7 Measurement procedure**

The warm-up procedure consisted of driving at approximately 80 km/h during 15 minutes.

As every team had a different measurement method, everyone performed his test program individually while communicating by walkie-talkie with the other teams.

Weather conditions (temperature, wind, ...) were registered continuously by a weather station and could thereby be linked to the measurement results afterwards.

## 8 Measurement results

### 8.1 Wind

Wind direction and speed were studied, using data registered by the weather station of IFSTTAR. Maximum wind speed registered during BRRC measurements was for example 5,4 m/s. The direction of the wind ranged between 216° (southwest) and 354° (northwest); 180°, 270° and 360° being the south, west and north respectively. It was not considered further as a disturbing factor because wind speeds were low and only a wind direction west was registered.

### 8.2 Temperature correction

It was verified if temperature correction would have a large influence on measurement results.

BRRC and BAsT linked all measurement runs to the ambient air temperature registered by the weather station of IFSTTAR.

TUG measured ambient air temperature and reported an average value per tyre-speed combination (for example one average temperature for all measurements performed with SRTT at 50 km/h).

Temperature correction is applied following ISO 28580 [6]:

$$C_{r,25} = C_{r,T} \{1 + k(T - T_{ref})\}$$

$$C_r = (R/F)$$

With

R = rolling resistance, expressed in Newtons

F = tyre load, expressed in Newtons

k = constant = 0.008

T = temperature during measurement, expressed in °C

T<sub>ref</sub> = reference temperature = 25 °C

Table 8.1 demonstrates the linked temperatures and their influence on C<sub>r</sub>. The influence on C<sub>r</sub> was calculated using following formula:

$$(C_{r,T} - C_{r,25})/C_{r,T}$$

**Table 8.1: Temperatures linked to various institutes with influence on C<sub>r</sub>**

	BAsT	BRRC	TUG
<b>Minimum temperature [°C]</b>	14.2	15.2	16.5
<b>Maximum temperature [°C]</b>	18.0	17.8	21.0
<b>Temperature interval minimum – maximum [°C]</b>	3.8	2.6	4.5



<b>Influence in relation to <math>T_{ref}</math> [%]</b>	Approx. -6.9	Approx. -6.6	Approx. -5.2
<b>Influence of the variation in temperature [%]</b>	3.0	2.1	3.6

A higher temperature effect was reported by Descornet in 1990 [7]. Additionally the influence of the variation in temperature has been calculated using the formula from that research:

$$C_{r,T_0} = C_{r,T} \exp\left\{\frac{(T_0 - T)}{T_1}\right\}$$

$$T_1 = 50^\circ C$$

for BAsT, BRRC and TUG resulting in 7.9 %, 5.3 % and 9.4 % influence of variation in temperature respectively.

Ambient air temperature seems to differ between TUG and IFSTTAR weather station data (for example maximum temperature 17.8 °C versus 21.0 °C) even though all measurements took place on the same days. Moreover the influence on  $C_r$  is so small, that it would not affect the results and comparison much.

Therefore it is decided not to apply any temperature correction in this report.

### **8.3 Repeatability of the RR devices**

Results are considered over the whole length of the test section. A distinction is made between short term and day-to-day repeatability. Short term repeatability investigates measurement runs performed the one after the other on the same test section. Day-to-day repeatability looks into the measurements that were performed on different days on the same test section.

#### **8.3.1 BAsT**

##### **8.3.1.1 Short term repeatability**

BAsT repeated measurements on test tracks M1 and L2 for the SRTT, AAV4, ES14 and ES16 tyres at 50 and 80 km/h. For every case some measurements were done heading east and some heading west. The “east” and “west” measurements are considered here separately.

Standard deviations were calculated for all cases, which are given in Table 8.2. Standard deviation (%) is calculated as follows:

For each combination tyre/speed/direction several measurements of  $C_r$  were carried out on tracks L2 and M1 and the average and the standard deviation were calculated. This standard deviation was divided by the mean value and expressed as a percentage. These percentages can be found in the right column of Table 8.2. The mean value of the percentages is then calculated:

- for all combinations
- per direction
- per track M1 and L2

- per speed 50 and 80 km/h
- per tyre

**Table 8.2: Short term repeatability expressed as standard deviations for the BAST trailer**

Tyre	Speed [km/h]	Test track	Direction	Standard deviation [%]
SRTT	50	L2	E	2.0
			W	3.5
		M1	E	1.9
			W	2.5
	80	L2	E	2.0
			W	5.6
		M1	E	3.1
			W	2.5
AAV4	50	L2	E	2.4
			W	3.1
		M1	E	2.3
			W	1.1
	80	L2	E	3.8
			W	2.1
		M1	E	3.3
			W	3.0
ES16	50	L2	E	0.5
			W	1.8
		M1	E	2.4
			W	2.6
	80	L2	E	1.9
			W	2.9
		M1	E	1.8
			W	4.7
			overall <sup>2</sup>	2.6
			E	2.3
			W	3.0
			L2	2.6
			M1	2.6
			50	2.2
			80	3.1
			SRTT	2.9
			AAV4	2.6
			ES16	2.3

The overall short term repeatability of the BAST trailer is 2.6 %, which appears to be tyre and surface independent.

### 8.3.1.2 Day-to-day repeatability

BAST carried out measurements on the tracks with the SRTT tyre at 50 and 80 km/h both on 6 and 9 June 2011. Figure 8.1 shows the measured  $C_r$  at 50 km/h and Figure

<sup>2</sup> Arithmetic mean

8.2 at 80 km/h. The overall relative RMS variation  $\sigma$  is 7 % for both speed values, which is calculated as follows:

$$\sigma^2 = \sum_{\text{all tracks } i} [(C_{r,i,6 \text{ June}} - C_{r,i,9 \text{ June}}) / C_{r,i,6 \text{ June}}]^2 / N$$

with

- N the number of test tracks
- $C_{r,i,x}$  the rolling resistance coefficient measured on track i on date x

Measurements performed on 9 June at 50 km/h appear to be higher compared to measurements performed on 6 June, while those at 80 km/h tend to be lower. The authors do not know how to explain this.

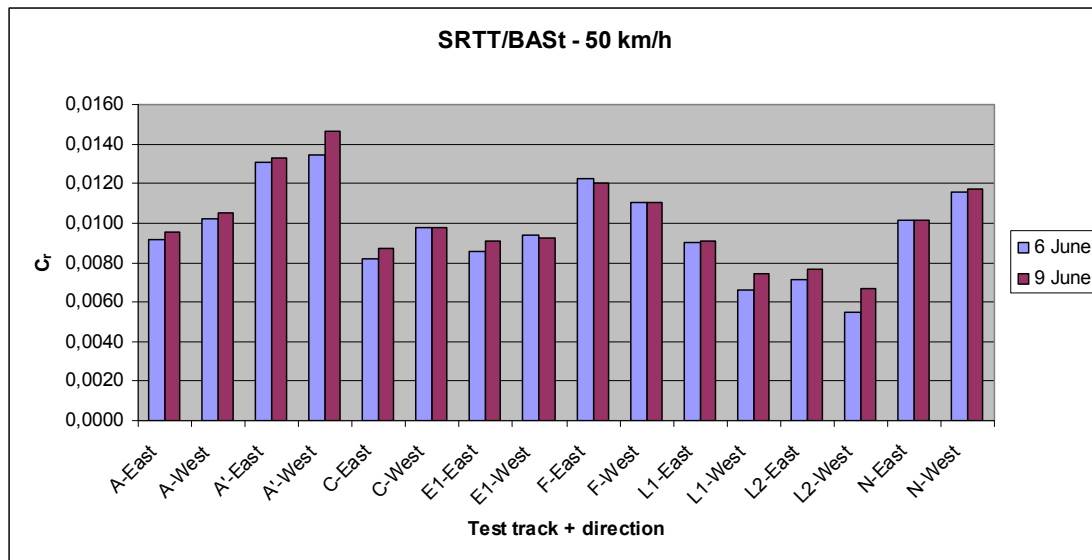


**Figure 8.1: Day-to-day variability for the BASt trailer with the SRTT/BASt mounted and at 50 km/h.**

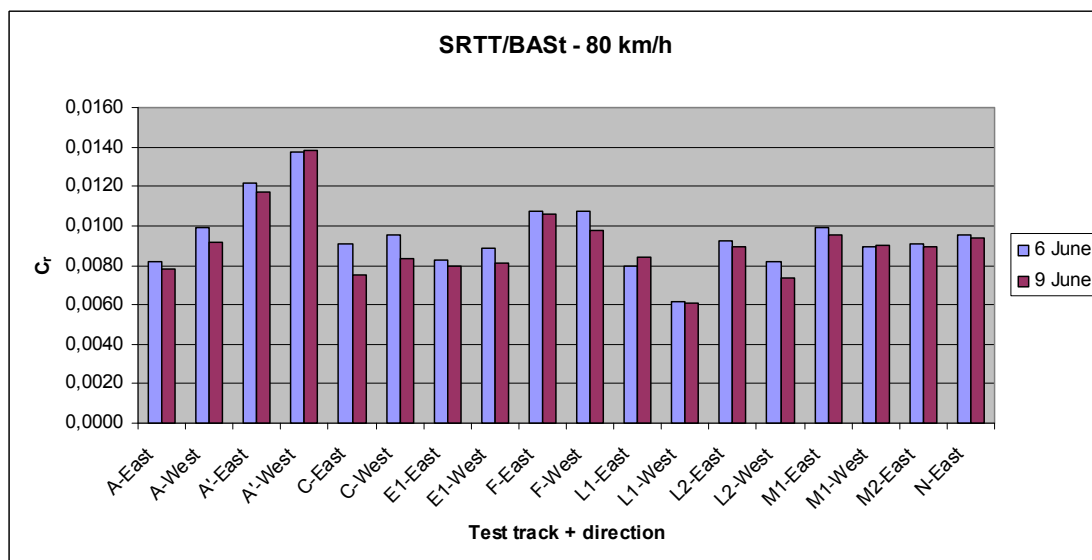


**Figure 8.2: Day-to-day variability for the BASt trailer with the SRTT/BASt mounted and at 80 km/h.**

## 8.3.2 BRRC

### 8.3.2.1 Short term repeatability

BRRC repeated measurements on test tracks M1 and L2 for the ES14 tyre at 50 and 80 km/h. For every case eight runs were done heading east and eight heading west. The “east” and “west” measurements are considered here separately. Standard deviation (%) is the standard deviation of all  $C_r$  divided by the average of all  $C_r$ . The values are given in Table 8.3.

**Table 8.3: Repeatability expressed as standard deviations for the BRRC trailer**

Tyre	Speed [km/h]	Test track	Direction	Standard deviation [%]
ES14	50	L2	E	2.5
			W	1.2
		M1	E	3.6
			W	1.1
	80	L2	E	2.6
			W	2.8
		M1	E	5.1
			W	2.7
			<b>overall</b>	<b>2.7</b>
			<b>E</b>	3.5
			<b>W</b>	2.0
			<b>L2</b>	2.3
			<b>M1</b>	3.1
			<b>50</b>	2.1
			<b>80</b>	3.3

One may conclude that the short term repeatability of the BRRC trailer is 2.7 %. The short term repeatability seems to be better for 50 km/h than for 80 km/h, which may be due to the influence of the wind.

Two measurement runs are shown in Figure 8.3. The graph reveals a good short term repeatability.

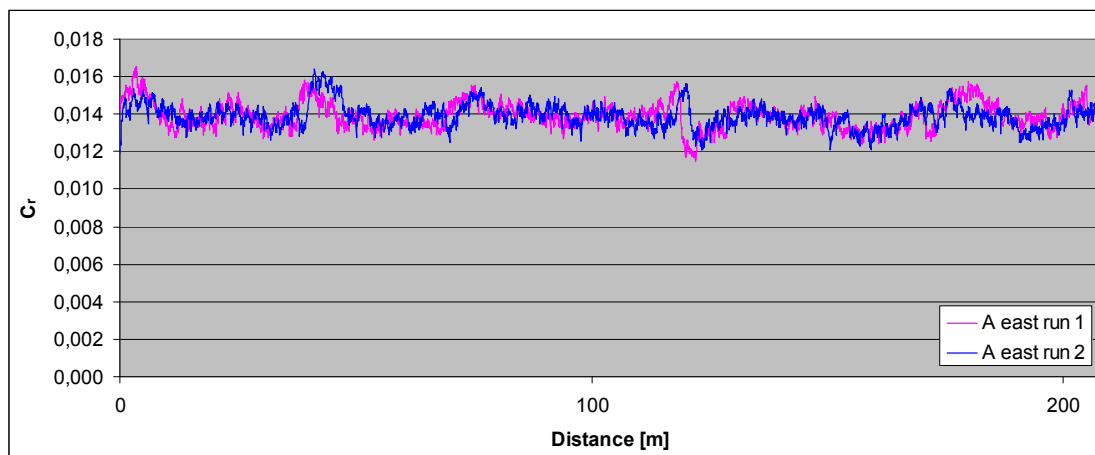


**Figure 8.3:  $C_r$  as a function of distance – Two measurement runs performed by BRRC on test section A direction east at 50 km/h**

### 8.3.2.2 Day-to-day repeatability

BRRC measured  $C_r$  on 6 and 9 June on all the test tracks. Only part of the results is relevant as during the measurement campaign on the 9<sup>th</sup> the trailer hit an object, disrupting the device.

**Table 8.4: Identical measurements carried out on different dates**

Test track	Speed [km/h]	Direction	Date	$C_r$	Change between 6 and 9 June
F	80	E	6/jun	0.0197	
F	80	W	6/jun	0.0205	
F	80	E	9/jun	0.0232	17.8 %
F	80	W	9/jun	0.0242	18.0 %
L1	80	E	6/jun	0.0160	
L1	80	W	6/jun	0.0169	
L1	80	E	9/jun	0.0188	17.5 %
L1	80	W	9/jun	0.0196	16.0 %
L2	80	E	6/jun	0.0169	
L2	80	W	6/jun	0.0183	
L2	80	E	9/jun	0.0189	11.8 %
L2	80	W	9/jun	0.0202	10,4 %
A	80	E	6/jun	0.0170	
A	80	E	9/jun	0.0206	21.2 %
C	80	E	6/jun	0.0174	
C	80	E	9/jun	0.0217	24.7 %
A'	80	E	6/jun	0.0203	
A'	80	E	9/jun	0.0240	18.2 %

There appears to be a systematic increase of the measurement results of 10 up to 25 %, most probably caused by a calibration error. For more information about calibration procedures, see [4]. This will be investigated further.

### 8.3.3 TUG

#### 8.3.3.1 Short term repeatability

TUG did a number of runs on ten test tracks in both directions, at two speeds and with four types of tyres. The repeatability values are summarized in Table 8.5. The overall short term repeatability for the TUG trailer is 1.1 %. There is no significant difference due to speed or direction. The repeatability is expressed as standard deviation (%) which is the standard deviation of all  $C_r$  (of different runs) divided by the average of all  $C_r$ .

**Table 8.5: Short term repeatability values of the TUG trailer (%)**

	SRTT				AAV4				ES16				ES14			
	50		80		50		80		50		80		50		80	
Section	East	West	East	West	East	West	East	West	East	West	East	West	East	West	East	West
M1	1.6%	1.2%	3.1%	-	0.8%	0.6%	0.1%	0.8%	0.7%	2.6%	3.2%	0.3%	0.6%	0.4%	1.4%	0.3%

<b>F</b>	1.1%	0.2%	2.0%	-	0.1%	0.8%	0.7%	0.6%	0.3%	1.0%	2.3%	1.1%	0.5%	0.1%	1.8%	0.6%
<b>M2</b>	3.1%	1.5%	1.3%	0.6%	0.8%	1.0%	0.5%	0.9%	1.1%	1.8%	2.3%	2.5%	3.0%	1.6%	1.7%	0.8%
<b>L1</b>	5.0%	0.8%	4.2%	2.5%	0.5%	0.7%	0.3%	0.3%	0.0%	1.0%	1.7%	3.9%	0.1%	1.0%	0.2%	0.8%
<b>L2</b>	3.0%	1.6%	1.7%	2.3%	1.5%	0.8%	0.1%	0.4%	1.0%	1.3%	0.7%	0.7%	0.5%	0.2%	1.0%	0.5%
<b>E1</b>	0.7%	1.0%	0.7%	2.0%	0.2%	0.5%	0.3%	0.6%	3.1%	0.5%	3.6%	5.5%	1.0%	1.2%	0.0%	0.4%
<b>E2</b>	1.0%	0.8%	1.3%	1.4%	0.6%	0.6%	0.3%	0.3%	0.5%	0.5%	2.5%	0.3%	0.8%	1.4%	0.3%	0.4%
<b>C</b>	0.5%	1.8%	2.5%	0.5%	0.0%	0.4%	0.3%	0.2%	0.4%	0.2%	1.1%	1.1%	0.8%	0.9%	0.4%	0.3%
<b>A'</b>	0.9%	1.7%	2.2%	1.5%	0.2%	0.7%	0.1%	0.7%	1.3%	0.4%	1.0%	3.5%	0.2%	0.6%	0.5%	0.2%
<b>A</b>	1.4%	2.3%	4.4%	1.8%	0.4%	0.4%	0.1%	0.6%	0.4%	0.8%	1.8%	0.9%	0.1%	0.2%	0.9%	0.9%
<b>overall</b>	<b>1.1%</b>															
<b>E</b>	<b>1.2%</b>															
<b>W</b>	<b>1.0%</b>															
<b>50</b>	<b>1.0%</b>															
<b>80</b>	<b>1.2%</b>															

Two measurement runs are shown in Figure 8.4. The graph reveals an excellent short term repeatability.

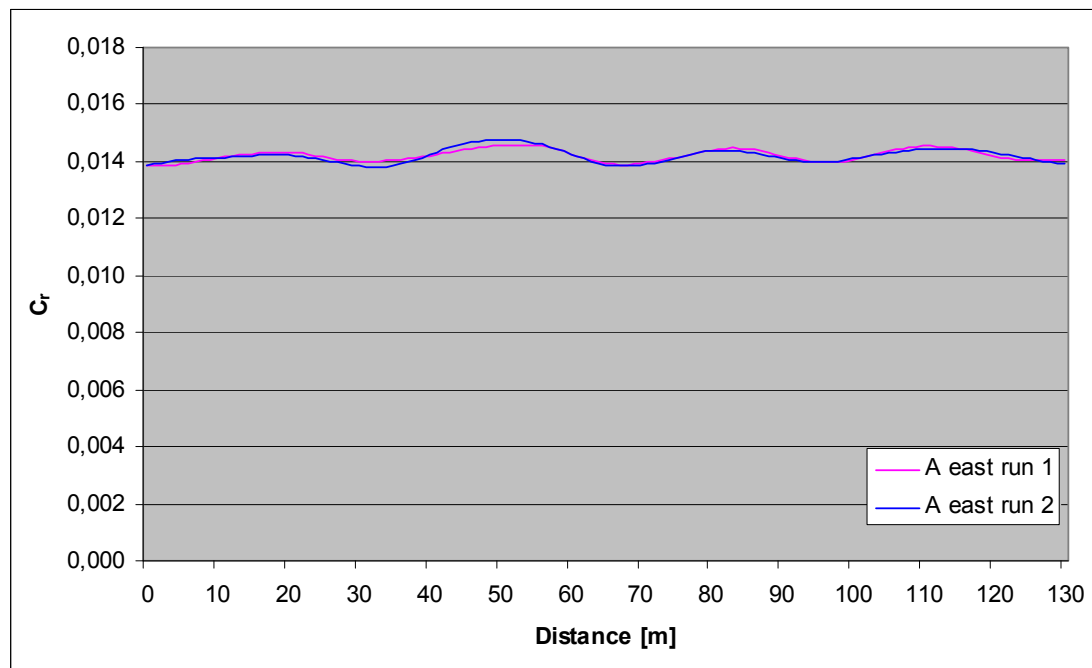


**Figure 8.4:  $C_r$  as a function of distance – Two measurement runs performed by TUG on test section A direction east at 50 km/h**

### 8.3.3.2 Day-to-day repeatability

As TUG already had a full test program by performing measurements with all tyres, TUG did not repeat measurements on different days.

## 8.4 Reproducibility of the RR devices

Results are considered over the whole length of the test section.

## 8.4.1 BAST – TUG

### 8.4.1.1 All measurements

All measurements performed by BAST and TUG with AAV4, ES16 and SRTT are plotted in Figure 8.5 and Figure 8.6. Graphs representing BAST measurements are drawn with full line, while the TUG graphs are drawn with dashed line.

BAST performed SRTT/BAST measurements on 2 days: 6 June and 9 June (see also section 8.3.1.2). Both results are shown in the graphs.

Except for two inconsistent BAST values for surfaces M1 and L2 at 80 km/h, the absolute values of AAV4 for TUG and BAST are situated not too far from each other (the difference is approx. 10 %) at 50 km/h but much closer at 80 km/h. Such a speed influence on the similarity of results is difficult to explain.

SRTT and ES16 values measured by BAST are substantially higher than measured by TUG at both speeds.

All graphs show similar patterns with respect to the effect of road surface.

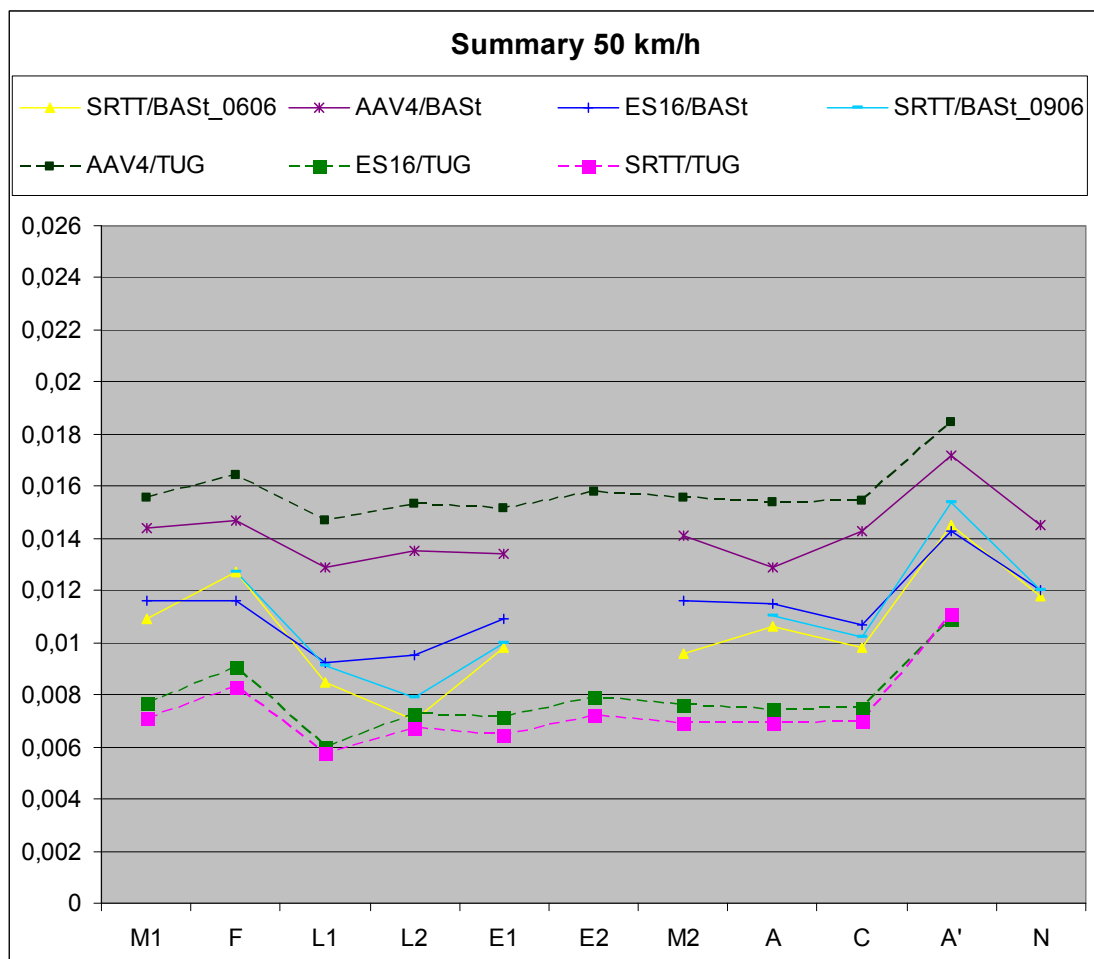
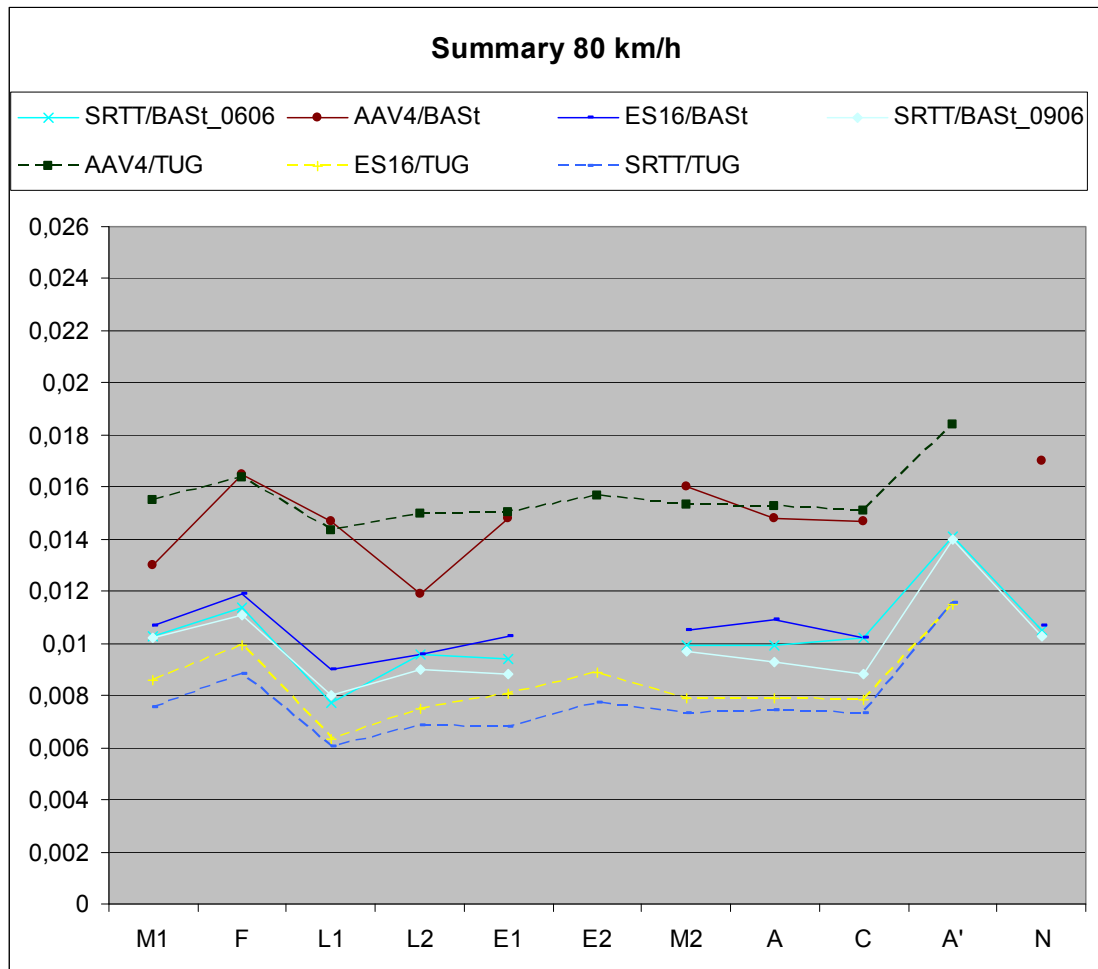


Figure 8.5:  $C_r$  for different test sections measured by BAST and TUG at 50 km/h



**Figure 8.6:**  $C_r$  for different test sections measured by BAST and TUG at 80 km/h

#### 8.4.1.2 Relation between BAST and TUG ES16 tyre measurements

Very good correlations between the TUG and BAST ES16 tyres are found for both speeds (see Figure 8.7 and Figure 8.8). However, the difference to a 1:1 line is substantial, indicating a poor reproducibility.



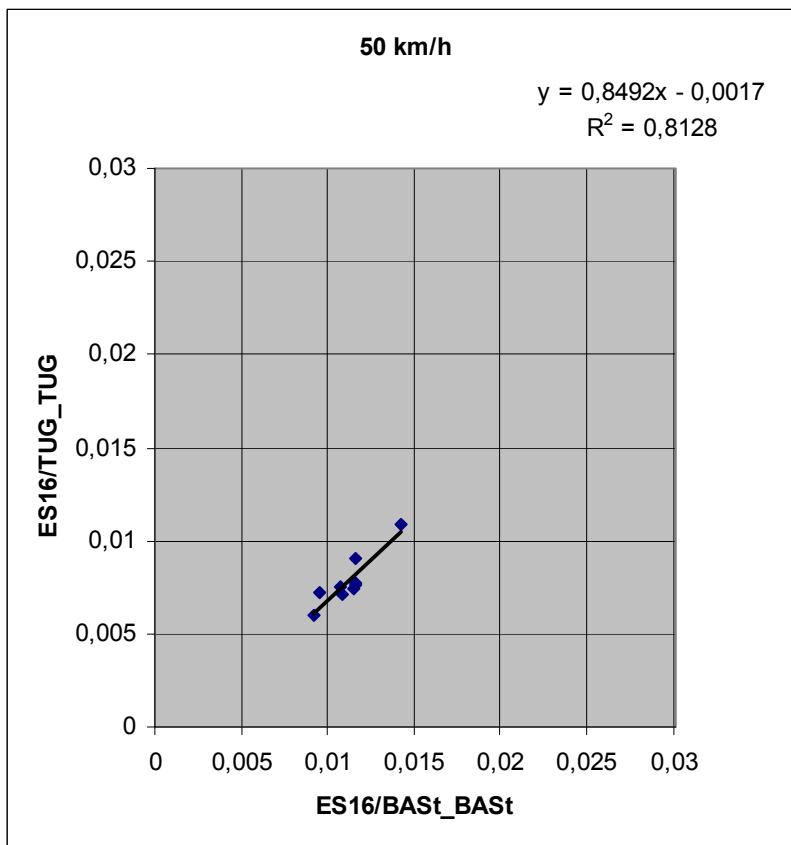


**Figure 8.7: Correlation between  $C_r$  measured by BASt and TUG with ES16 at 50 km/h**

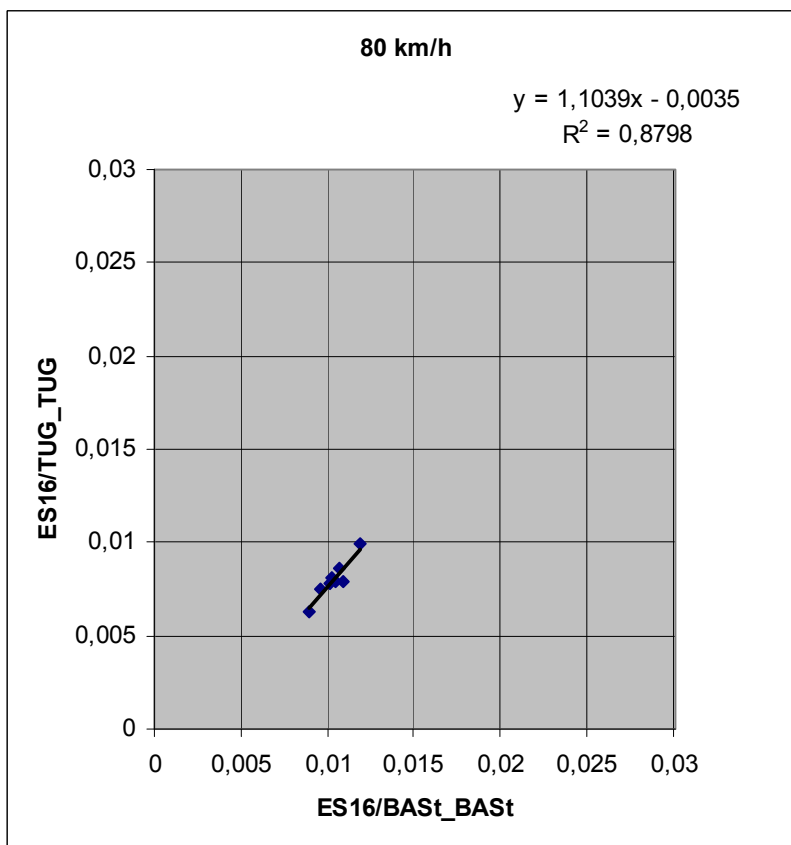


**Figure 8.8: Correlation between  $C_r$  measured by BASt and TUG with ES16 at 80 km/h**

### 8.4.1.3 Relation between BAST and TUG SRTT tyre measurements

Very good correlations are found between the TUG and BAST tyres when comparing SRTT measurements. At 80 km/h it is even an excellent correlation (0.984). However, the regression line is situated far from the 1:1 relation (albeit slope coefficient is 0.914), which again means that reproducibility is poor.

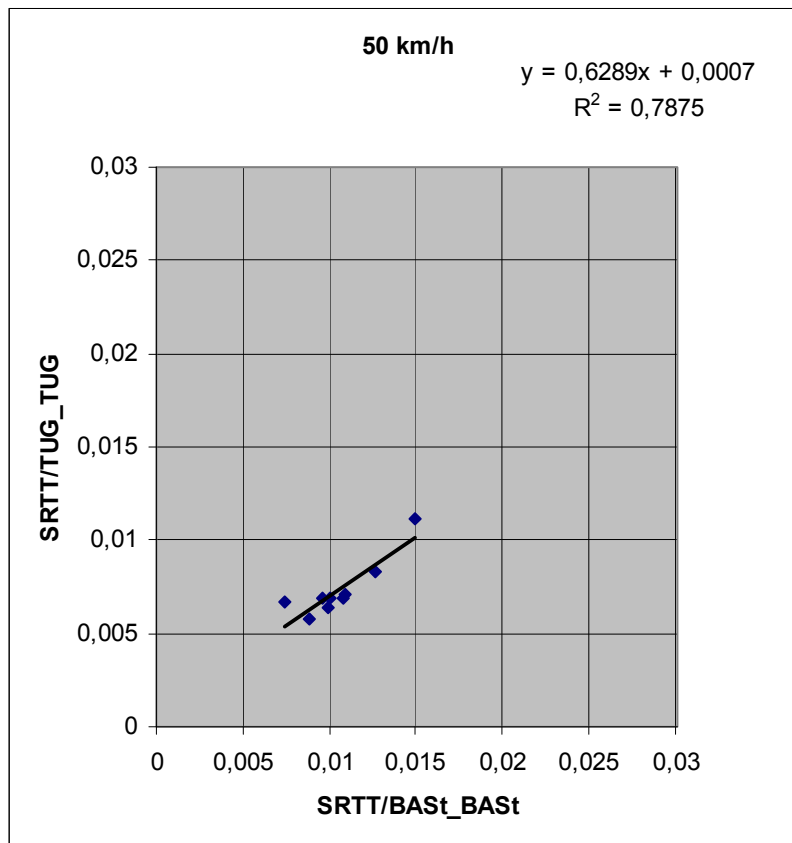


Figure 8.9: Correlation between  $C_r$  measured by BAST and TUG with SRTT at 50 km/h

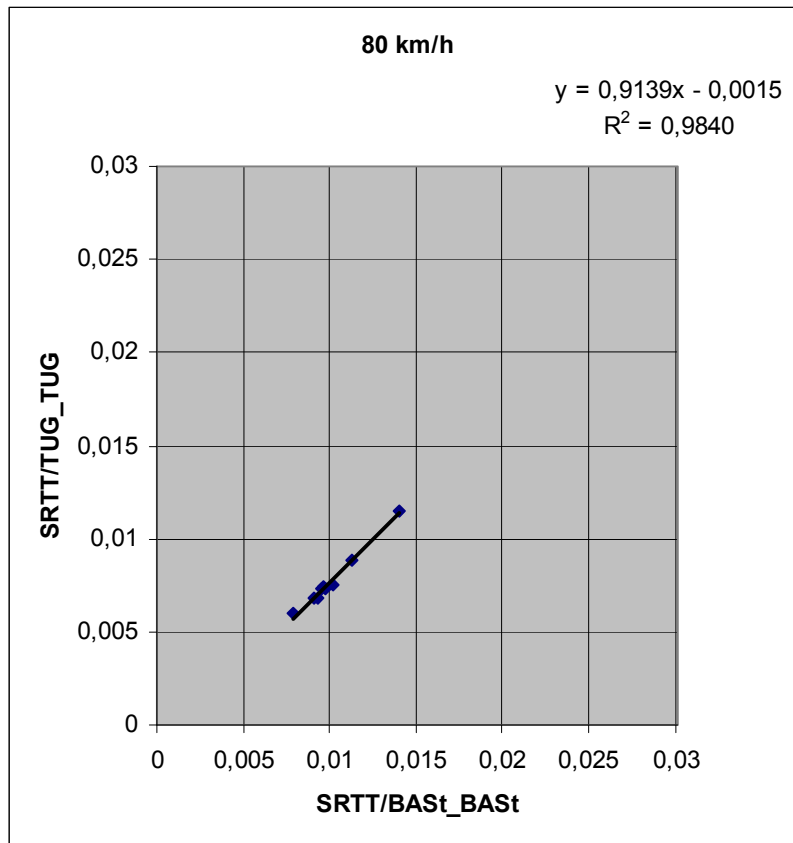
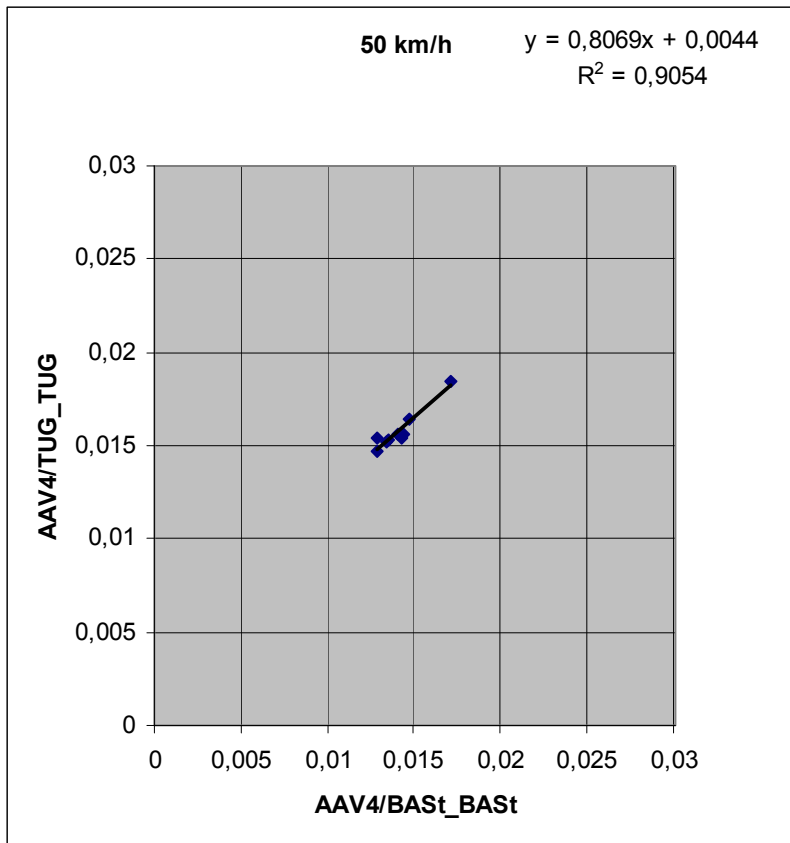


Figure 8.10: Correlation between  $C_r$  measured by BASt and TUG with SRTT at 80 km/h

#### 8.4.1.4 Relation between BASt and TUG AAV4 tyre measurements

The correlation chart of 50 km/h demonstrates a very good correlation, while the one of 80 km/h indicates that there is no correlation (see Figure 8.11 and Figure 8.12). This is due to the two inconsistent BASt values (see Figure 8.6).



**Figure 8.11: Correlation between  $C_r$  measured by BASt and TUG with AAV4 at 50 km/h**

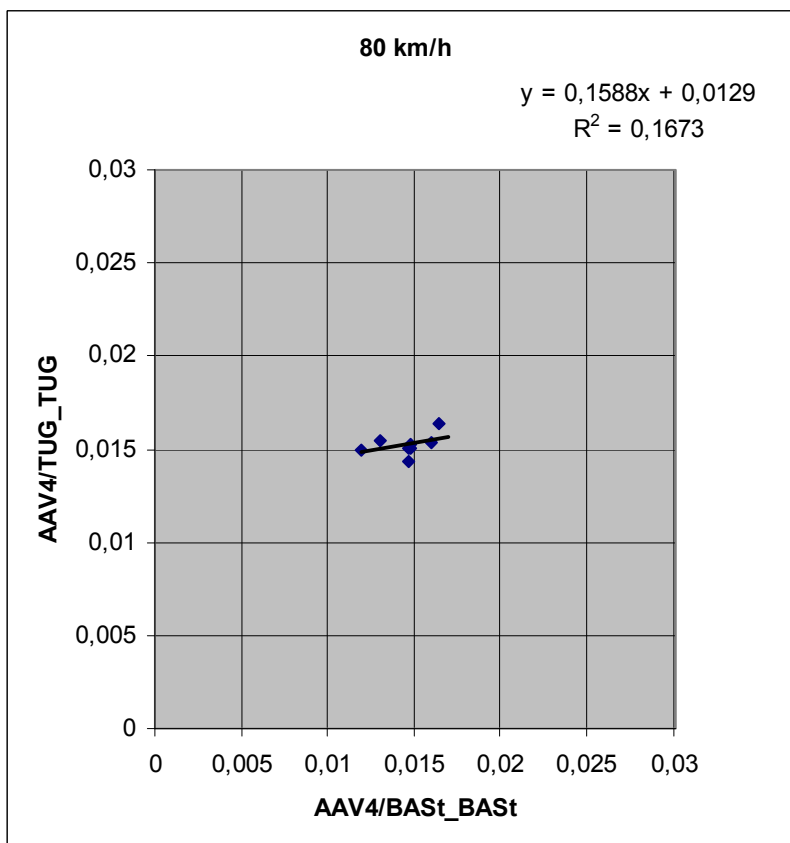


**Figure 8.12: Correlation between  $C_r$  measured by BASt and TUG with AAV4 at 80 km/h**

## 8.4.2 BRRC – TUG

### 8.4.2.1 All measurements

All measurements performed by BRRC and TUG with ES14 are plotted in Figure 8.13. Graphs representing BRRC are drawn with full line, while those representing TUG are drawn with dashed line.

It can clearly be seen that BRRC has an outlier for test section M2. The  $C_r$  values are too high. This may be due to the fact that BRRC measured this surface separately, turning with the vehicle with a small turning radius and accelerating very strongly on a small distance. These manipulations of the trailer even caused an impact with the vehicle at a certain moment. The acceleration may have caused higher  $C_r$  values for M2. This problem will be verified by BRRC in the near future.

At 50 km/h the absolute values of ES14 lie together very closely, when discarding outlier M2.

However, TUG drum measurements show a difference between ES14/BRRC and ES14/TUG (see Figure 10.2 and Figure 10.3), which is surface and speed dependent ( $C_r$  0.001 – 0.003).

Also a different load was used. TUG used a load of 4000 N while BRRC used only a load of 2000 N due to suspension limitations of the trailer. A higher difference because of this was expected, which is not the case.

A similar pattern can be seen for all graphs.

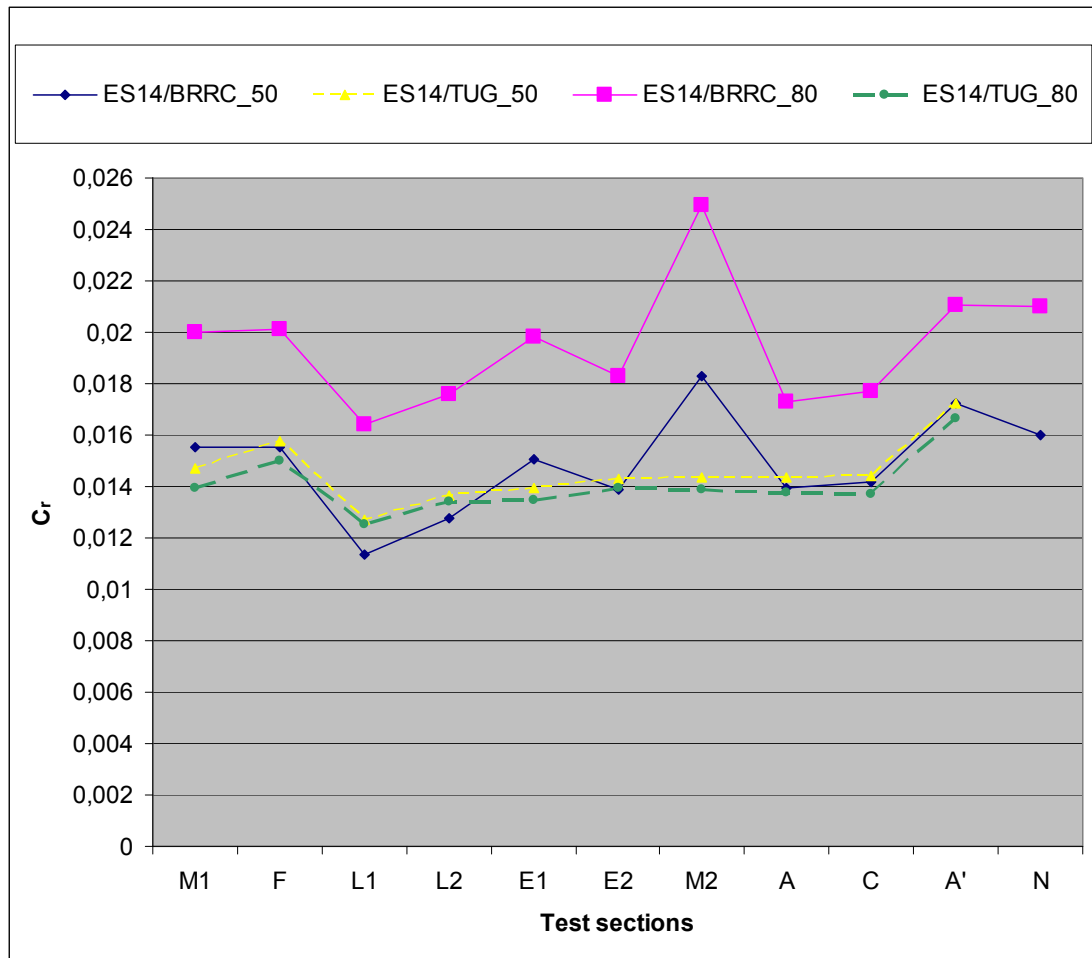
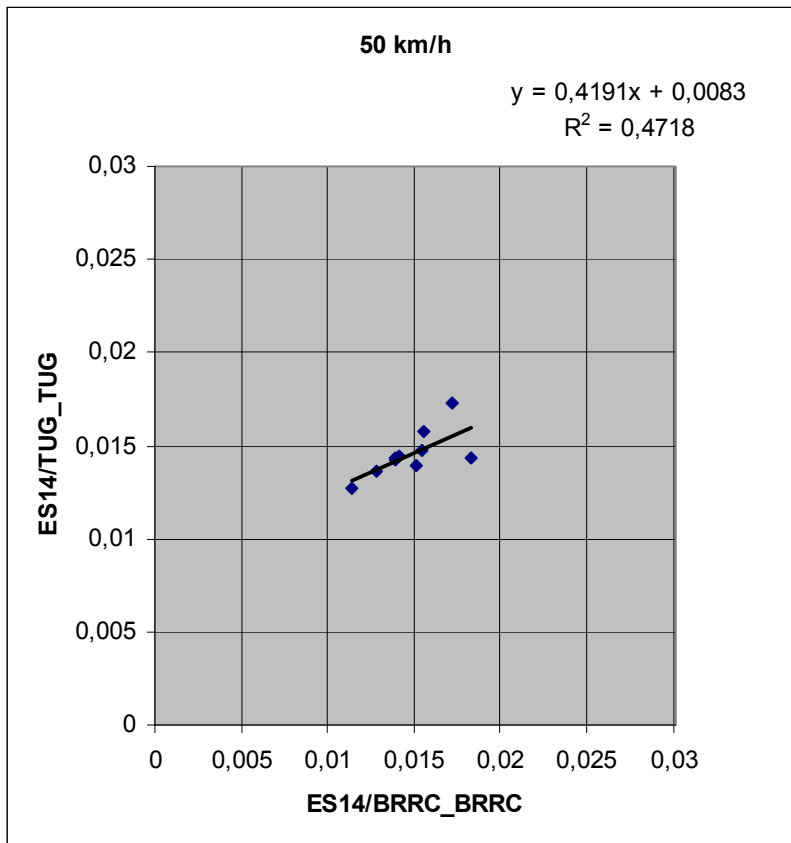


Figure 8.13:  $C_r$  for different test sections measured by BRRC and TUG at 50 and 80 km/h

#### 8.4.2.2 Relation between BRRC and TUG ES14 tyre measurements

A fair correlation is found at 50 km/h (see Figure 8.14). However if M2 would have been discarded, even a very good relation would be found ( $R^2 = 0.818$ ).

No correlation appears at 80 km/h (see Figure 8.15). However if M2 would have been discarded, a rather good correlation would be found ( $R^2 = 0.612$ ), but reproducibility would be very poor as the BRRC values are consistently much higher.



**Figure 8.14: Correlation between  $C_r$  measured by BRRc and TUG with ES14 at 50 km/h**

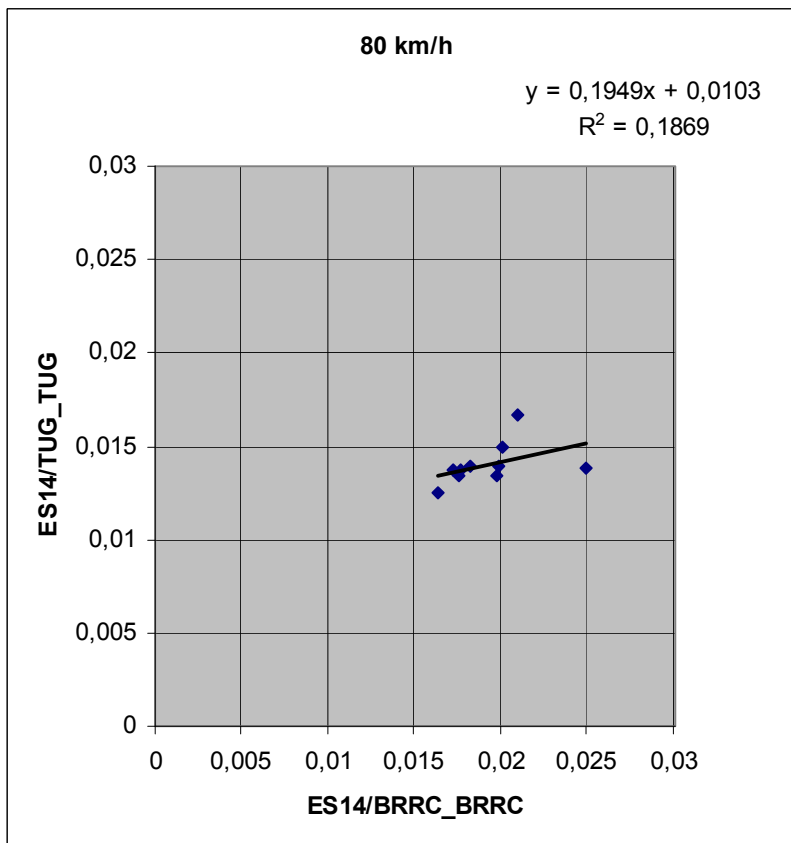


**Figure 8.15: Correlation between  $C_r$  measured by BRRc and TUG with ES14 at 80 km/h**

### 8.4.3 BAsT - BRRC

#### 8.4.3.1 All measurements

Even though BAsT and BRRC did not perform measurements with the same tyre type and thereby no conclusions about reproducibility can be made, it is interesting to compare the measurement results.

All measurements performed by BAsT and BRRC with ES16 and ES 14 are plotted in Figure 8.16. To make a clearer distinction between institutes, all measurements of BAsT are plotted with full line, while those of BRRC are plotted with dashed line.

BRRC values are clearly higher, which is due to the tyre size. Based on TUG measurements performed with ES14 and ES16, it can be assumed that the difference in  $C_r$  at 50 km/h is about 0.006 to 0.007 (see Figure 9.3). The graphs of the measurements at 50 km/h show a  $C_r$  difference of the same order of magnitude (see Figure 8.16). The higher values at 80 km/h are also partly caused by the lack of wind shielding of the BRRC trailer.

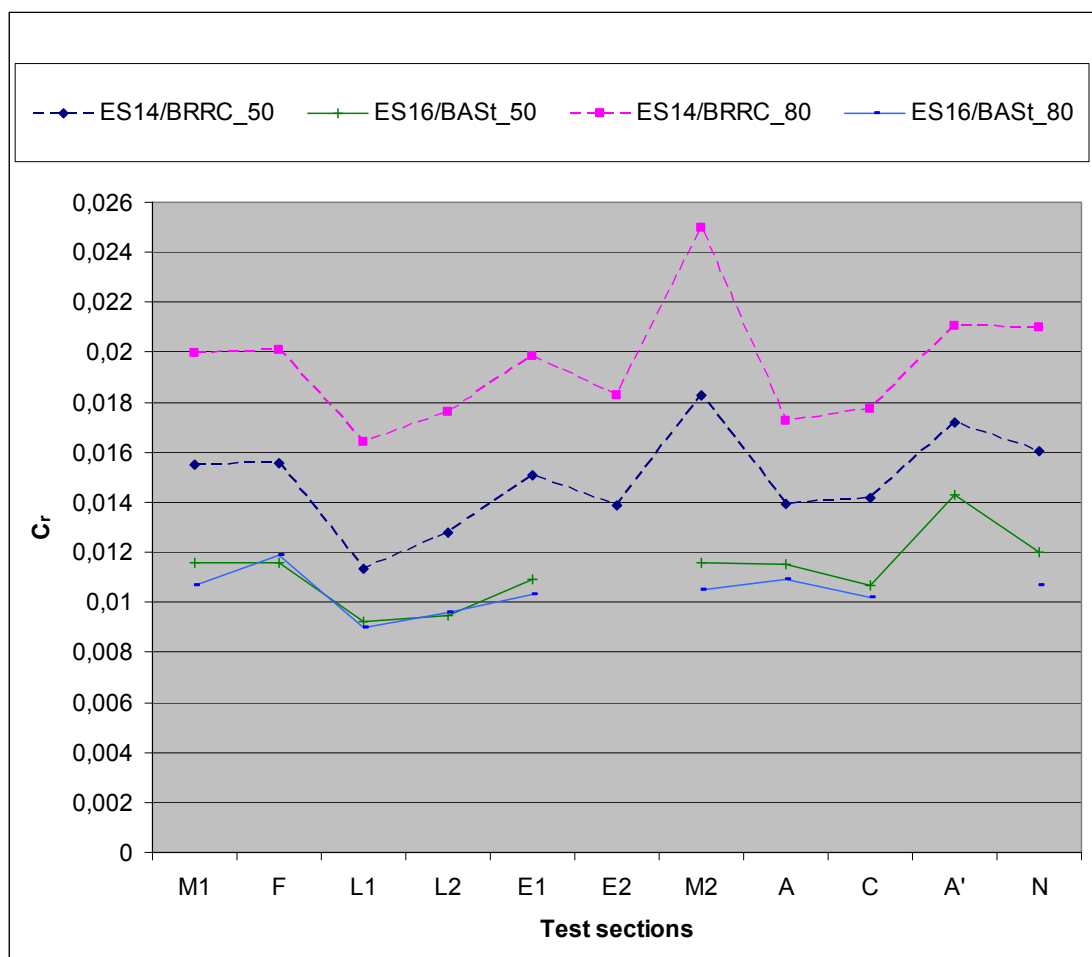


Figure 8.16:  $C_r$  for different test sections measured by BAsT and BRRC



### 8.4.3.2 Relation between ES16/BASt and ES14/BRRC tyre measurements

Correlations between ES16/BASt and ES14/BRRC are analyzed. A good correlation is achieved at 50 km/h while there is not found any correlation at 80 km/h (see Figure 8.17 and Figure 8.18). This may be due to the high influence of wind at higher speed of the BRRC trailer.

If outlier M2 would have been discarded, a very good relation at 50 km/h ( $R^2 = 0.838$ ) and a rather low correlation at 80 km/h would be found ( $R^2 = 0.429$ ).

No conclusions about reproducibility can be drawn.

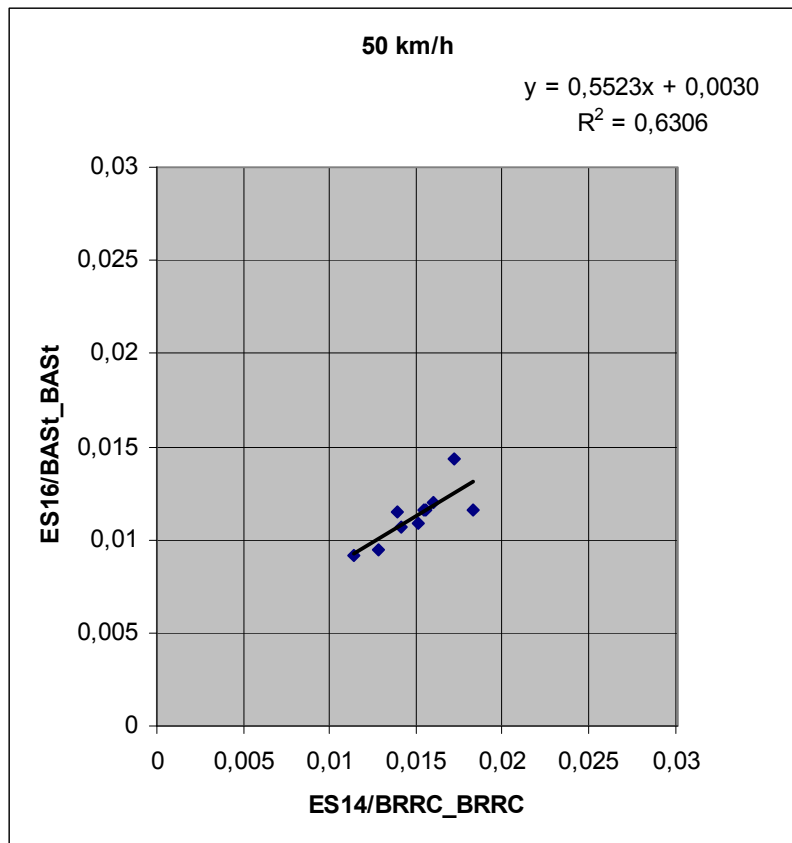


Figure 8.17: Correlation between  $C_r$  ES16/BASt and ES14/BRRC at 50 km/h

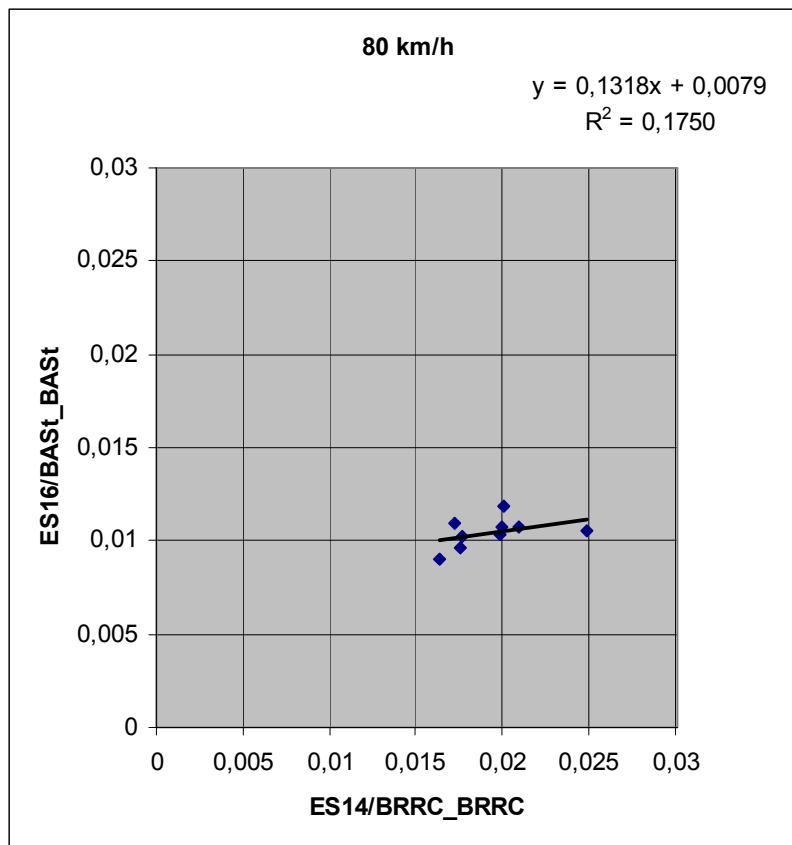


Figure 8.18: Correlation between  $C_r$  ES16/BASt and ES14/BRRC at 80 km/h

## 9 Additional tests

### 9.1 Tyres

#### 9.1.1 Measurements

TUG performed measurements on the test track with all tyres to detect differences between tyres of the same type. However ES14/BRRRC and ES16/BAS<sub>t</sub> were not measured. The measurement results are shown in Figure 9.1 and Figure 9.2.

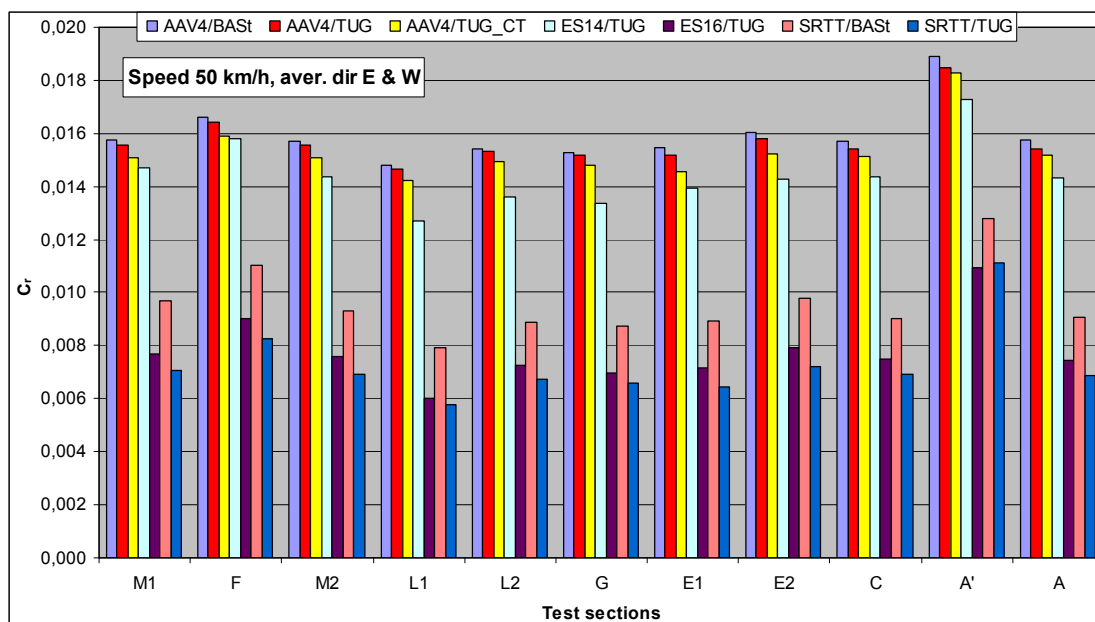


Figure 9.1: Measurements performed by TUG with all tyres at 50 km/h on test track

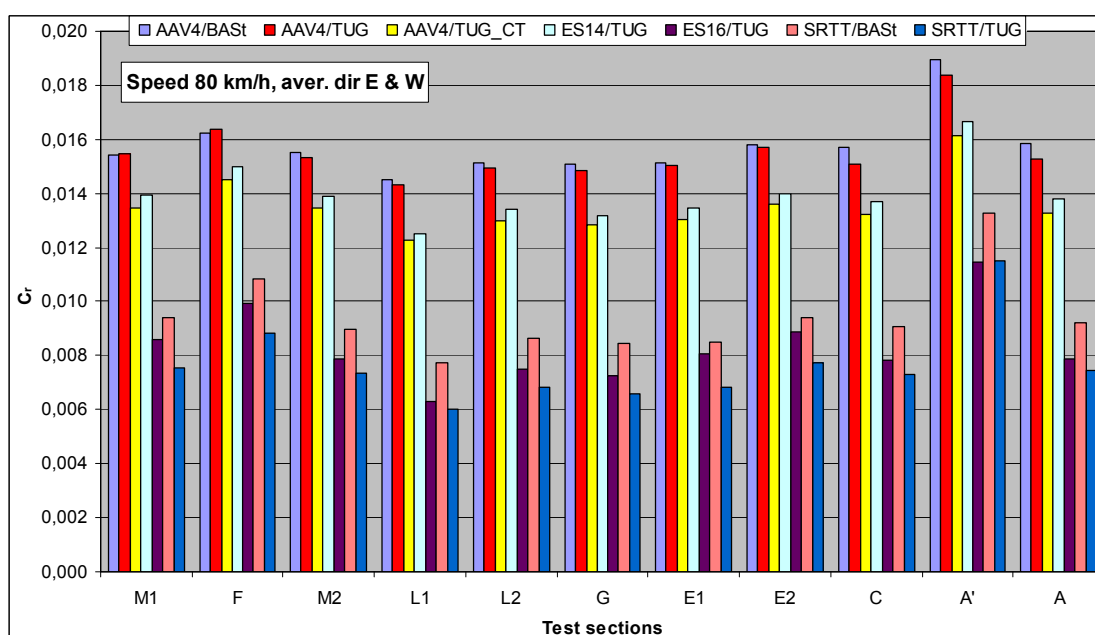


Figure 9.2: Measurements performed by TUG with all tyres at 80 km/h on test track

It appears that the AAV4 tyres give values close to each other, but the TUG and BAST SRTT tyres differ substantially.

### 9.1.2 Tyre related corrections

When looking at differences between tyres of the same type (SRTT, AAV4), only a small difference was noted between the two AAV4 tyres (see Figure 9.3 and Figure 9.4). The AAV4 tyres came from the same batch unlike the SRTT tyres and one of them even had a corrupted tread pattern. At 80 km/h the differences are slightly larger than at 50 km/h. The two SRTT's differ by approx. 30 %, which is alarming. The reason must be studied. The difference between ES14 and ES16 can be found in the graph for TUG test tyres. These may be used when comparing tyres with different sizes. It is amazing that tyre size may have such a dramatic influence.

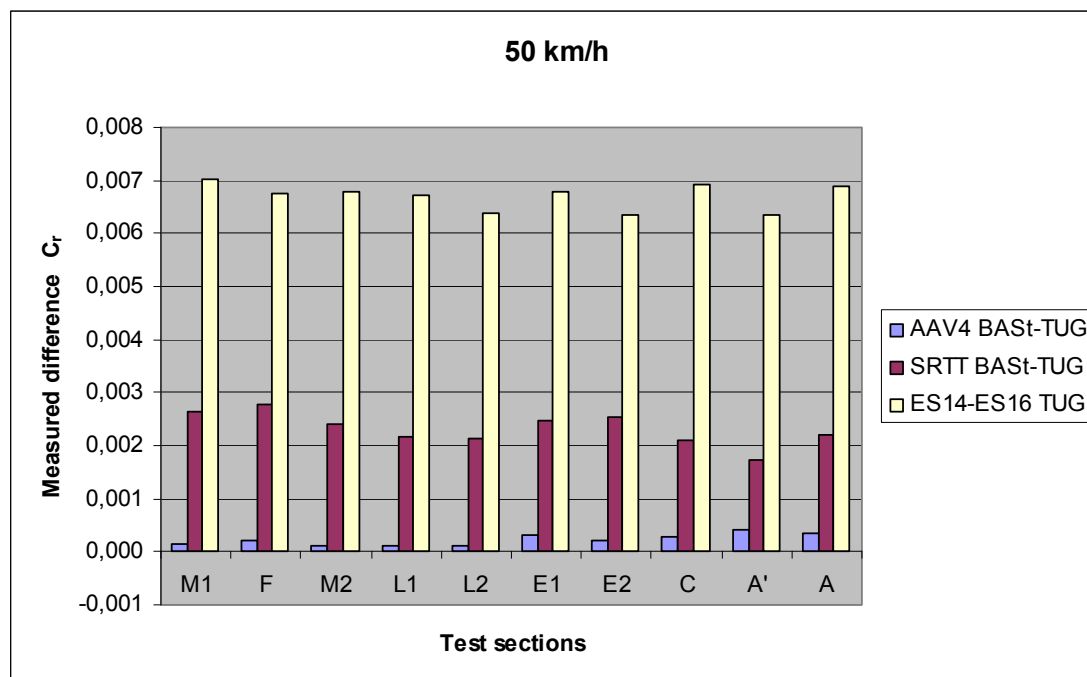
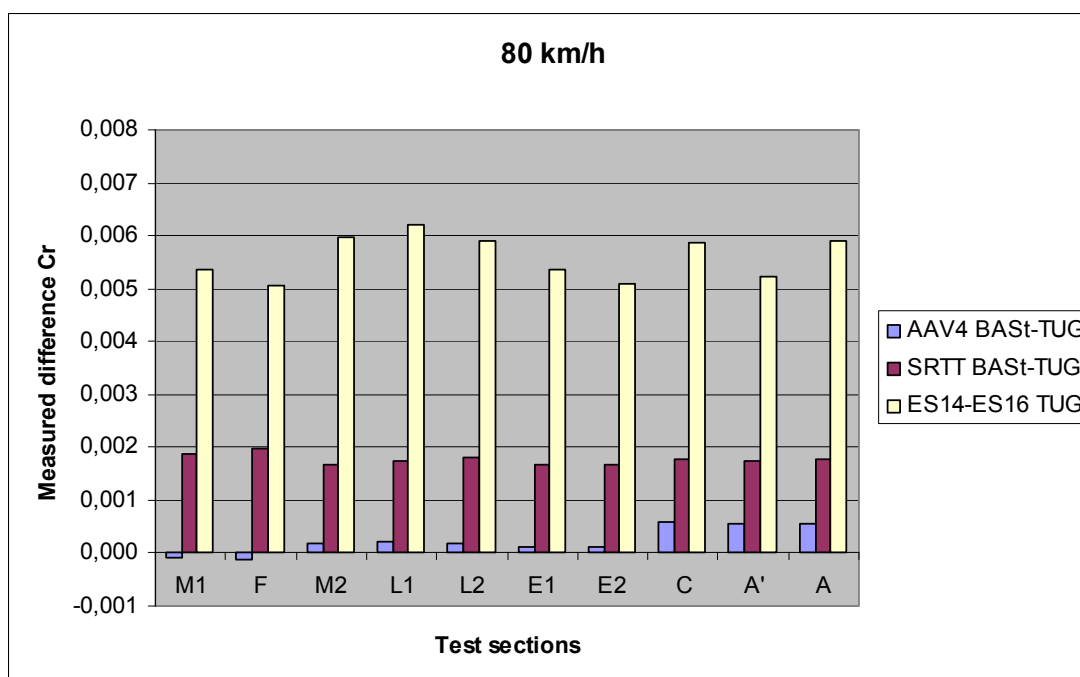


Figure 9.3:  $C_r$  difference between tyres measured by TUG on test sections



**Figure 9.4:  $C_r$  difference between tyres measured by TUG on test sections**

The relative difference expressed in percentage is shown in Table 9.1. A positive value means that  $C_r$  measured with the BAST tyre is higher. It can clearly be seen that the SRTT's differ the most at 50 km/h: 19.7 - 39.5 %. The difference is slightly smaller at 80 km/h: 15.5 - 28.7 %. The highest difference between the two AAV4's with normal tread is only 3.8 % at 80 km/h.

**Table 9.1: Relative difference in percentage between tyres measured by TUG on test sections**

Speed	50 km/h		80 km/h	
Test section	AAV4 BAST-TUG	SRTT BAST-TUG	AAV4 BAST-TUG	SRTT BAST-TUG
M1	1.0%	37.1%	-0.5%	24.7%
F	1.3%	33.4%	-0.8%	22.4%
M2	0.8%	34.6%	1.2%	22.7%
L1	0.8%	37.5%	1.5%	28.7%
L2	0.8%	31.9%	1.2%	26.6%
E1	2.0%	37.5%	0.8%	25.5%
E2	1.5%	39.5%	0.9%	24.6%
C	1.7%	29.1%	3.8%	23.0%
A'	2.6%	24.7%	3.6%	23.7%
A	1.8%	19.7%	3.1%	15.5%

Table 9.2 shows the relative difference in percentage between the AAV4/TUG tyre with normal and with corrupted tread. A positive value means that  $C_r$  measured with the tyre with normal tread is higher. The difference between the tyres is higher at higher speed: approximately 3 % at 50 km/h and approximately 15 % at 80 km/h.

**Table 9.2: Relative difference in percentage between AAV4/TUG\_CT and AAV4/TUG**

<b>Test section</b>	<b>50 km/h</b>	<b>80 km/h</b>
<b>M1</b>	3.2%	15.0%
<b>F</b>	3.2%	12.9%
<b>M2</b>	3.1%	13.8%
<b>L1</b>	3.1%	16.6%
<b>L2</b>	2.6%	15.2%
<b>E1</b>	2.8%	15.6%
<b>E2</b>	4.3%	15.2%
<b>C</b>	3.7%	15.3%
<b>A'</b>	1.9%	14.3%
<b>A</b>	1.1%	14.0%

Analyses were made to explore the influence of this difference between tyres. This was done for tyres of the same type, namely AAV4 and SRTT. AAV4/BAS<sub>t</sub>\_BAS<sub>t</sub> and SRTT/BAS<sub>t</sub>\_BAS<sub>t</sub> were corrected to AAV4/TUG\_BAS<sub>t</sub> and SRTT/TUG\_BAS<sub>t</sub> by subtracting the difference found in Figure 9.3 and Figure 9.4.

For SRTT the graphs are now situated rather close to each other. They almost show the same absolute values (see Figure 9.5) within about 20 %. However the relative difference between the institutes is still quite high: approximately 16 % at 50 km/h and approximately 7 % at 80 km/h.

The tyre correction also improves the correlation at 50 km/h (see Figure 9.6 and Figure 8.9). The correlation at 80 km/h remains the same, which is excellent (see Figure 9.7 and Figure 8.10).

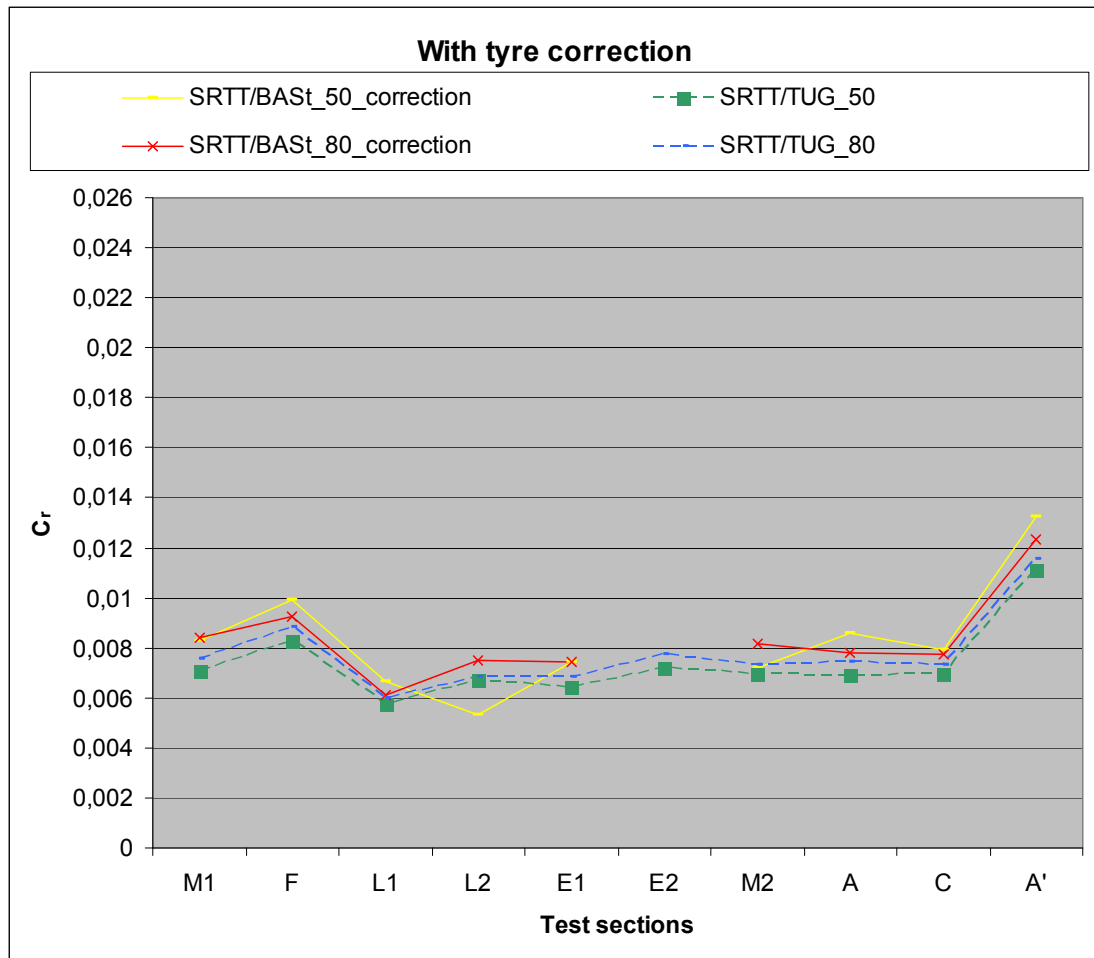


**Figure 9.5:  $C_r$  for different test sections measured by BAST and BRRC with SRTT tyre correction**

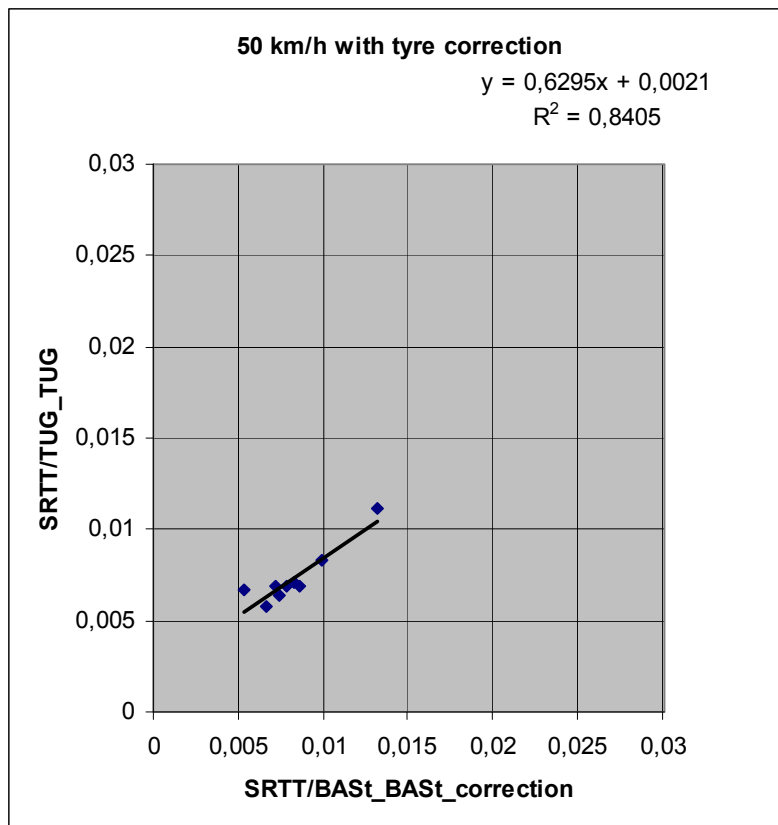


**Figure 9.6: Correlation  $C_r$  measured by TUG and BASSt with SRTT corrected for tyre difference at 50 km/h**

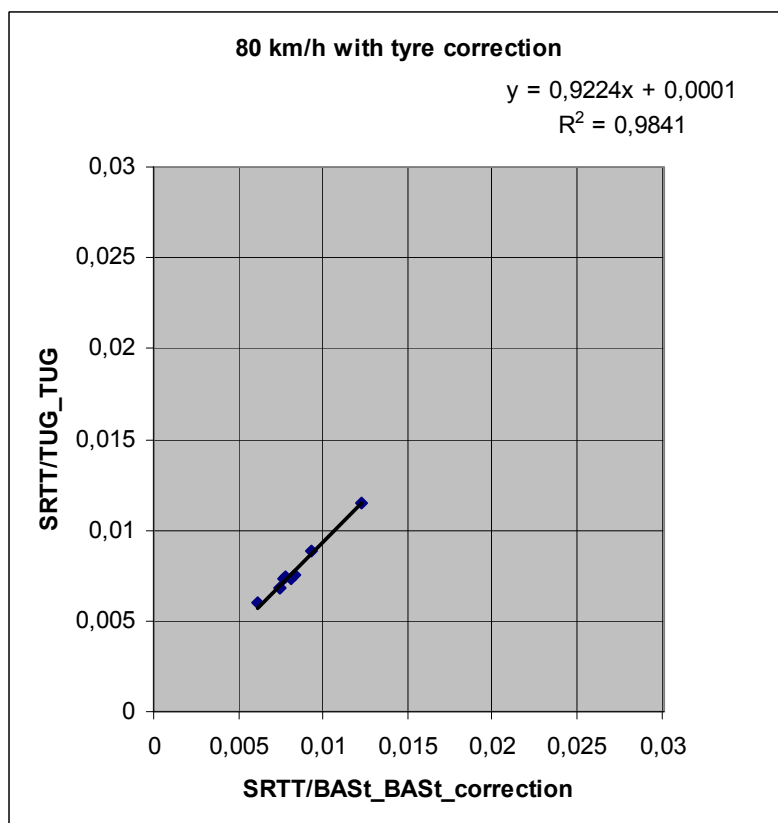


**Figure 9.7: Correlation  $C_r$  measured by TUG and BASSt with SRTT corrected for tyre difference at 80 km/h**



The tyre correction does not improve the comparison between absolute AAV4 values much (see Figure 9.8). The relative difference between the institutes is quite high: approximately 12 % at 50 km/h and approximately 6 % at 80 km/h.

Moreover the correlation at 50 km/h is lower than without corrections (see Figure 9.9 and Figure 8.11). The correlation at 80 km/h on the contrary did improve (see Figure 9.10 and Figure 8.12).

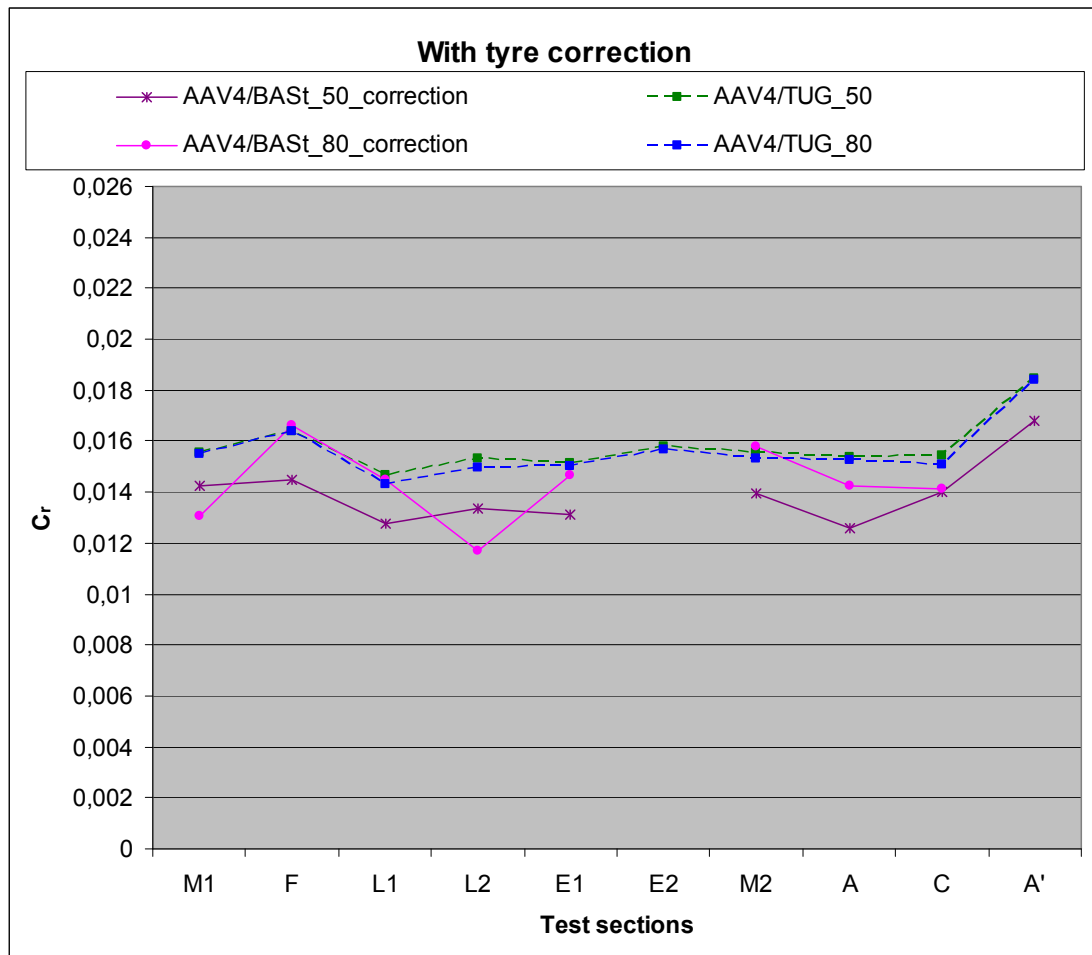


**Figure 9.8:  $C_r$  for different test sections measured by BAST and BRRC with AAV4 tyre correction**

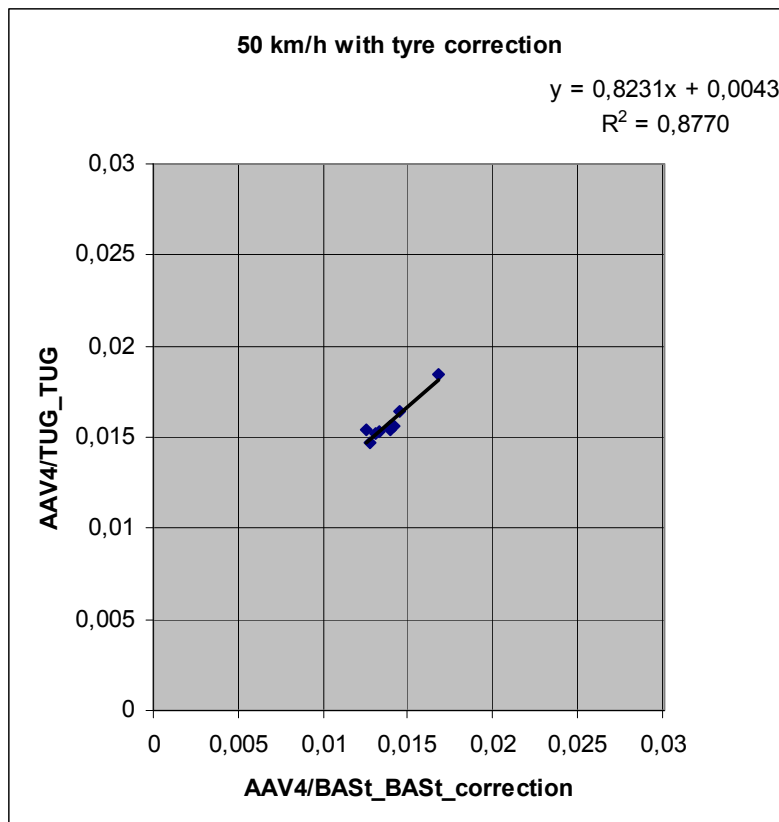


**Figure 9.9: Correlation  $C_r$  measured by TUG and BASSt with SRTT corrected for tyre difference at 50 km/h**

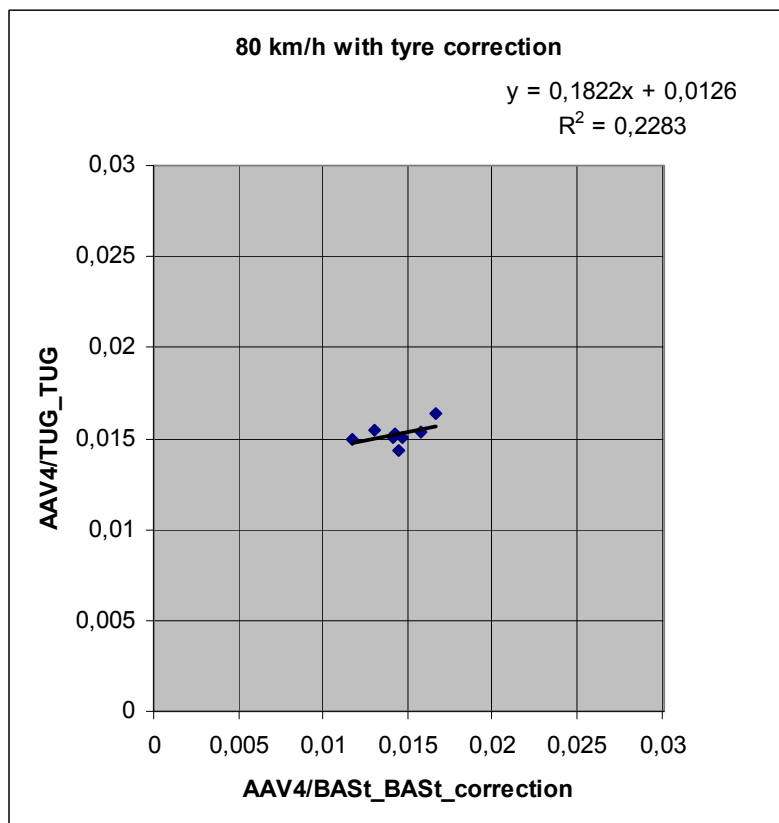


**Figure 9.10: Correlation  $C_r$  measured by TUG and BASSt with SRTT corrected for tyre difference at 80 km/h**

### 9.1.3 Trailer related differences

Trailer related differences between measurements can be detected by comparing measurements performed by TUG and BAST with exactly the same tyres. For SRTT/BAST\_BAST the average value of measurements performed on 6 and 9 June is used.

The trend of the AAV4 graphs measured by TUG and BAST are very similar at 50 km/h. There appears to be a significant offset (see Figure 9.11). As TUG used higher inflation pressure than BAST, the difference should have been the opposite.

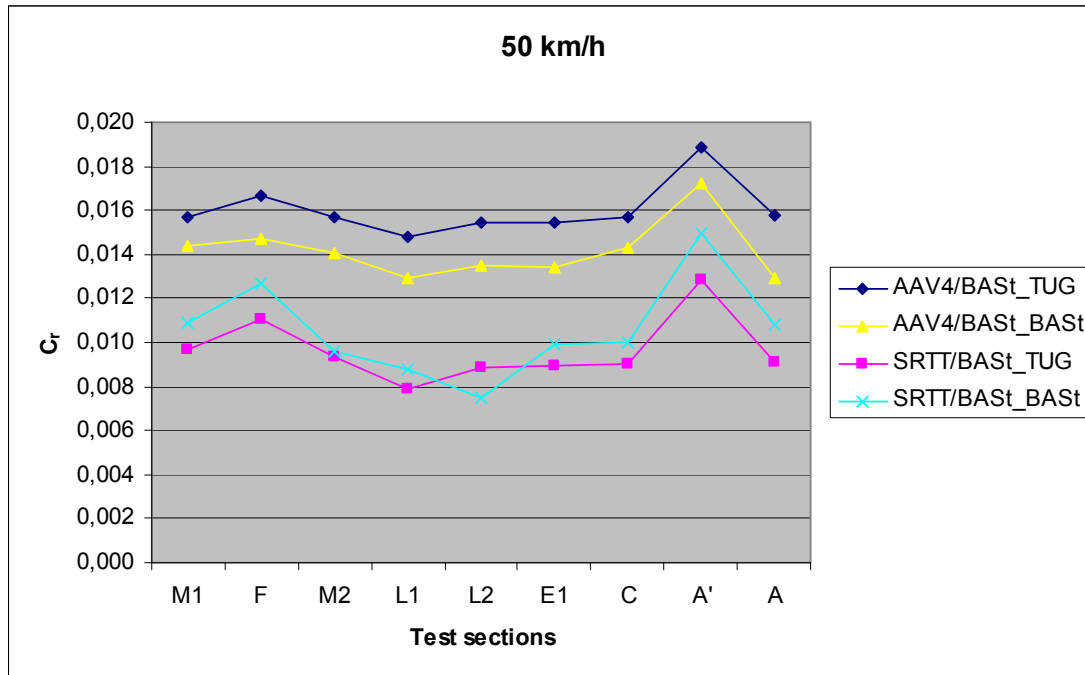


**Figure 9.11:  $C_r$  for different test sections measured by BAST and TUG with AAV4/BAST and SRTT/BAST at 50 km/h**

The SRTT graphs measured by TUG and BAST lie somewhat closer to each other. At 50 km/h, the TUG values are lower than the BAST values, which is opposite to the case for the AAV4 tyre. The offset that was noted at 50 km/h doesn't appear for 80 km/h (see Figure 9.12). The graph of AAV4/BAST\_BAST shows some strange values for test sections M1 and L2. The results of the other test sections lie close to the TUG measurements.

Overall, these results are inconsistent; as the differences depend on tyre and speed. It is difficult to find an explanation.

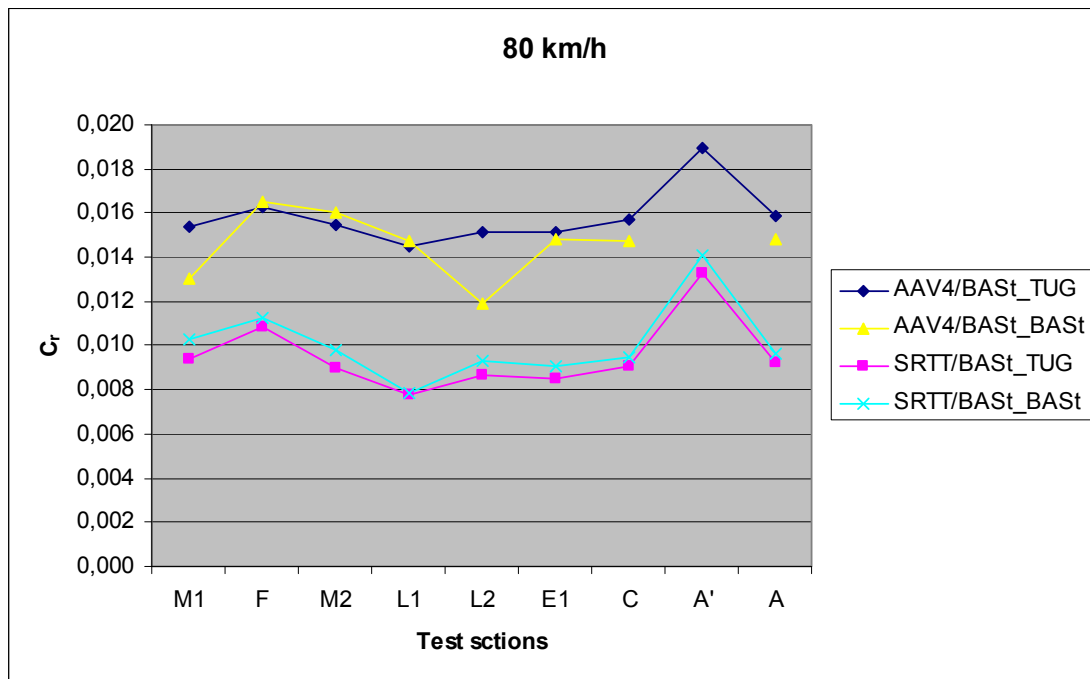


**Figure 9.12:  $C_r$  for different test sections measured by BASt and TUG with AAV4/BASt and SRTT/BASt at 80 km/h**

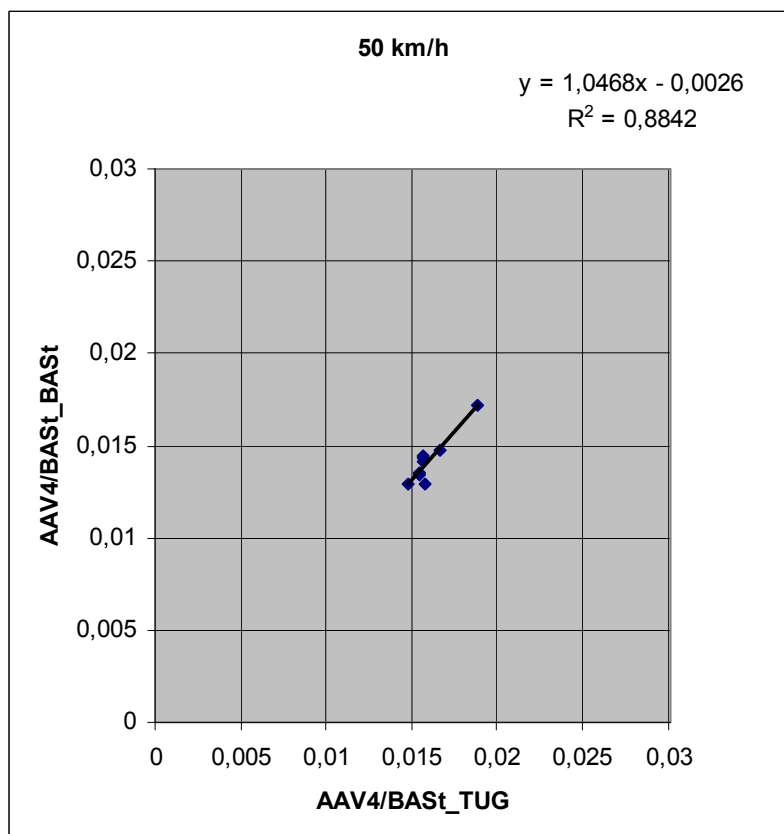


**Figure 9.13: Correlation between  $C_r$  measured by BASt and TUG with AAV4/BASt at 50 km/h**

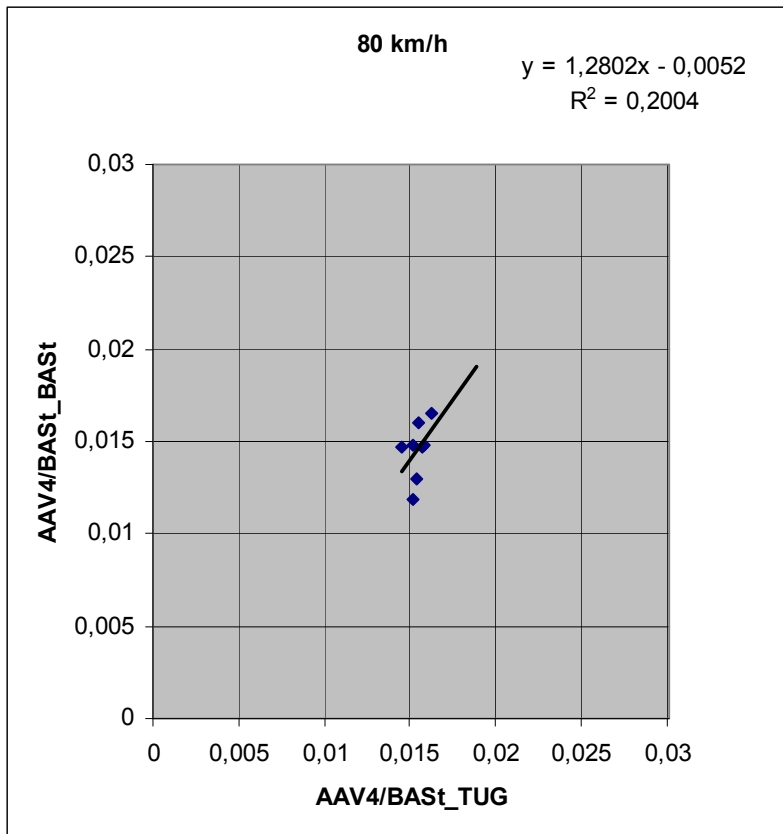


**Figure 9.14: Correlation between  $C_r$  measured by BASSt and TUG with AAV4/BASSt at 50 km/h**

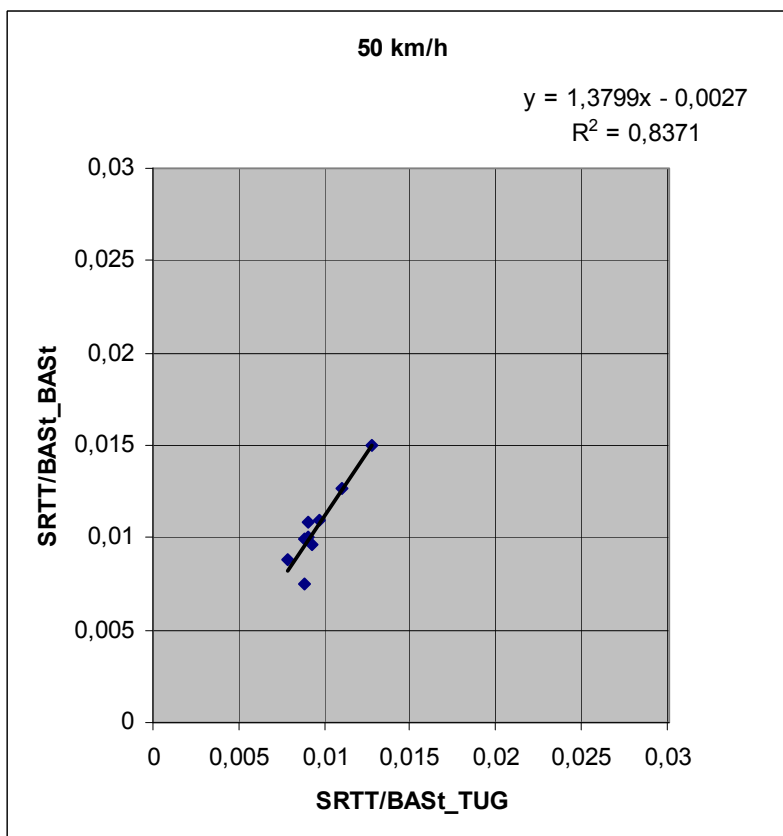


**Figure 9.15: Correlation between  $C_r$  measured by BASSt and TUG with SRTT/BASSt at 50 km/h**

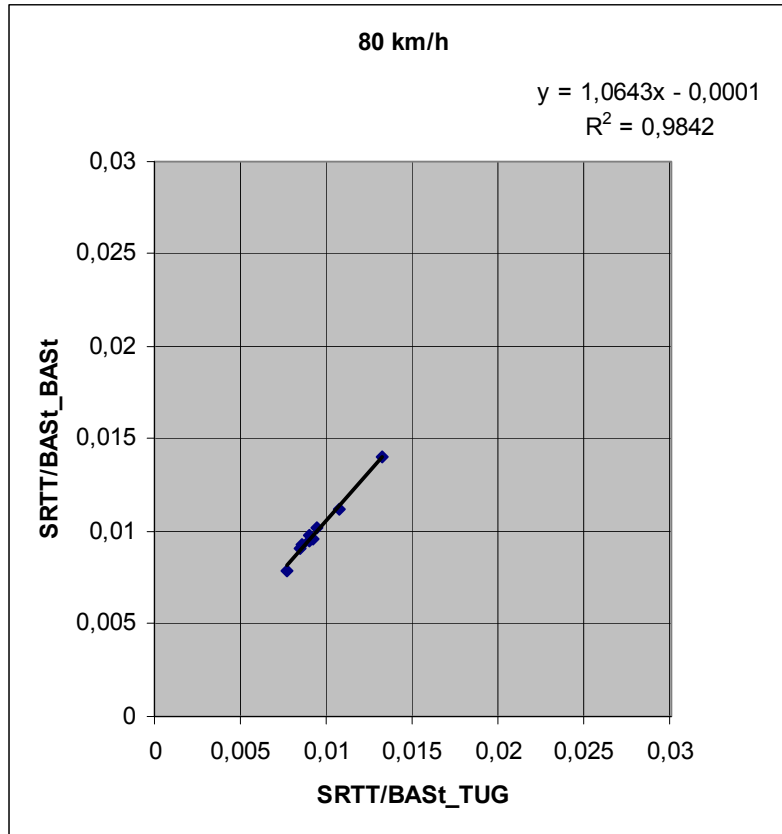


**Figure 9.16: Correlation between  $C_r$  measured by BASSt and TUG with SRTT/BASSt at 80 km/h**

The charts show very good correlations except for measurements with AAV4/BASSt at 80 km/h (see Figure 9.13 to Figure 9.16). This may be due to the measurements performed by BASSt with AAV4 at 80 km/h which are not in line with the others (see Figure 9.12). An excellent correlation can be noted for measurements with SRTT at 80 km/h. The different offset at 50 km/h versus 80 km/h may be an indication of a different speed dependency of these trailers.

## 9.2 Speed influence

Only a small speed influence can be noted (see Figure 9.17 and Figure 9.18). The best correlation between speed and  $C_r$  is given by SRTT/TUG. The difference between SRTT/BASSt and SRTT/TUG becomes smaller at higher speeds.

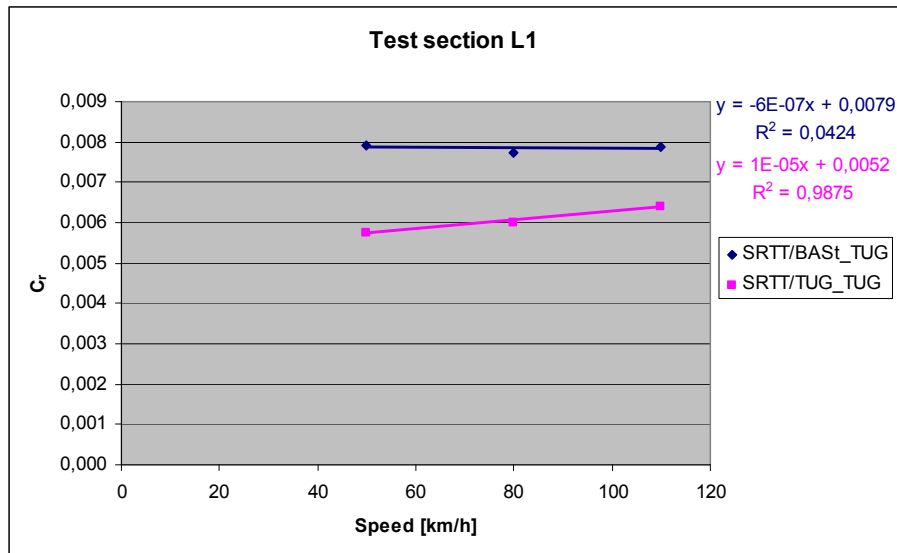


**Figure 9.17:  $C_r$  as a function of speed for tyres SRTT/BASt and SRTT/TUG measured by TUG on test section L1**

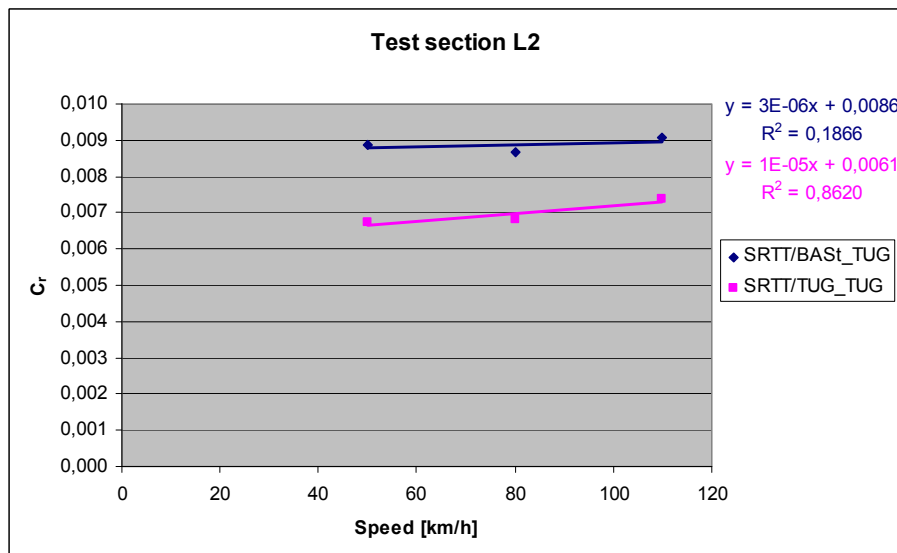


**Figure 9.18:  $C_r$  as a function of speed for tyres SRTT/BASt and SRTT/TUG measured by TUG on test section L2**

BASt and BRRC measure in general larger differences between 50 and 80 km/h than TUG (see Figure 8.13 and Figure 9.19). The largest difference is measured by BRRC (see Figure 8.13) but is probably due to the lack of wind shielding and thereby the influence of wind (higher  $C_r$  at higher speed). BASt and TUG often measure lower  $C_r$  at higher speed, which is unexpected and contradictory to Figure 9.17 and Figure 9.18.

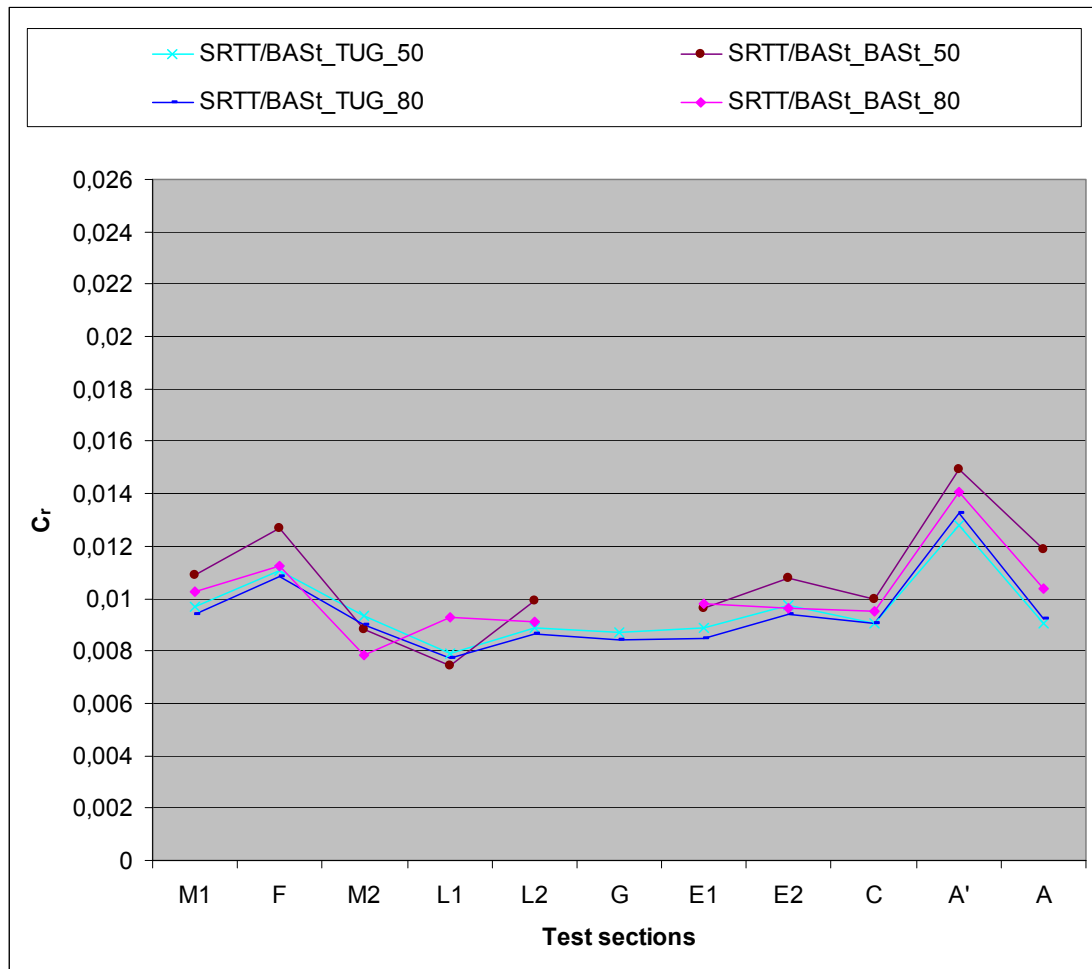


**Figure 9.19:  $C_r$  for different test sections measured by BASt and TUG with SRTT at 50 and 80 km/h**

### 9.3 Warm-up

Measurements were performed by BRRC on a highway near Nantes to gain knowledge about the evolution of tyre temperature and the difference between measuring temperature at the shoulder of the tyre or at the interior of the tyre.

After driving to the test site, the vehicle stood still for 15 and 25 minutes before starting the measurement with nitrogen and air respectively to allow the tyre to cool down before the start.

The measurements were performed by driving at a constant speed of 80 km/h for 45 minutes, however due to other traffic and road works the vehicle sometimes had to slow down (70 km/h) and accelerate again for a short period.

Tyre inflation, ambient air temperature, interior and exterior tyre temperature were measured every 15 minutes during a short standstill (4-5 minutes). The precision of the tyre inflation measuring tool is  $\pm 0.05$  bar.

The measurement was repeated two times: one time with air inside the tyre, the second time with nitrogen inside the tyre. The tyre was filled up three times to make sure all air/nitrogen was gone before inserting another.

After 15 minutes the maximum tyre inflation is already reached (2.15 bar) in both cases (see Figure 9.20 and Figure 9.21).



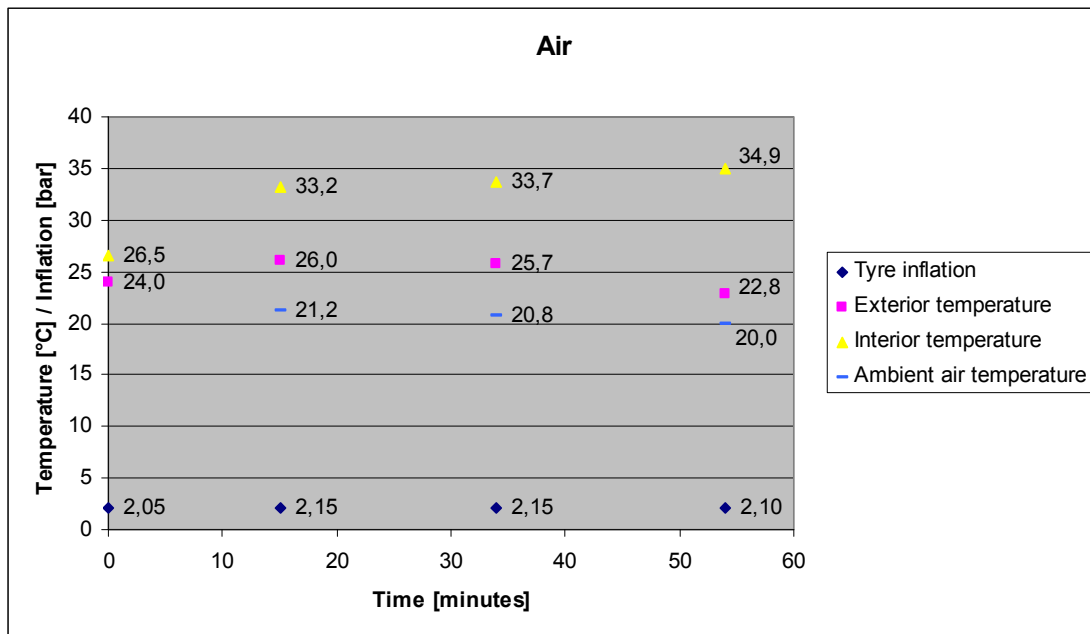


**Figure 9.20: Warm-up test with air inside ES14/BRRC tyre: data measured during short standstill 0 – 15 – 30 – 45 minutes**

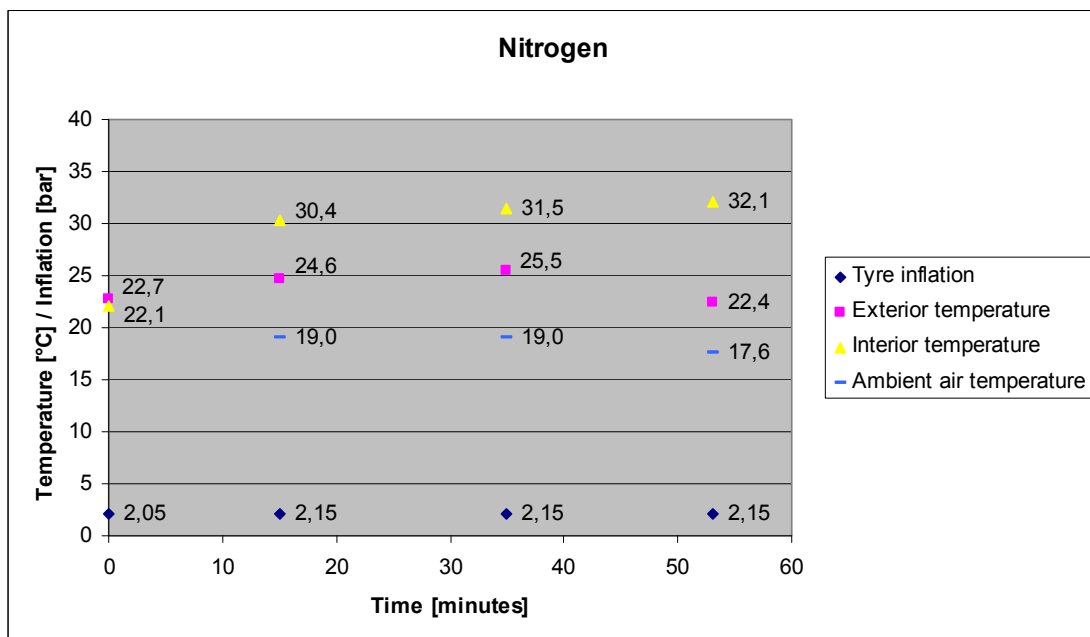


**Figure 9.21: Warm-up test with nitrogen inside ES14/BRRC tyre: data measured during short standstill 0 – 15 – 30 – 45 minutes**

Temperature measured at the tyre shoulder fluctuates a lot and is more subject to radiation of the sun (see Figure 9.22 and Figure 9.23). Temperature seems to be more stable with nitrogen inside the tyre. Interior temperature drops less at standstill with nitrogen than with air. A higher interior temperature is reached with air than with nitrogen and temperature increases faster while driving.

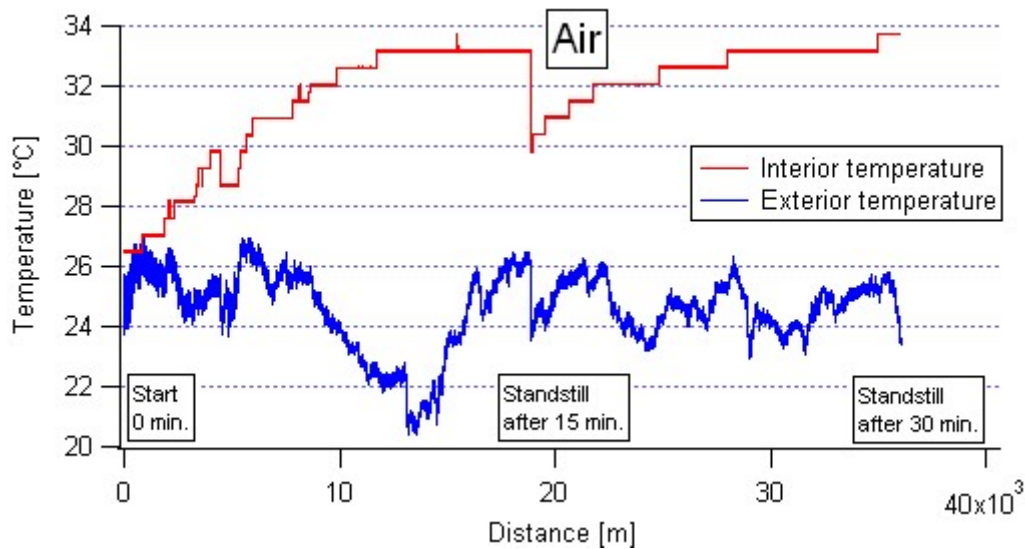


**Figure 9.22: Warm-up test with air inside ES14/BRRC tyre – Continuous measurement of temperatures while driving 2 times 15 minutes**

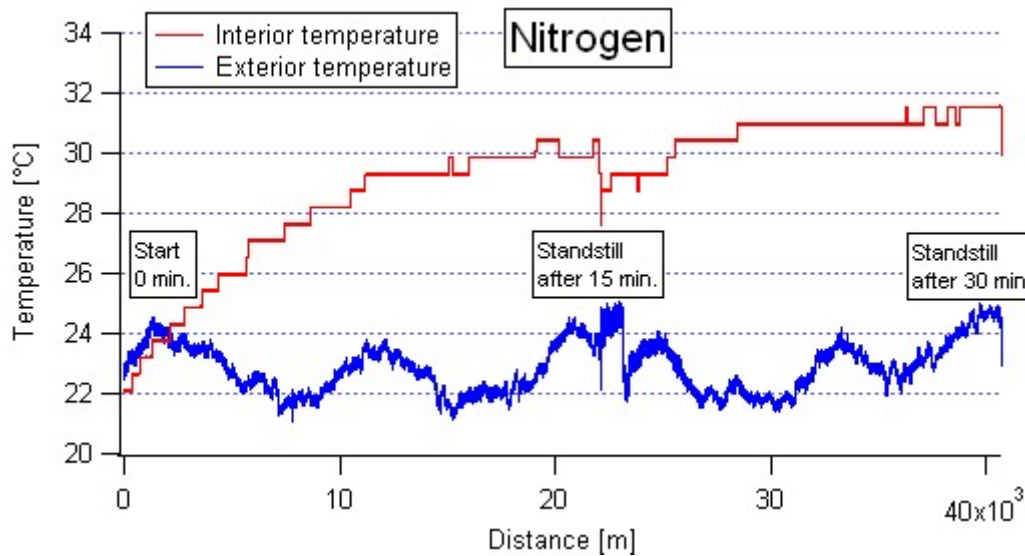


**Figure 9.23: Warm-up test with nitrogen inside ES14/BRRC tyre – Continuous measurement of temperatures while driving 2 times 15 minutes**

## 9.4 Influence of side forces

When driving in a curve, the tyre reacts to the steering by developing a slip angle  $\Theta$  (see Figure 9.24). More information about side forces and slip angle can be found in [8] (section 9.2.2). Even a half degree slip angle may change  $C_r$  by a significant amount [2].

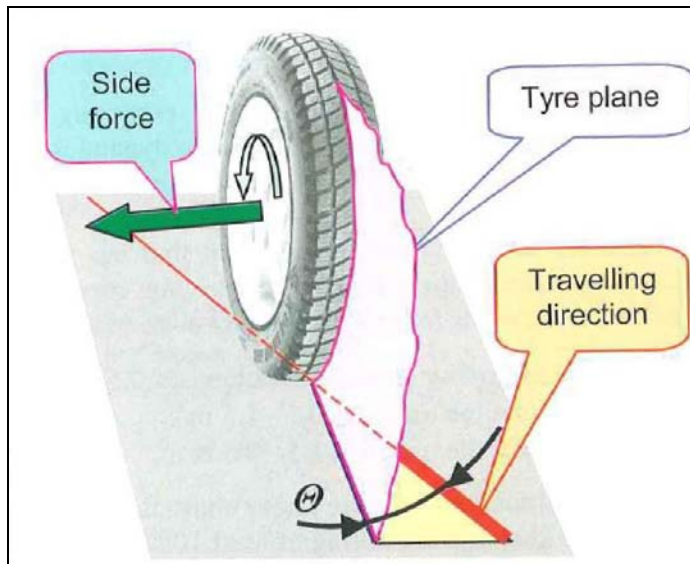


**Figure 9.24: Tyre moving in direction of red line [8]**

To simulate the effect of wheel adjustment and to see the effect of side forces measurements have been performed at various speeds (30, 50 and 70 km/h) by BRRC in the small bend at the east end of the test track.

All measurements were performed three times at each speed in direction west. The average values and standard deviation per speed are shown in Figure 9.25.

Due to a lack of wind shielding, measurements performed by BRRC at higher speed are found to be strongly influenced by the wind. The difference in  $C_r$  between 50 and 80 km/h is about 0.005 (see Figure 8.13). This is more than the difference that was measured for this test (see Figure 9.25) so it is believed by the authors that this test is not very reliable as the change in  $C_r$  might be caused by the effect of the wind only. The test should be performed with appropriate wind shielding on the trailer.

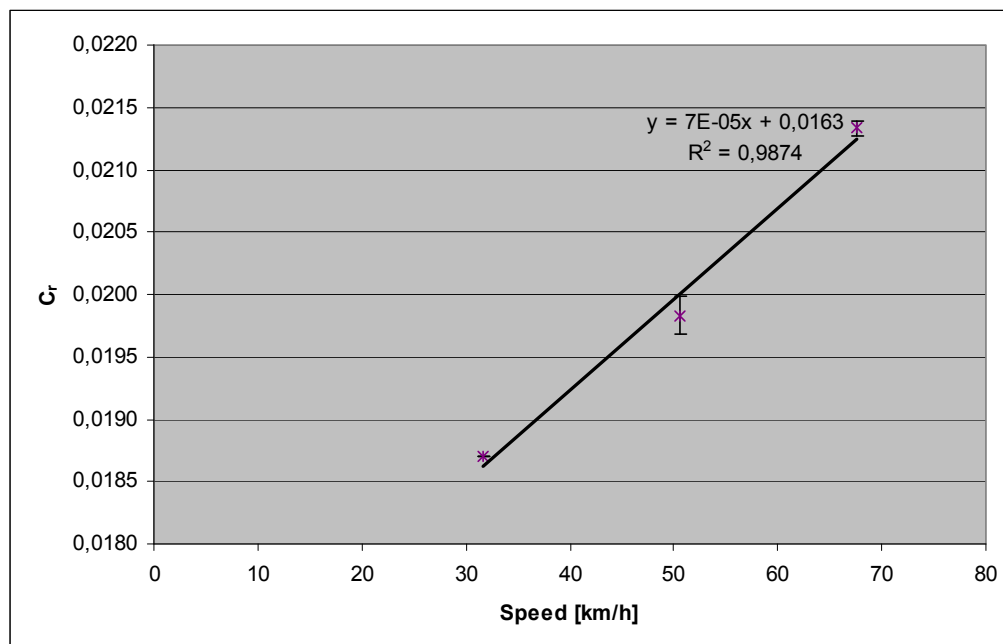


**Figure 9.25:  $C_r$  as a function of speed. measured by BRRC with tyre ES14/BRRC in small bend**

## **9.5 Cement concrete**

A very low rolling resistance was measured on cement concrete (0.009) while porous cement concrete (N) gave a very high rolling resistance (0.016). The  $C_r$  of cement concrete is even lower than on epoxy resin (L1) which is unexpected.

When considering texture spectra it can be seen that cement concrete has very low texture levels for most wavelengths (see Figure 4.3). Porous cement concrete has the highest texture levels for most wavelengths.

It is believed by the authors that something is wrong with this value for cement concrete so follow-up will be made.

## 10 Drum measurements

### 10.1 BAST

Drum measurements were performed with a tyre inflation after warm-up of 200 kPa and a tyre load of 4000 N to conform to the measurement conditions on site in Nantes.

Additionally a drum measurement was performed with the conditions specified by ISO 28580 [6] with ES16/BAST tyre at 80 km/h: steel drum, cold tyre inflation 210 kPa and tyre load 5890 N.

No temperature corrections were applied. See Figure 10.1 for measurement results.

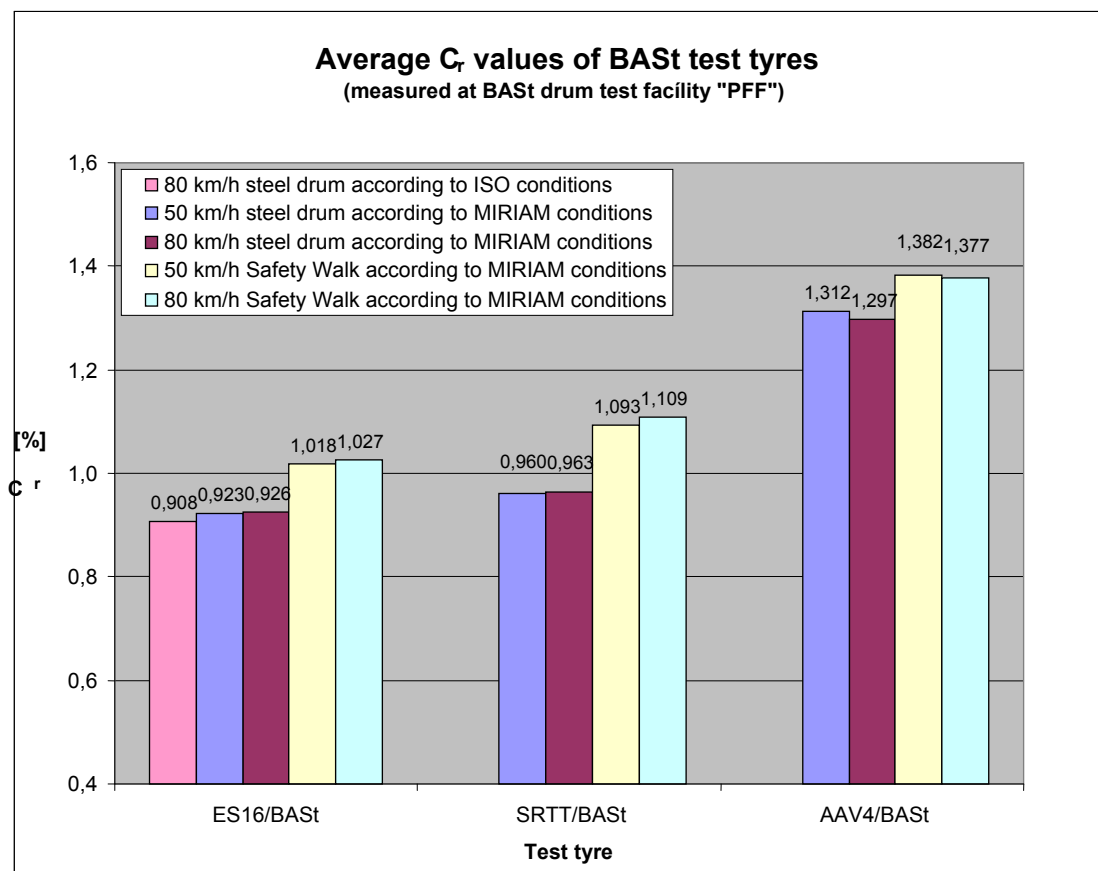


**Figure 10.1: Average  $C_r$  values of BAST test tyres measured in laboratory on drum BAST**

### 10.2 TUG

Drum measurements were performed with a tyre load of 4000 N to conform to the measurement conditions on-site in Nantes. Tyre inflation was 210 kPa. Drum results were corrected to correspond to a flat surface (drum curvature correction). The results were not corrected for temperature. Results are shown in Figure 10.2.

APS-4 is a rough-textured surface used in the TUG laboratory, imitating a surface dressing with 11 mm max. aggregate.



**Figure 10.2: Average  $C_r$  values of various test tyres measured in laboratory on drum TUG**

The  $C_r$  differences between test tyres of the same type vary between 0.0003 and 0.0028 (see Figure 10.3). Expressed in percentage this is 2.3 to 17.3 % (see Figure 10.4).

The largest difference is found between ES14/TUG and ES14/BRRc on APS-4 surface for all speeds (see Figure 10.3). Because of this, the comparison in section 8.4.2 should be interpreted with care.

Differences between test tyres are clearly speed and surface dependent.

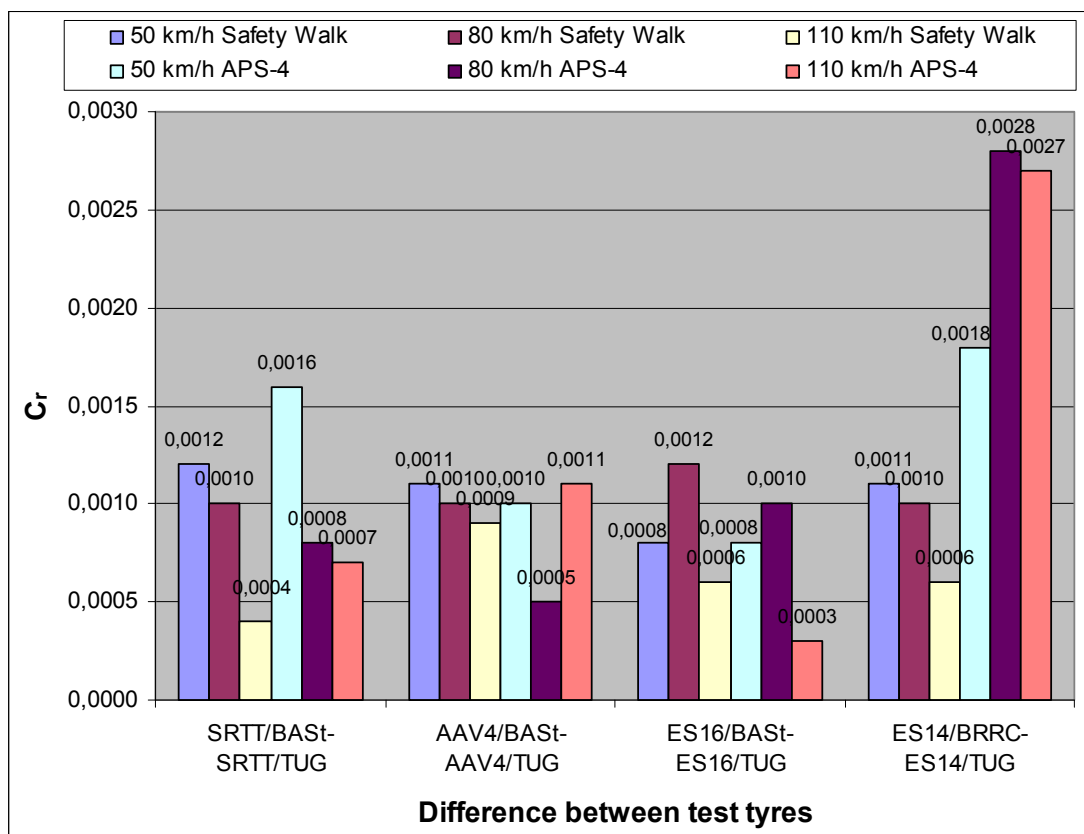


Figure 10.3:  $C_r$  difference (absolute values) between test tyres of the same type measured in laboratory on drum TUG

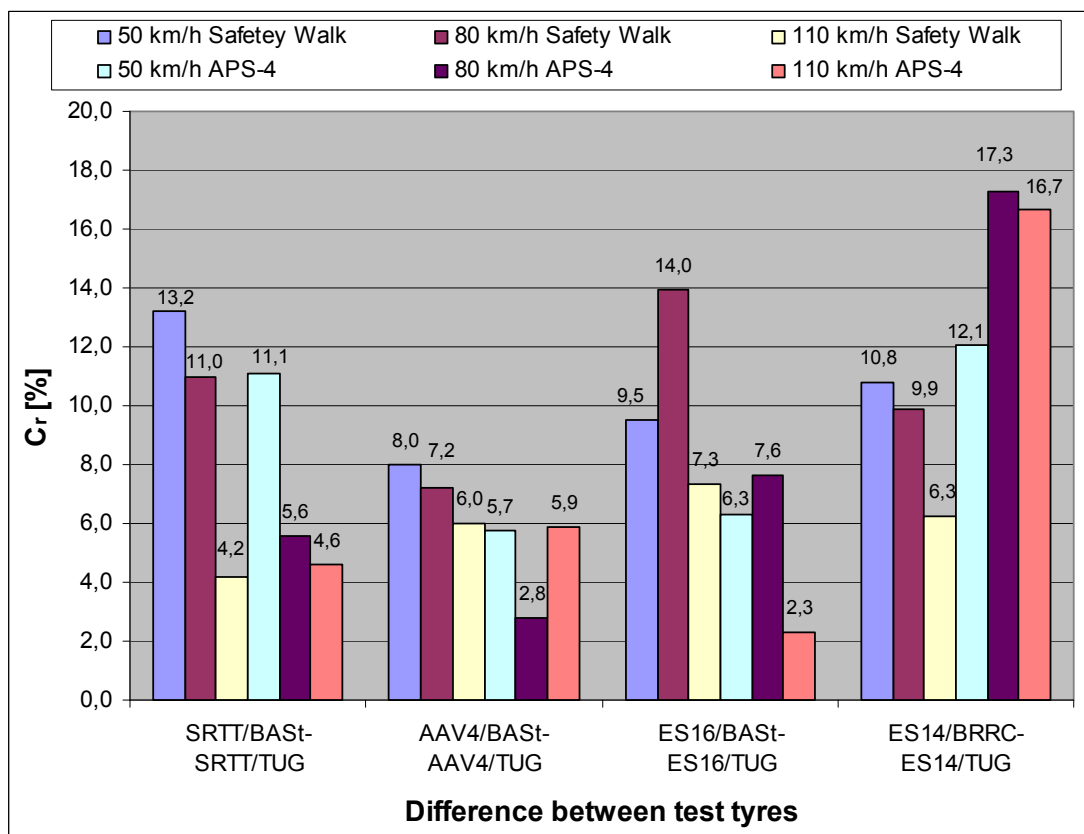
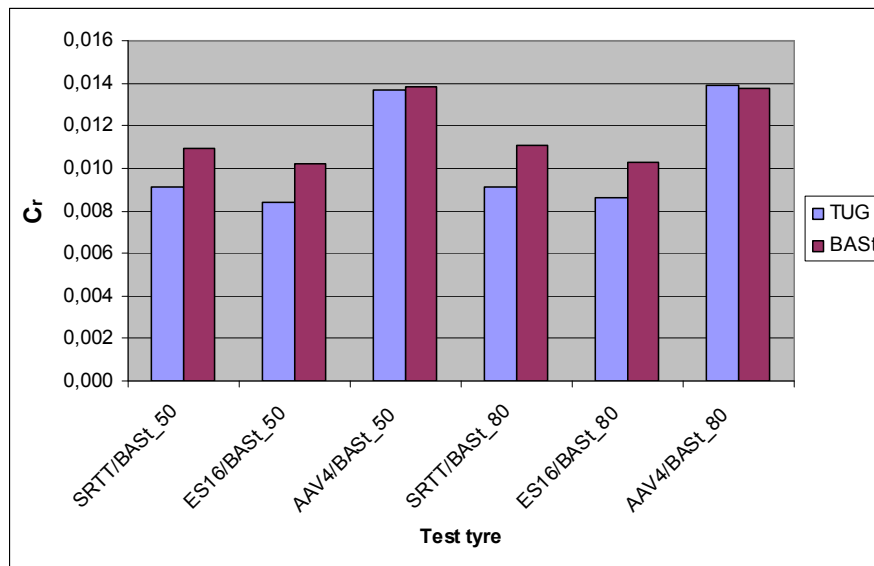


Figure 10.4:  $C_r$  difference in percentage between test tyres of the same type measured in laboratory on drum TUG

### 10.3 BAST – TUG

BAST and TUG performed drum measurements on the same tyres: AAV4/BAST. ES16/BAST and SRTT/BAST. The comparing graph is shown in Figure 10.5.



**Figure 10.5: Comparison drum measurements performed by TUG and BAST on BAST test tyres on Safety Walk**

Some differences may be due to:

- drum methods (outer drum BAST versus flat surface correction TUG)
- absence of temperature correction
- different tyre inflation (200 kPa BAST versus 210 kPa TUG)

### 10.4 Data from Michelin

Two test reports from Michelin were obtained of a SRTT and an ES16 tyre that came from other batches than the tyres used for MIRIAM.

A drum with diameter 1.7 m was used for the test but the results are expressed for a drum with diameter 2.0 m. Results were corrected for drum curvature to a 1.7 m drum and to flat (as TUG) according to ISO 28580 [6].

All results are specified in Table 10.1. Unfortunately they can not be compared with TUG because a different tyre load and pressure was used during the test. BAST however measured ES16/BAST in ISO conditions so this test may be used to get an impression of the value, although it was not performed with exactly the same tyre. The Michelin test result is similar to the BAST test result (see also Figure 10.1).

**Table 10.1: Results from measurements on a drum by Michelin**

Tyre	Speed	Tyre load	Tyre pressure	Ambient air temperature	Nominal design radius r	Drum diameter R1	C <sub>r_drum1</sub>	Drum diameter R2	C <sub>r_drum2</sub>	C <sub>R_flat</sub>
	[km/h]	[N]	[kPa]	[°C]	[m]	[m]		[m]		
SRTT/Michelin	80	5730	?	25	0.338	2.0	0.0087	1.7	0.0088	0.0080
ES16/Michelin	80	5890	210	25	0.338	2.0	0.0079	1.7	0.0080	0.0073



# 11 Texture influence on rolling resistance

## 11.1 Texture measurement devices

### 11.1.1 BRRRC

Texture was measured with the dynamic laser profilometer of BRRRC. The laser has a high sample frequency (78 kHz) and a small diameter laser beam (0.2 mm). The laser is mounted on a vehicle which allows performing measurements very efficiently. Vehicle speed may vary between 0 and 40 km/h when measuring in steps of 0.2 mm while theoretically a speed of 200 km/h may be used to measure in steps of 1 mm. The laser profilometer has a vertical measuring range of 64 mm and is a 16-bit system. The vertical resolution is thereby 1  $\mu\text{m}$ . It has a horizontal resolution of 0.2 mm.



Figure 11.1: BRRRC dynamic laser profilometer

### 11.1.2 IFSTTAR / CETE of Lyon

Texture was measured with the dynamic laser profilometer of CETE of Lyon (Department Laboratory of Lyon). The laser has a 62.5 kHz sample frequency and a laser beam of 0.55 mm diameter. The laser is mounted inside a passenger car C5, which allows performing measurements very efficiently. The laser makes the measurement on the right wheel tracks. Vehicle speed may vary between 0 and 120 km/h. A value of 50 km/h was chosen to allow measuring in steps of 0.6 mm. The laser profilometer has a vertical measuring range of 64 mm and is a 16-bit system. The vertical resolution is thereby 32  $\mu\text{m}$ .



Figure 11.2: CETE of Lyon dynamic laser profilometer

### 11.1.3 Comparison texture measurements performed by IFSTTAR and BRRC on test track

Texture measurements were verified by comparing measurements performed by BRRC and IFSTTAR. Two examples of comparisons are shown in Figure 11.3 and Figure 11.4.

The comparison between texture spectra in the megatexture range is fairly good. Due to the higher accuracy of the BRRC equipment, the values at the shorter wavelengths are more reliable. In general wavelengths higher than 6.3 mm can be considered as accurate for both laser profilometers.

Texture measurements performed by BRRC were used for all further analyses in this report as they were performed on the same days as the rolling resistance measurements.

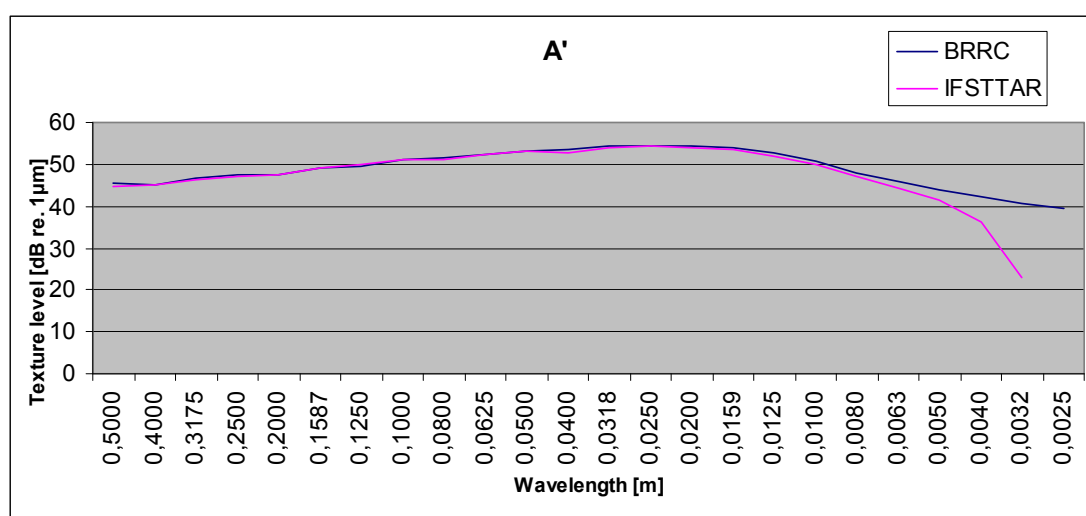


Figure 11.3: Comparison texture spectrum A' measured by BRRC and IFSTTAR

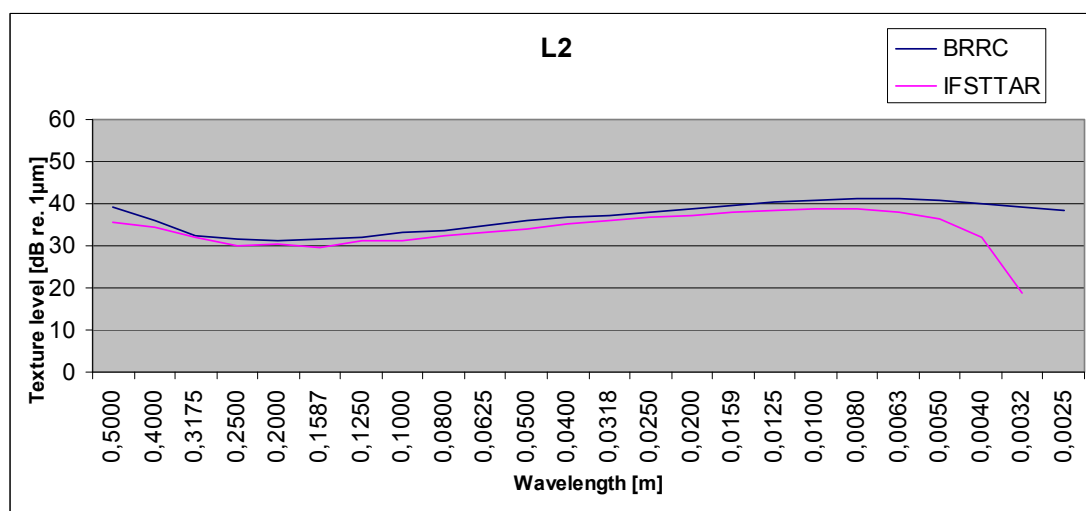
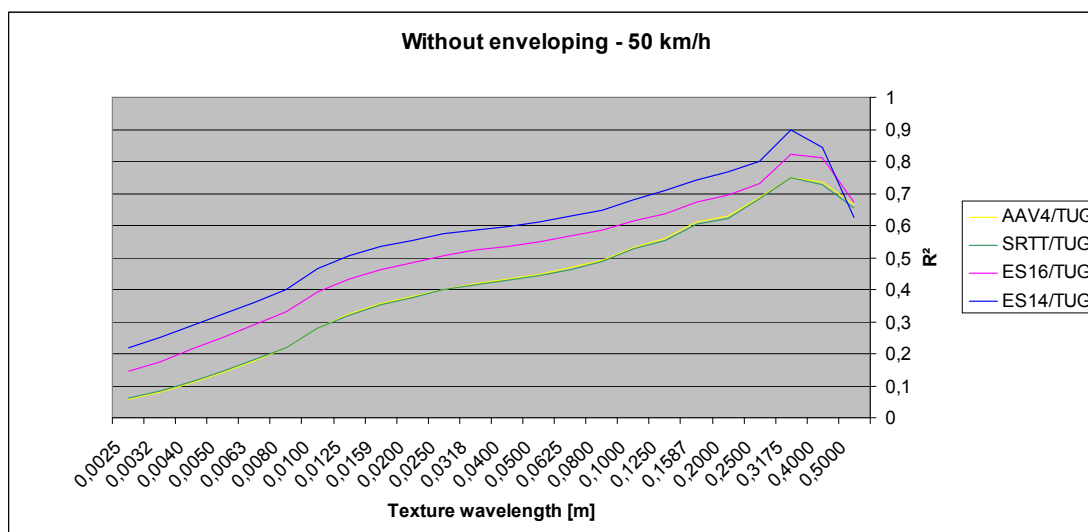


Figure 11.4: Comparison texture spectrum L2 measured by BRRC and IFSTTAR

## 11.2 One-third-octave band texture levels

The correlation between rolling resistance one-third-octave band texture levels (measured by BRRC) has been determined based on rolling resistance measurements performed by TUG on test sections A, A', F, E1, E2, M1, M2, L1 and L2. Test section C has been excluded because of the many irregularities of the surface. The correlation has been calculated for texture levels without and with enveloping.

### 11.2.1 Without enveloping



**Figure 11.5: Correlations at various texture wavelengths and tyres for measurements performed at 50 km/h – without enveloping**

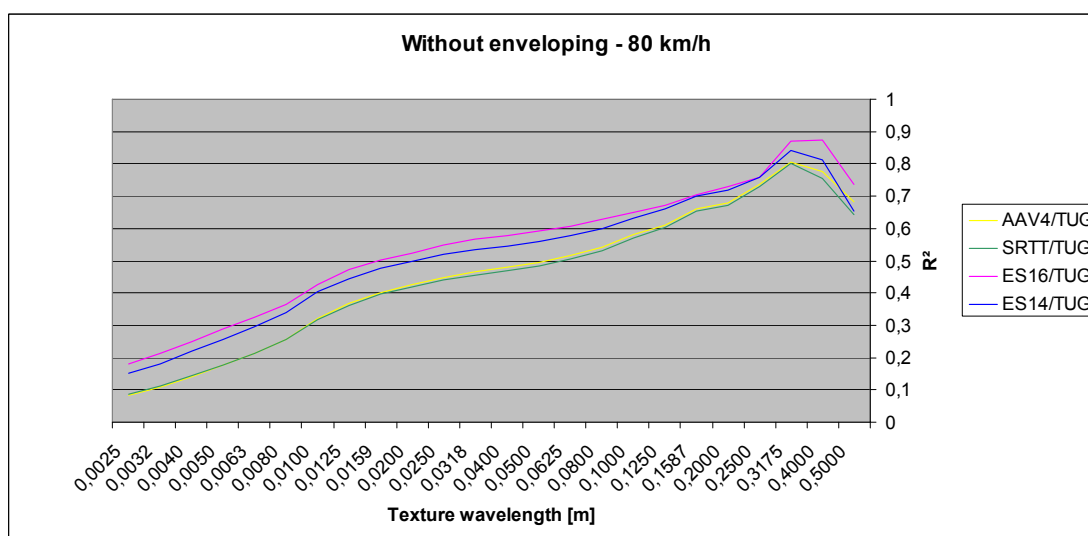


**Figure 11.6: Correlations at various texture wavelengths and tyres for measurements performed at 80 km/h – without enveloping**

Michelin Energy Saver tyres show the highest correlations for all texture wavelengths. The highest correlations for all tyres are found at the longest texture wavelengths. The results for SRTT/TUG and AAV4/TUG lie very close together.

## 11.2.2 With enveloping

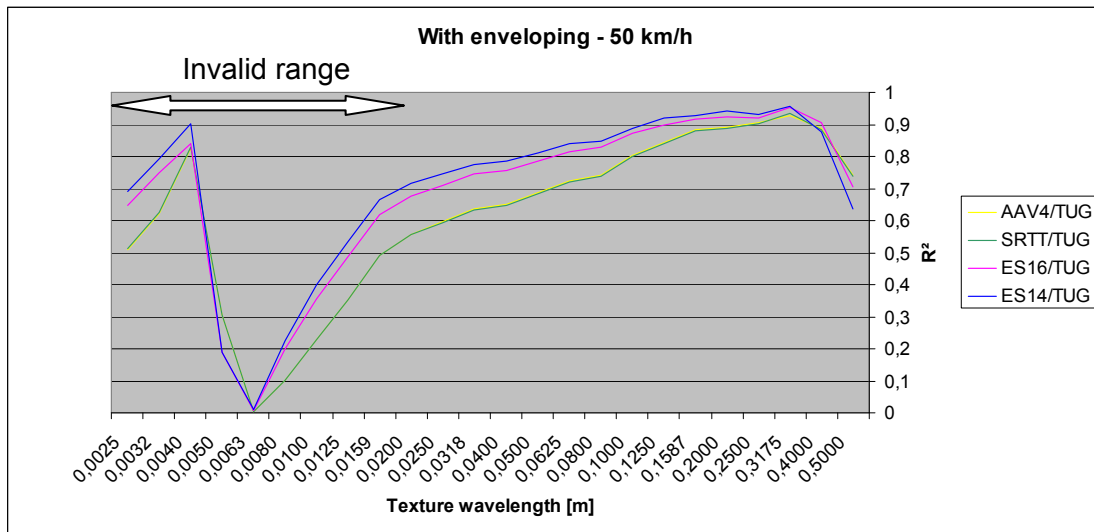


**Figure 11.7: Correlations at various texture wavelengths and tyres for measurements performed at 50 km/h – with enveloping**

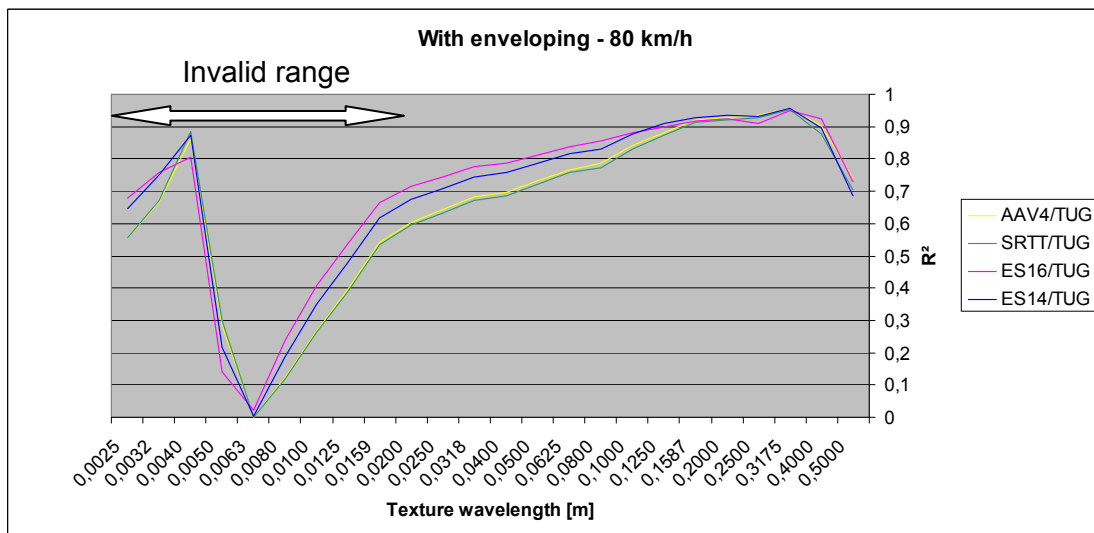


**Figure 11.8: Correlations at various texture wavelengths and tyres for measurements performed at 80 km/h – with enveloping**

Michelin Energy Saver tyres show the highest correlations for most texture wavelengths. The correlations are better than without enveloping. Results of SRTT/TUG and AAV4/TUG are situated very closely together. In the macrotexture range a peak can be noted at 0.0040 m. The highest correlations are found in the megatexture range.

Please do not pay any attention to the range at shorter wavelengths than 0.02 m since the strange shape of the curve with a peak and a dip there is entirely due to an artefact of the enveloping procedure. Only the part with wavelengths longer than approximately 0.02 m should be considered.

## 11.3 MPD

### 11.3.1 Without enveloping

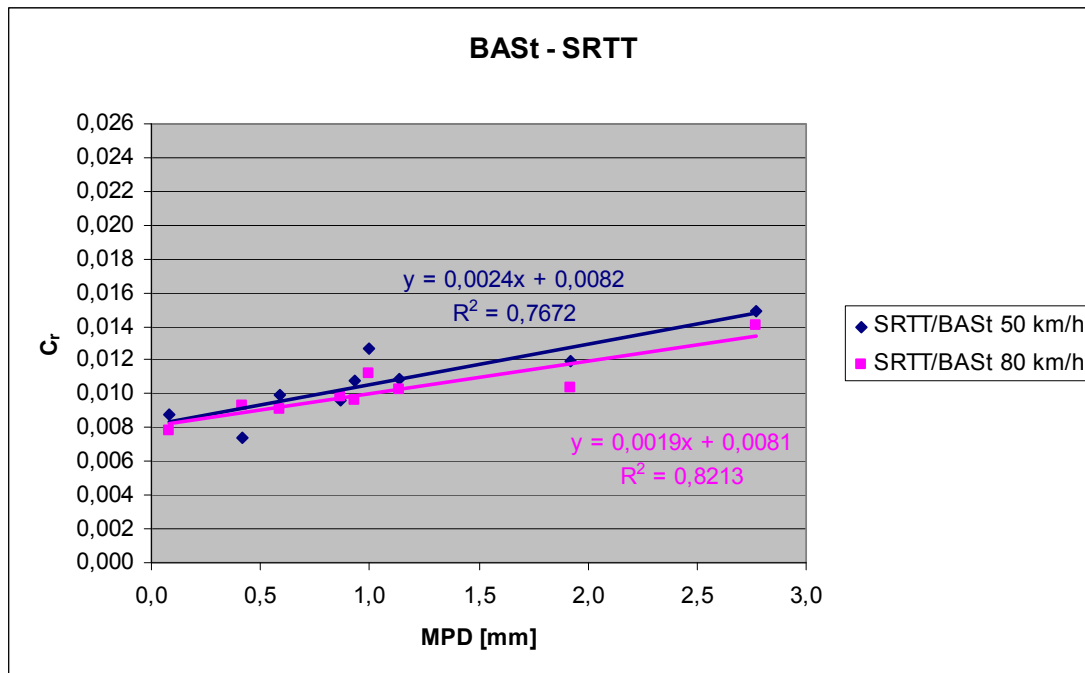


Figure 11.9: Correlation between MPD and  $C_r$  for SRTT/BASSt tyre (based on measurements performed by BASSt)

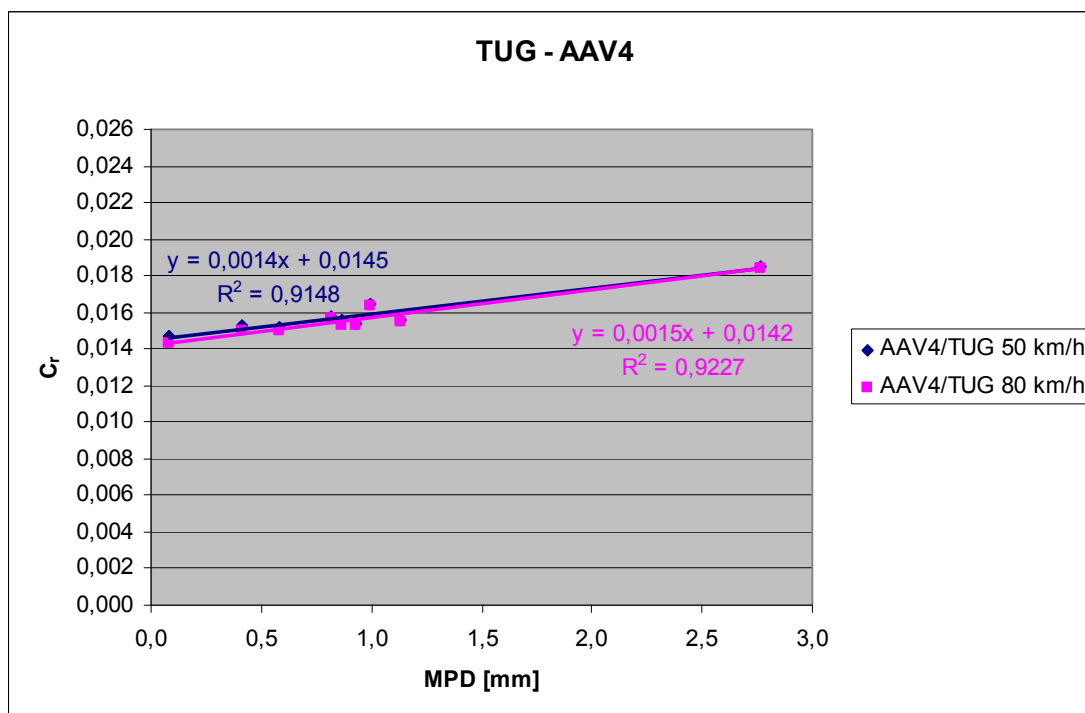


Figure 11.10: Correlation between MPD and  $C_r$  for AAV4/TUG tyre (based on measurements performed by TUG)

SRTT/BAS<sub>t</sub>\_BAS<sub>t</sub> and AAV4/TUG\_TUG have very good correlations between  $C_r$  and MPD. Table 11.1 and Table 11.2 summarize all results. Other graphs that are not shown in Figure 11.9 and Figure 11.10 can be found in Annex B.

**Table 11.1: Summarizing table of correlations between MPD and  $C_r$  for various tyres, institutes and speeds**

	BRRC		BAS <sub>t</sub>		TUG	
Speed [km/h]	50	80	50	80	50	80
AAV4	-	-	0.79	0.27	0.91	0.92
SRTT	-	-	0.77	0.82	0.91	0.92
ES16	-	-	0.87	0.40	0.88	0.81
ES14	0.43	0.19	-	-	0.88	0.90

**Table 11.2: Summarizing table of slope coefficients of regression lines of MPD as a unction of  $C_r$  for various tyres, institutes and speeds**

	BRRC		BAS <sub>t</sub>		TUG	
Speed [km/h]	50	80	50	80	50	80
AAV4	-	-	0.0014	0.0016	0.0014	0.0015
SRTT	-	-	0.0024	0.0019	0.0020	0.0020
ES16	-	-	0.0017	0.0010	0.0017	0.0018
ES14	0.0017	0.0014	-	-	0.0016	0.0015

### 11.3.2 With enveloping

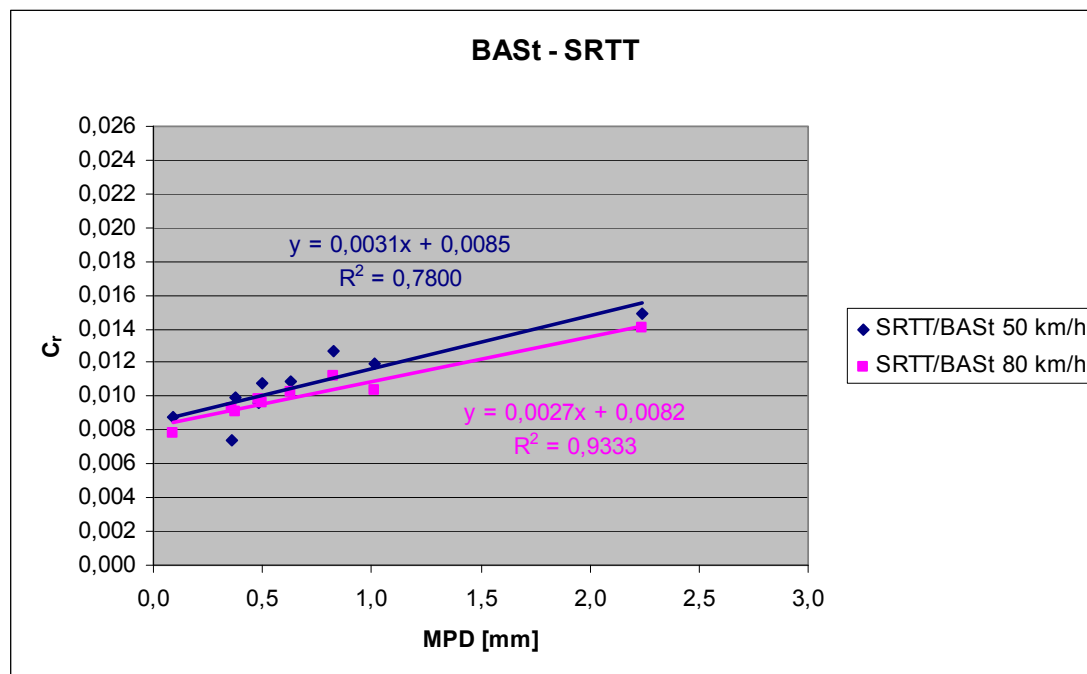


**Figure 11.11: Correlation between MPD and  $C_r$  for SRTT/BAS<sub>t</sub> tyre (based on measurements performed by BAS<sub>t</sub>) – with enveloping**

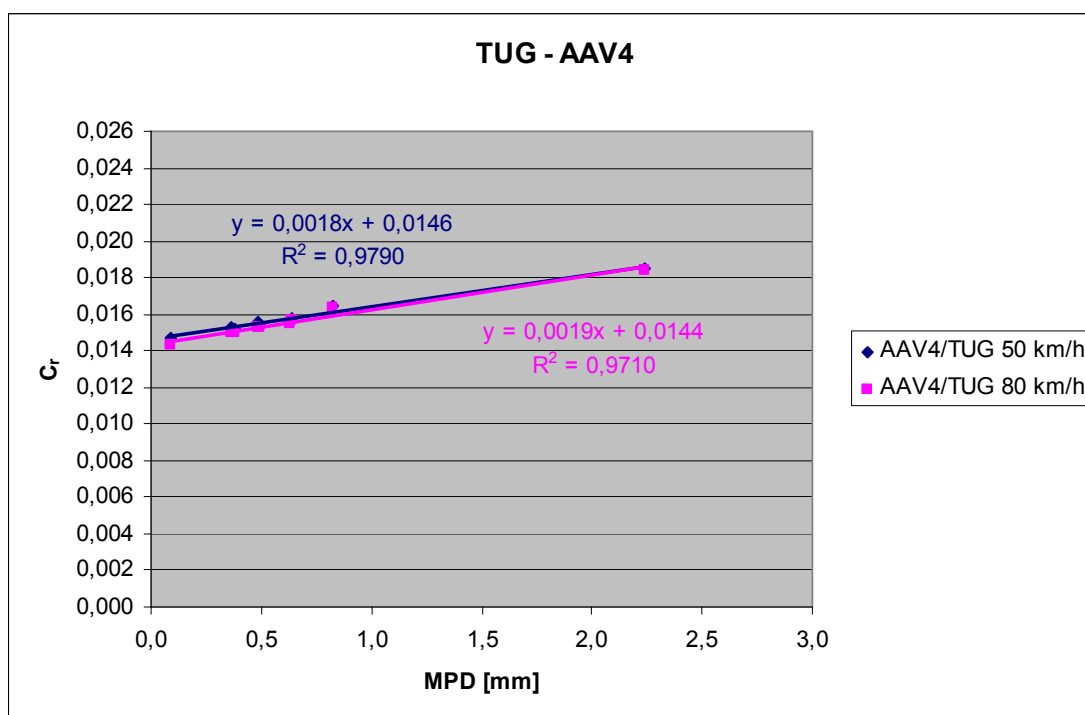


**Figure 11.12: Correlation between MPD and  $C_r$  for AAV4/TUG tyre (based on measurements performed by TUG) – with enveloping**

SRTT/BAS<sub>t</sub>\_BAS<sub>t</sub> and AAV4/TUG\_TUG have even better correlations between  $C_r$  and MPD with enveloping. Table 11.3 and Table 11.4 summarize all results. Other graphs that are not shown in Figure 11.11 and Figure 11.12 can be found in Annex C. Excellent correlations must be a sign that the measurements are very accurate.

**Table 11.3: Summarizing table of correlations between MPD and  $C_r$  for various tyres, institutes and speeds – with enveloping**

	BRRC		BAS <sub>t</sub>		TUG	
Speed [km/h]	50	80	50	80	50	80
AAV4	-	-	0.91	0.29	0.98	0.97
SRTT	-	-	0.70	0.93	0.98	0.97
ES16	-	-	0.82	0.60	0.92	0.84
ES14	0.33	0.12	-	-	0.87	0.93

**Table 11.4: Summarizing table of slope coefficients of regression lines of MPD as a function of  $C_r$  for various tyres, institutes and speeds – with enveloping**

	BRRC		BAS <sub>t</sub>		TUG	
Speed [km/h]	50	80	50	80	50	80
AAV4	-	-	0.0020	0.0032	0.0018	0.0019
SRTT	-	-	0.0031	0.0027	0.0025	0.0025
ES16	-	-	0.0021	0.0023	0.0021	0.0022
ES14	0.0020	0.0015	-	-	0.0020	0.0018

## 11.4 Band-limited macrotexture and megatexture levels

Broad band mega- and macrotexture levels LMe and LMa [1], are defined as follows:

$$LMe = 10 \log \sum_i 10^{L_i/10}$$

with  $L_i$  the level of the  $i$ -th one-third-octave band in the megatexture range of the texture scale. An analogue definition goes for LMa. Megatexture range is from 63 mm to 500 mm of centre wavelengths. Macrotexture range is from 0.63 mm to 50 mm of centre wavelengths.

The correlations of  $C_r$  with LMa and LMe have been calculated for the different tyre/trailer combinations. The following graphs show their correlation with the rolling resistance coefficient.

### 11.4.1 Macrotexture

#### 11.4.1.1 Without enveloping

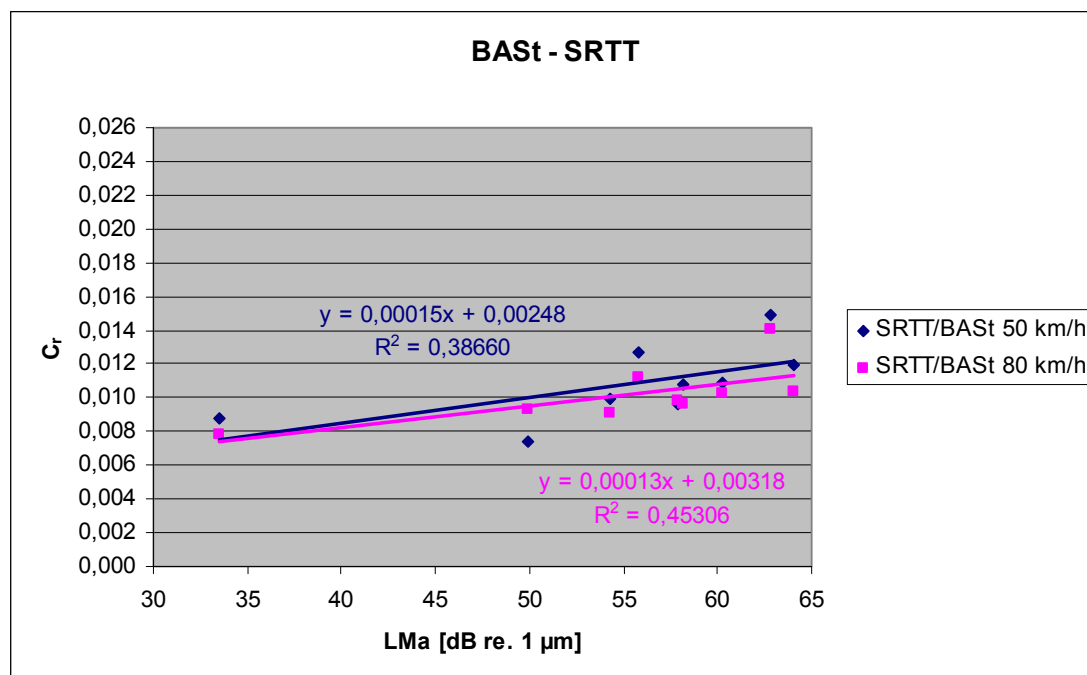
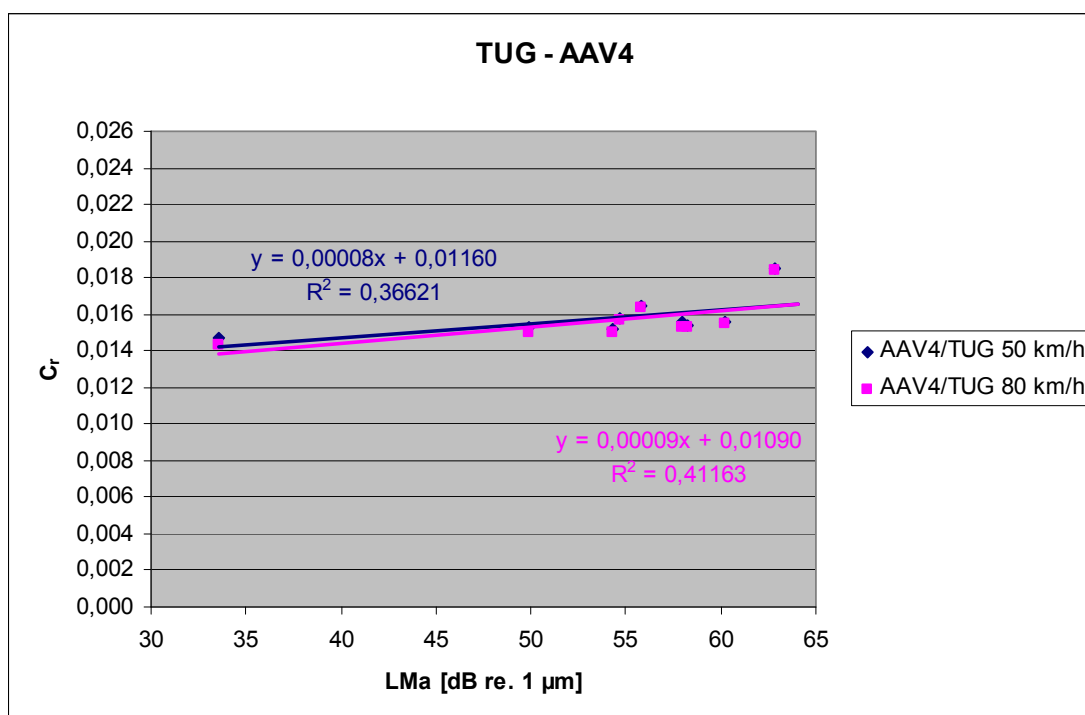


Figure 11.13: Correlation between macrotexture and  $C_r$  for SRTT/BASSt tyre (based on measurements performed by BAST)





**Figure 11.14: Correlation between macrotexture and  $C_r$  for AAV4/TUG tyre (based on measurements performed by TUG)**

SRTT/BAS<sub>t</sub>\_BAS<sub>t</sub> and AAV4/TUG\_TUG give rather low correlations between  $C_r$  and macrotexture. Table 11.5 and Table 11.6 summarize all results. Other graphs that are not shown in Figure 11.13 and Figure 11.14 can be found in Annex D.

**Table 11.5: Summarizing table of correlations between macrotexture and  $C_r$  for various tyres, institutes and speeds**

	BRRC		BAS <sub>t</sub>		TUG	
Speed [km/h]	50	80	50	80	50	80
AAV4	-	-	0.33	0.08	0.37	0.41
SRTT	-	-	0.39	0.45	0.37	0.41
ES16	-	-	0.65	0.54	0.48	0.51
ES14	0.62	0.35	-	-	0.55	0.49

**Table 11.6: Summarizing table of slope coefficients of regression lines of  $LMa$  as a unction of  $C_r$  for various tyres, institutes and speeds**

	BRRC		BAS <sub>t</sub>		TUG	
Speed [km/h]	50	80	50	80	50	80
AAV4	-	-	0.00008	0.00005	0.00008	0.00009
SRTT	-	-	0.00015	0.00013	0.00011	0.00012
ES16	-	-	0.00013	0.00007	0.00011	0.00012
ES14	0.00019	0.00017	-	-	0.00011	0.00010

### 11.4.1.2 With enveloping

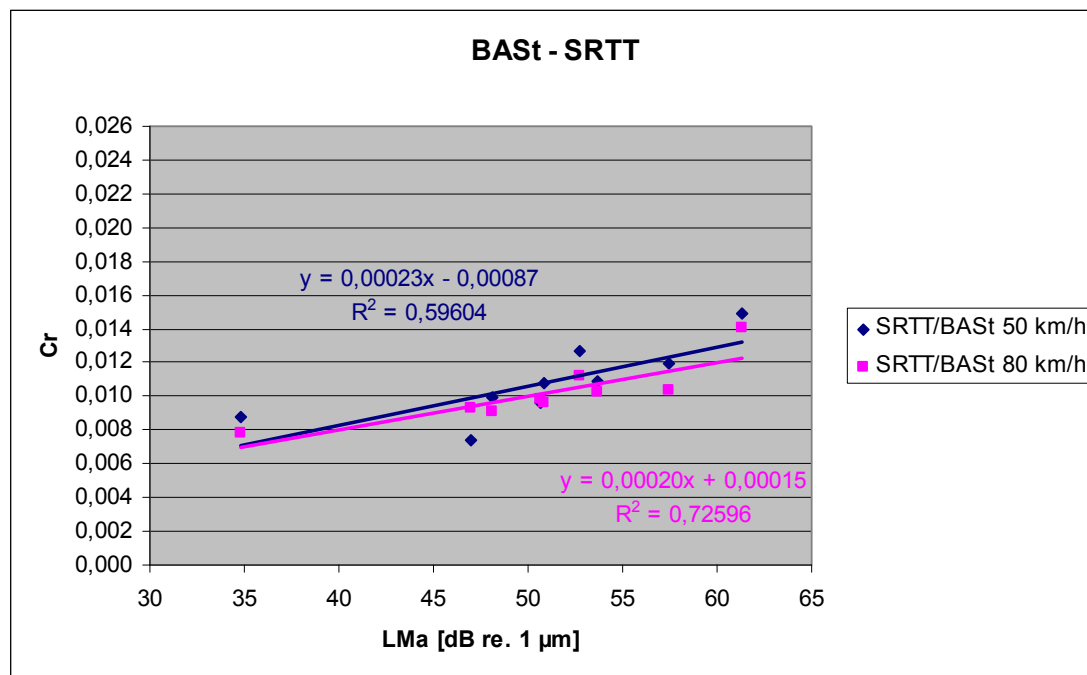


**Figure 11.15: Correlation between macrotexture and  $C_r$  for SRTT/BASt tyre (based on measurements performed by BASt) – with enveloping**

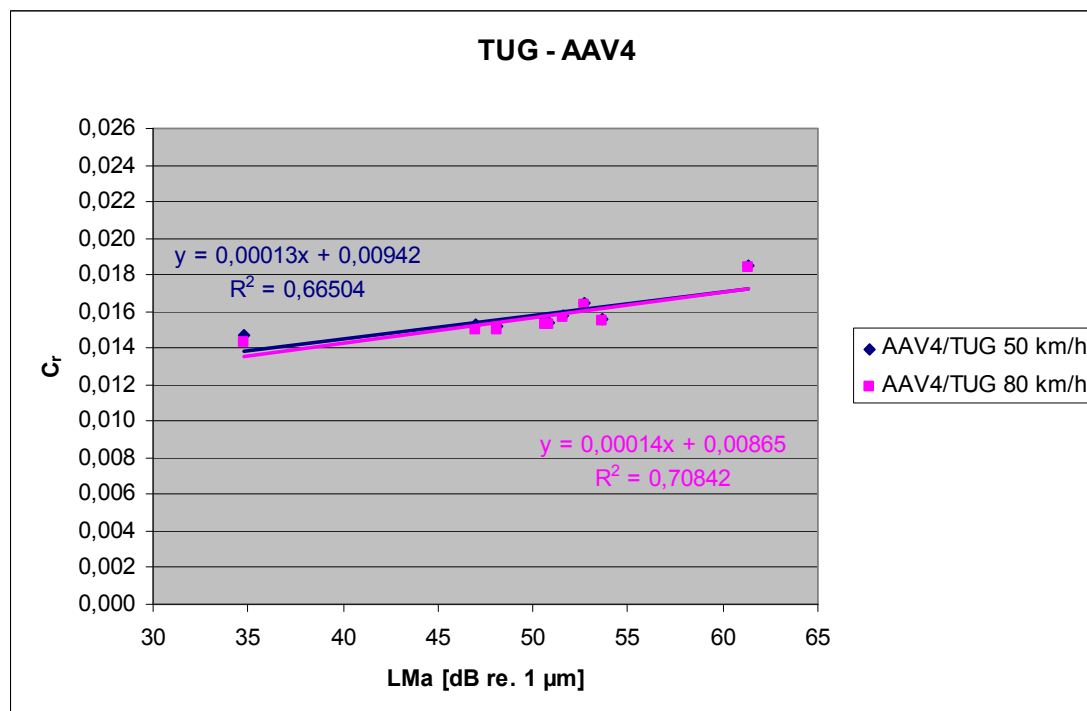


**Figure 11.16: Correlation between macrotexture and  $C_r$  for AAV4/TUG tyre (based on measurements performed by TUG) – with enveloping**

SRTT/BASt\_BASt and AAV4/TUG\_TUG have good correlations between  $C_r$  and macrotexture, much better than without enveloping. Table 11.7 and Table 11.8

summarize all results. Other graphs that are not shown in Figure 11.15 and Figure 11.16 can be found in Annex E.

**Table 11.7: Summarizing table of correlations between macrotexture and  $C_r$  for various tyres, institutes and speeds – with enveloping**

	BRRC		BAST		TUG	
Speed [km/h]	50	80	50	80	50	80
AAV4	-	-	0.60	0.10	0.67	0.71
SRTT	-	-	0.60	0.73	0.66	0.70
ES16	-	-	0.80	0.61	0.77	0.79
ES14	0.57	0.28	-	-	0.80	0.77

**Table 11.8: Summarizing table of slope coefficients of regression lines of  $L_{Ma}$  as a unction of  $C_r$  for various tyres, institutes and speeds – with enveloping**

	BRRC		BAST		TUG	
Speed [km/h]	50	80	50	80	50	80
AAV4	-	-	0.00014	0.00008	0.00013	0.00014
SRTT	-	-	0.00023	0.00020	0.00018	0.00019
ES16	-	-	0.00018	0.00010	0.00017	0.00019
ES14	0.00022	0.00018	-	-	0.00017	0.00015

## 11.4.2 Megatexture

### 11.4.2.1 Without enveloping

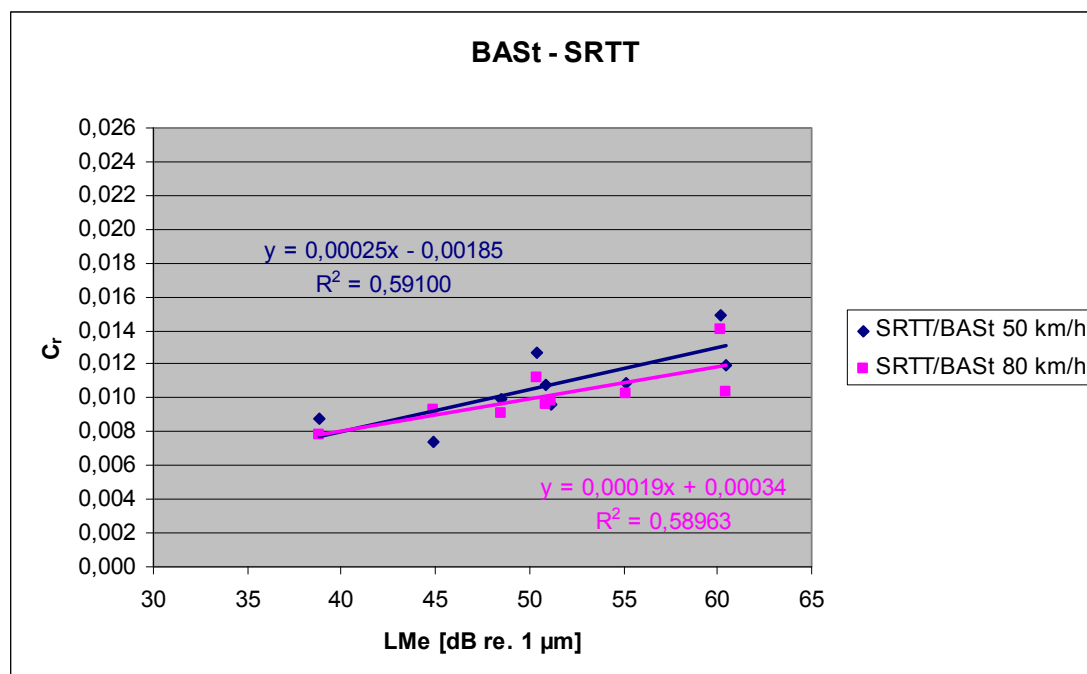


**Figure 11.17: Correlation between megatexture and  $C_r$  for SRTT/BAST tyre (based on measurements performed by BAST)**

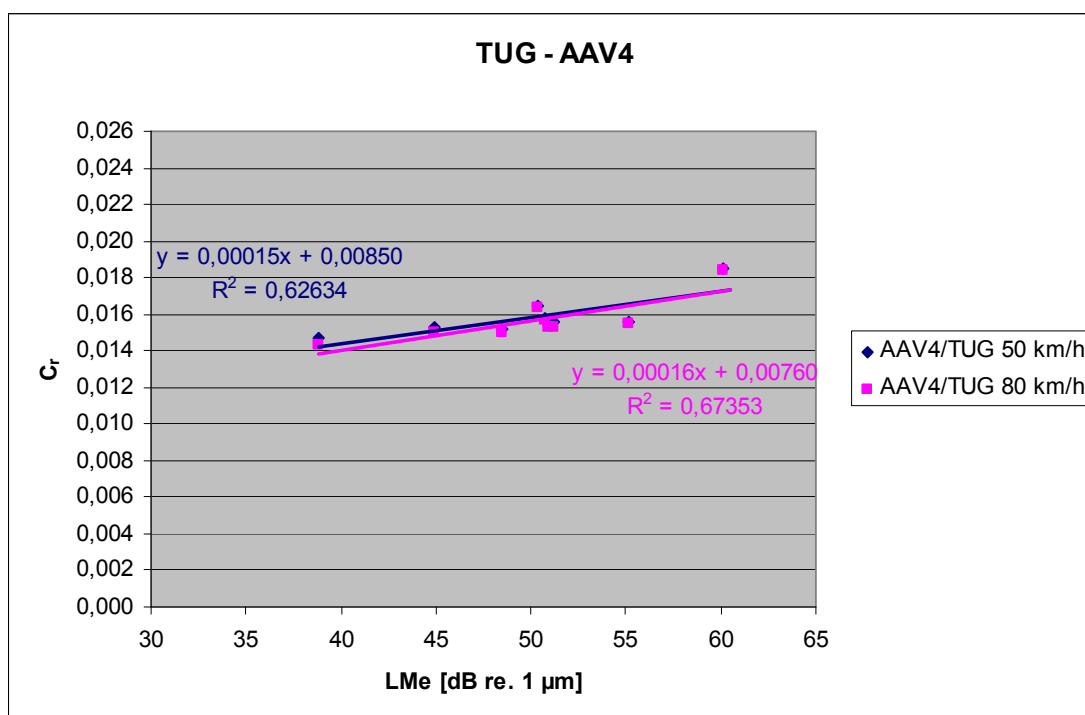


**Figure 11.18: Correlation between megatexture and  $C_r$  for AAV4/TUG tyre (based on measurements performed by TUG)**

SRTT/BAS<sub>t</sub>\_BAS<sub>T</sub> and AAV4/TUG\_TUG have rather good correlations between  $C_r$  and megatexture. Table 11.9 and Table 11.10 summarize all results. Other graphs that are not shown in Figure 11.17 and Figure 11.18 can be found in Annex F.

**Table 11.9: Summarizing table of correlations between megatexture and  $C_r$  for various tyres, institutes and speeds**

	BRRC		BAS <sub>t</sub>		TUG	
Speed [km/h]	50	80	50	80	50	80
AAV4	-	-	0.53	0.17	0.63	0.67
SRTT	-	-	0.59	0.59	0.62	0.66
ES16	-	-	0.79	0.43	0.69	0.72
ES14	0.56	0.30	-	-	0.76	0.71

**Table 11.10: Summarizing table of slope coefficients of regression lines of LMe as a function of  $C_r$  for various tyres, institutes and speeds**

	BRRC		BAS <sub>t</sub>		TUG	
Speed [km/h]	50	80	50	80	50	80
AAV4	-	-	0.00014	0.00011	0.00015	0.00016
SRTT	-	-	0.00025	0.00019	0.00020	0.00022
ES16	-	-	0.00019	0.00009	0.00019	0.00021
ES14	0.00024	0.00021	-	-	0.00019	0.00017

### 11.4.2.2 With enveloping

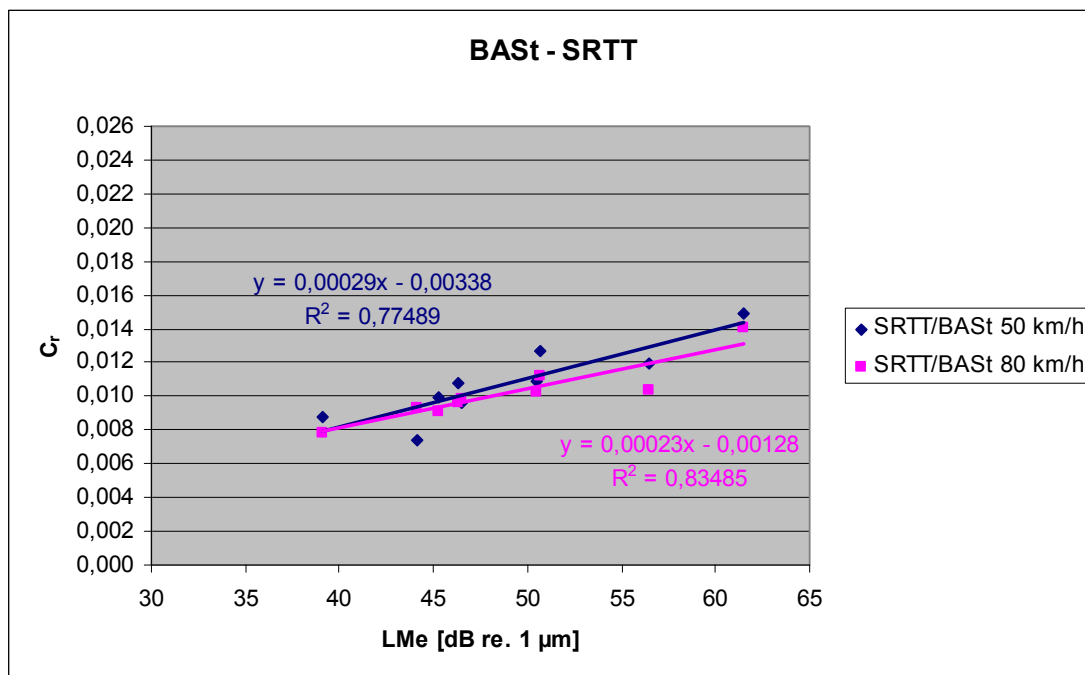


**Figure 11.19: Correlation between megatexture and  $C_r$  for SRTT/BASt tyre (based on measurements performed by BASt) – with enveloping**

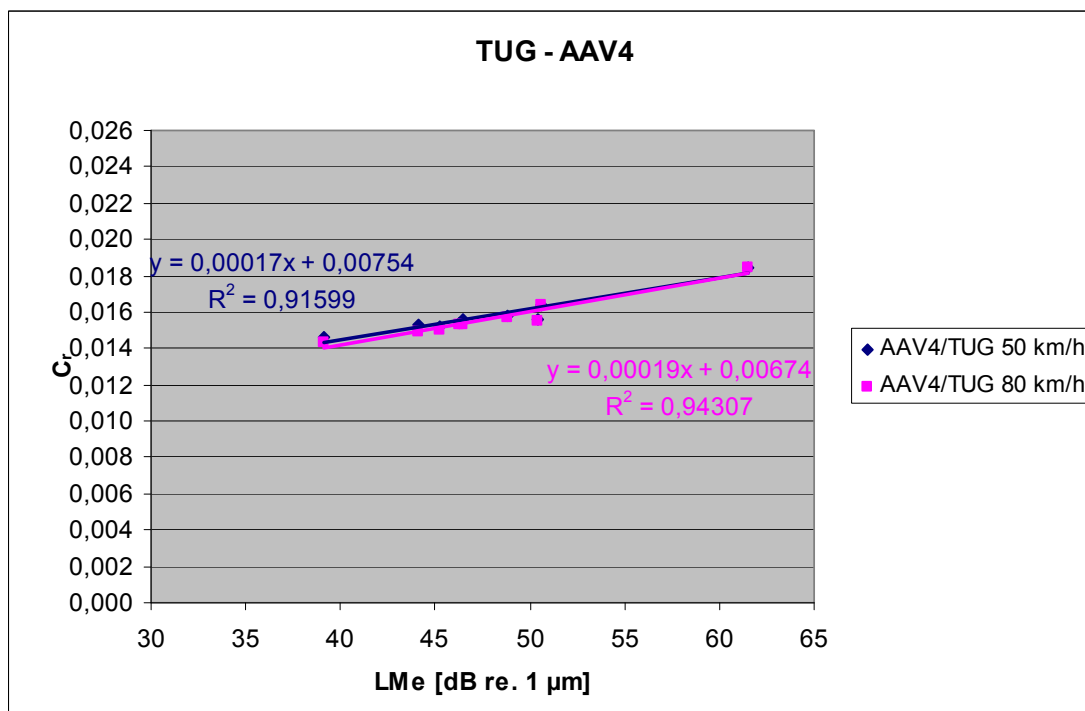


**Figure 11.20: Correlation between megatexture and  $C_r$  for AAV4/TUG tyre (based on measurements performed by TUG) – with enveloping**

SRTT/BASt\_BASt and AAV4/TUG\_TUG have very good correlations between  $C_r$  and megatexture, even better than without enveloping. Table 11.11 and Table 11.12 summarize all results. Other graphs that are not shown in Figure 11.19 and Figure 11.20 can be found in Annex G.

**Table 11.11: Summarizing table of correlations between megatexture and  $C_r$  for various tyres, institutes and speeds – with enveloping**

	<b>BRRC</b>		<b>BAS<sub>t</sub></b>		<b>TUG</b>	
<b>Speed [km/h]</b>	<b>50</b>	<b>80</b>	<b>50</b>	<b>80</b>	<b>50</b>	<b>80</b>
<b>AAV4</b>	-	-	0.80	0.22	0.92	0.94
<b>SRTT</b>	-	-	0.77	0.83	0.91	0.93
<b>ES16</b>	-	-	0.84	0.50	0.94	0.93
<b>ES14</b>	0.44	0.20	-	-	0.94	0.94

**Table 11.12: Summarizing table of slope coefficients of regression lines of LMe as a function of  $C_r$  for various tyres, institutes and speeds – with enveloping**

	<b>BRRC</b>		<b>BAS<sub>t</sub></b>		<b>TUG</b>	
<b>Speed [km/h]</b>	<b>50</b>	<b>80</b>	<b>50</b>	<b>80</b>	<b>50</b>	<b>80</b>
<b>AAV4</b>	-	-	0.00017	0.00016	0.00017	0.00019
<b>SRTT</b>	-	-	0.00029	0.00023	0.00024	0.00025
<b>ES16</b>	-	-	0.00020	0.00012	0.00022	0.00023
<b>ES14</b>	0.00021	0.00017	-	-	0.00021	0.00019

## **11.5 MPD, macrotexture and megatexture**

### **11.5.1 Correlations**

#### **11.5.1.1 Without enveloping**

A summary of all correlations with MPD, macrotexture and megatexture can be found in Figure 11.21. A better correlation is found with megatexture than with macrotexture. The best correlation is obtained with MPD. This may be related with the effects of positive/negative texture.

The worst correlation is found for AAV4/BAS<sub>t</sub> at 80 km/h. This is probably due to the “strange” measurement results for this tyre/speed which are not in line with the others.

ES14/BRRC also has a low correlation which is probably due to the lack of wind shielding and the high influence of wind at a speed of 80 km/h. Also the outlier M2 causes a low correlation. If this outlier would have been discarded, correlations for BRRC would be between 0.60 and 0.85.

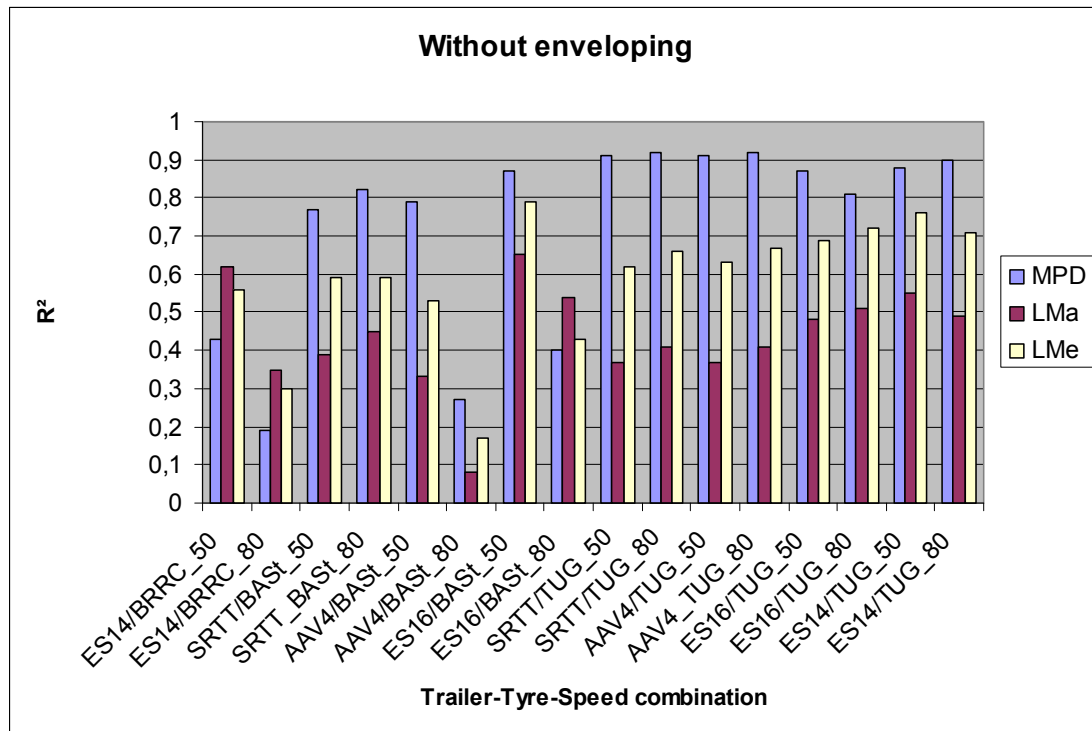


**Figure 11.21: Summarizing graph correlations MPD, LMa and LMe for all tyres and speeds**

### 11.5.1.2 With enveloping

A summary of all correlations with MPD, macrotexture and megatexture with enveloping can be found in Figure 11.22. A better correlation is found with megatexture than with macrotexture. MPD and megatexture show comparable correlations, which are excellent. By using enveloping the effects of positive/negative texture are eliminated.

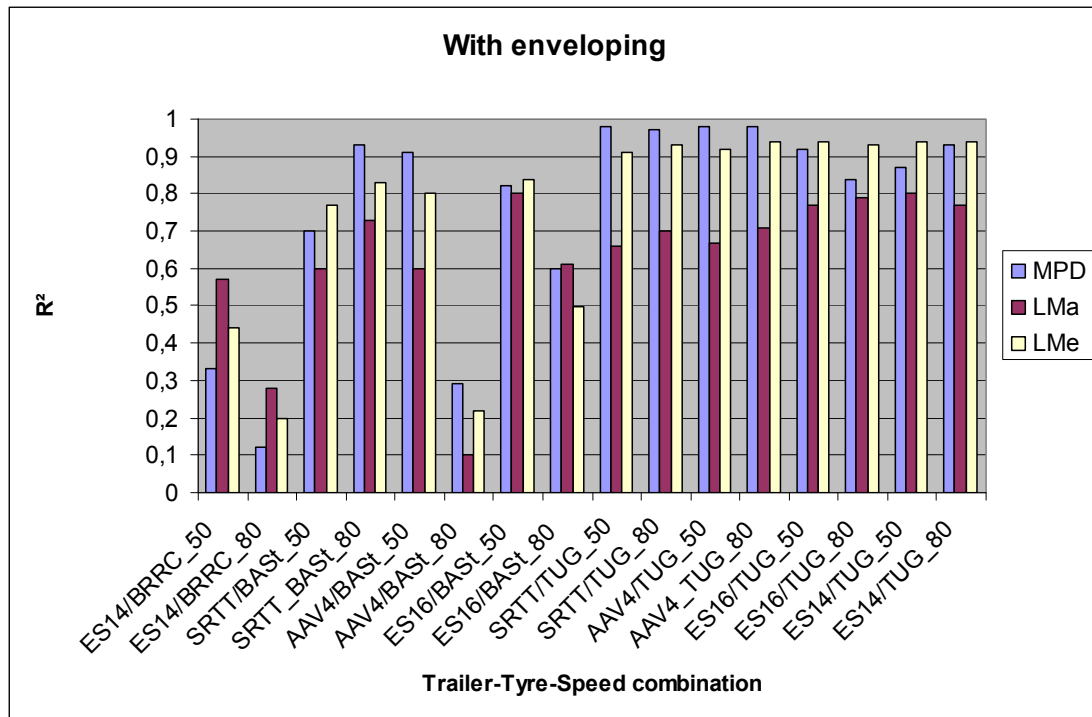


**Figure 11.22: Summarizing graph correlations MPD, LMa and LMe for all tyres and speeds – with enveloping**

## 11.5.2 Slope coefficients

To eliminate uncertainties, only the measurements of section 11.5.1 with correlations equal to or higher than 0.7 are considered in this section 11.5.2.

### 11.5.2.1 Without enveloping

All slope coefficients of regression lines found in sections 11.3 - 11.4 for analyses without enveloping and with correlations equal to or higher than 0.7, are summarized in Figure 11.23 and Figure 11.24.



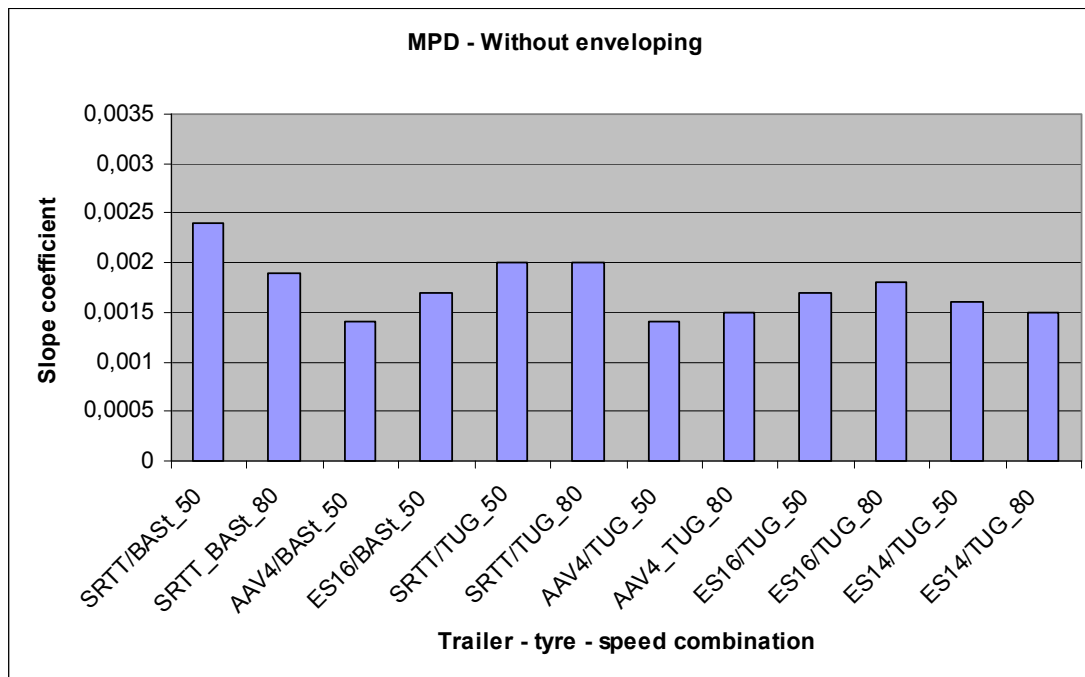


**Figure 11.23: Summarizing graph slope coefficients MPD for various tyres and speeds**

In Figure 11.24 for some trailer – tyre – speed combinations no values are given because of lack of data with high correlations.

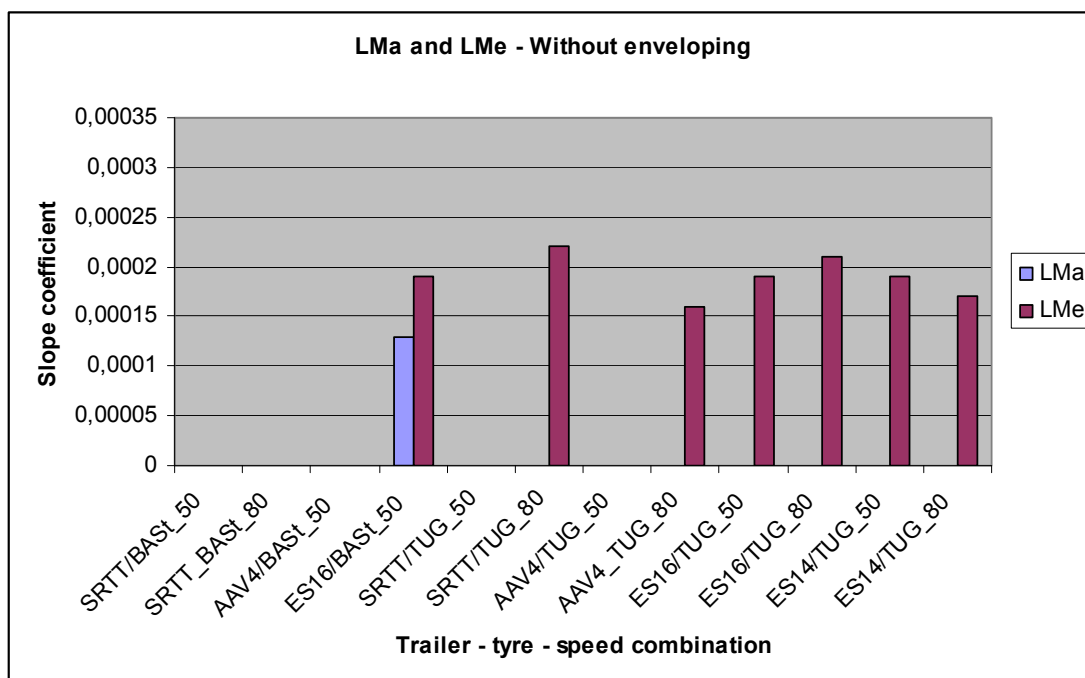


**Figure 11.24: Slope coefficients LMA and LMe for various tyres and speeds**

Based on Figure 11.25 and Figure 11.26 one can state that the slope coefficients without enveloping are independent of speed or institute but possibly dependent of tyre type. MPD, LMa and LMe have an overall average slope coefficient of 0.00174, 0.00013 and 0.00019 respectively.

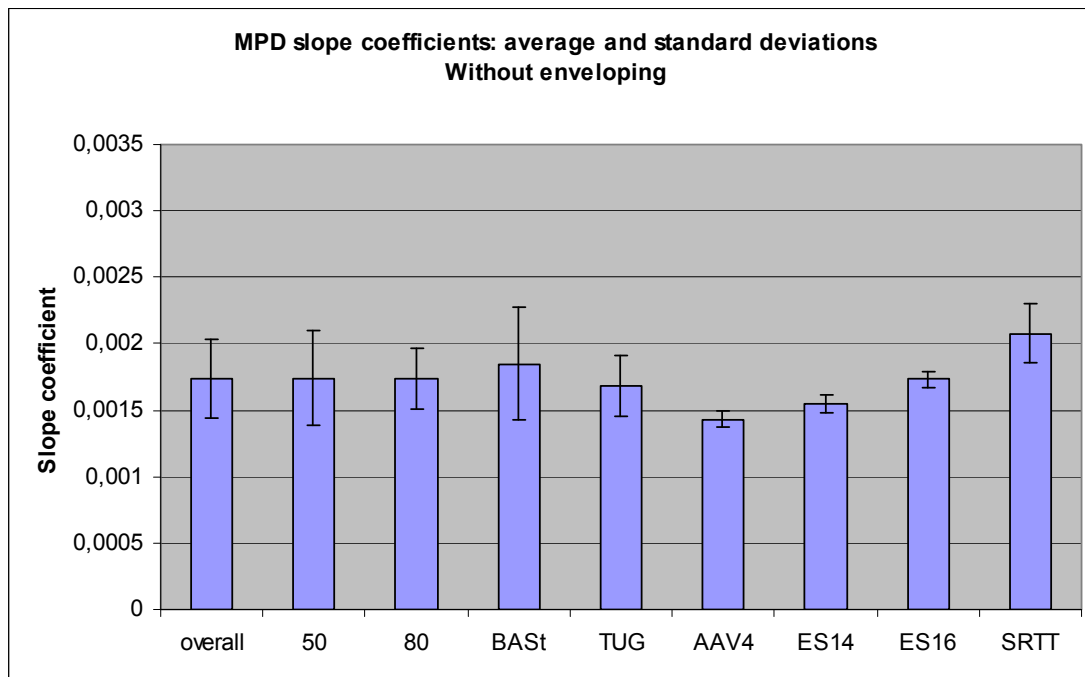


**Figure 11.25: Average values and standard deviations MPD per category (overall, speed, institute, tyre)**

In Figure 11.26 for some categories no standard deviations are given because of lack of data with high correlations.

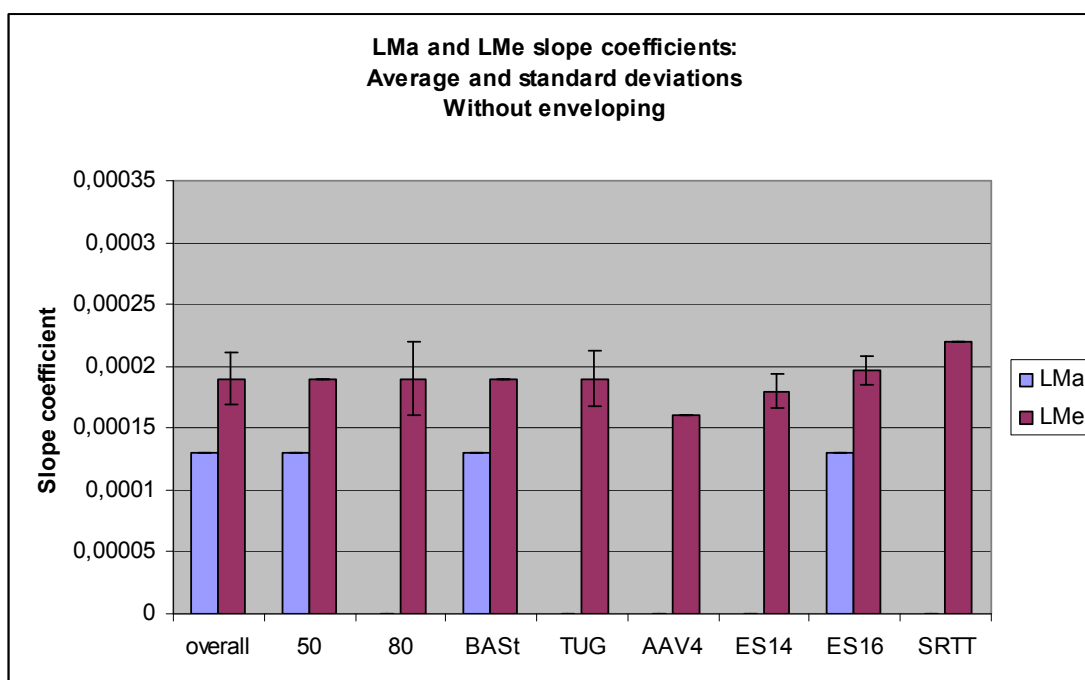


**Figure 11.26: Average values and standard deviations LMA, LMe per category (overall, speed, institute, tyre)**

### 11.5.2.2 With enveloping

All slope coefficients of regression lines found in section 11.3 - 11.4 for analyses with enveloping and with correlations equal to or higher than 0.7, are summarized in Figure 11.27 and Figure 11.28. All slope coefficients are larger with enveloping than without enveloping.

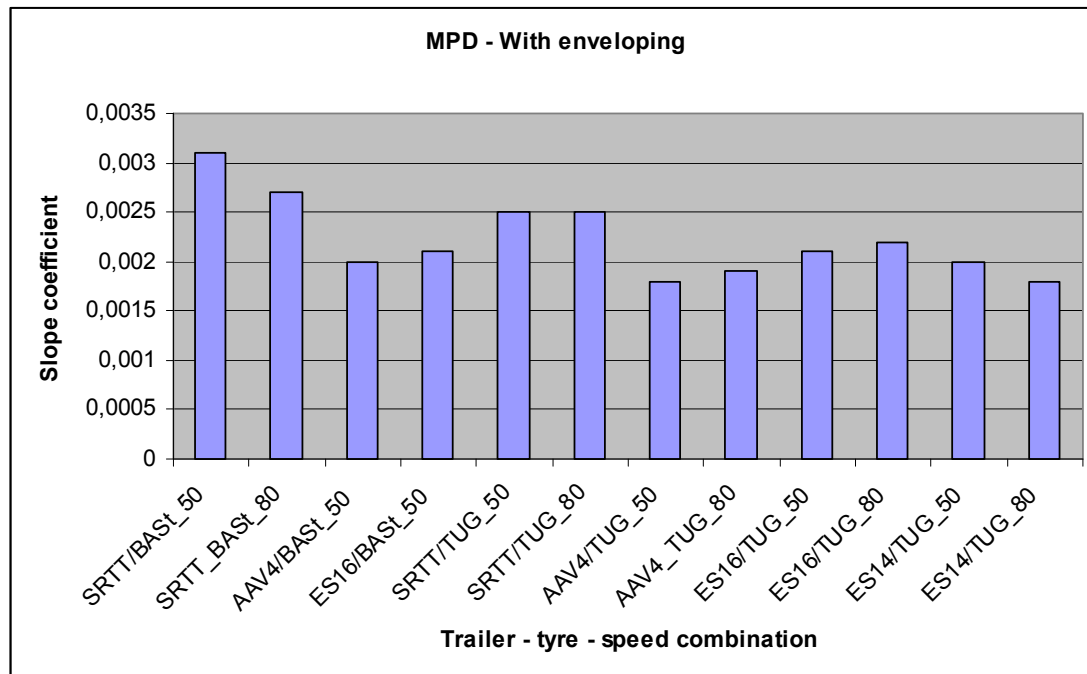


Figure 11.27: Summarizing graph slope coefficients MPD for various tyres and speeds – with enveloping

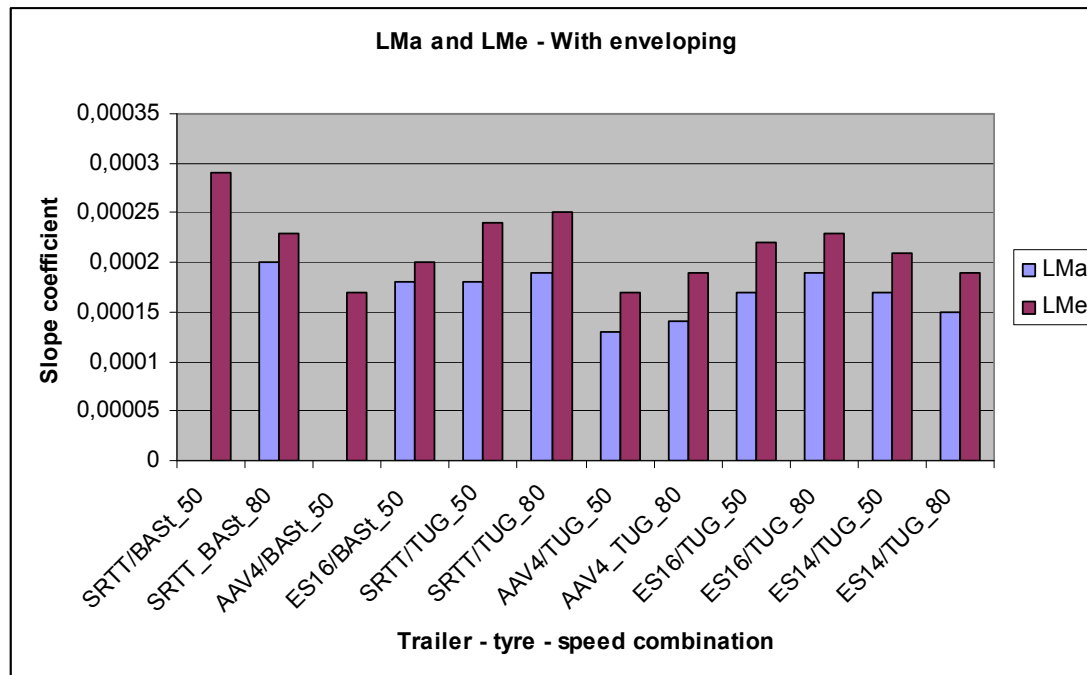
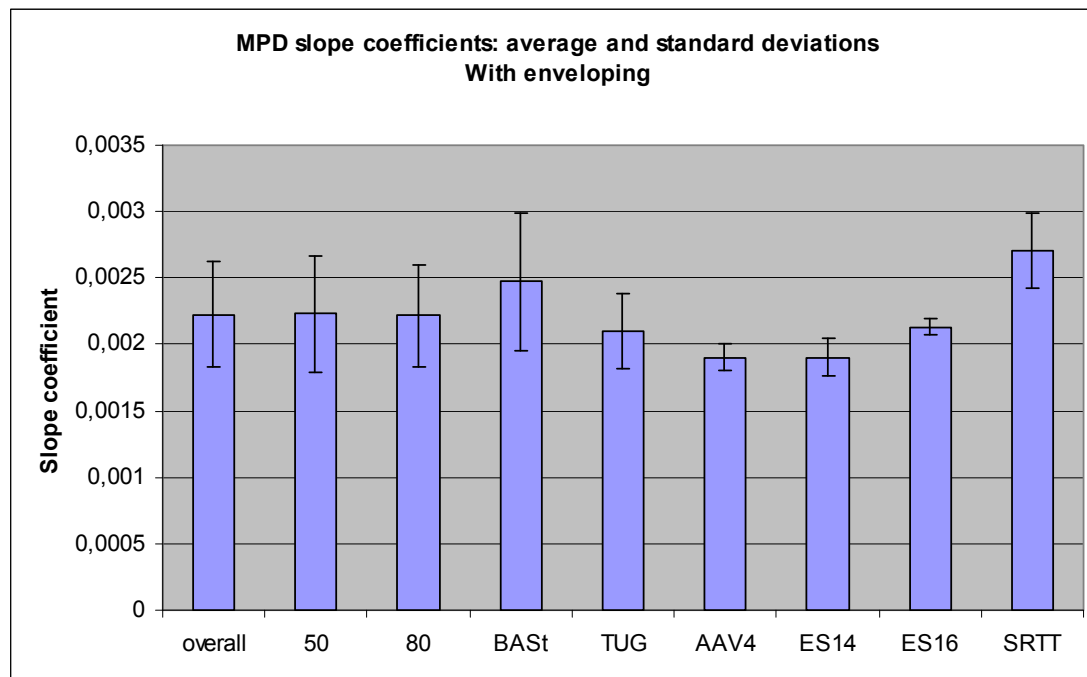
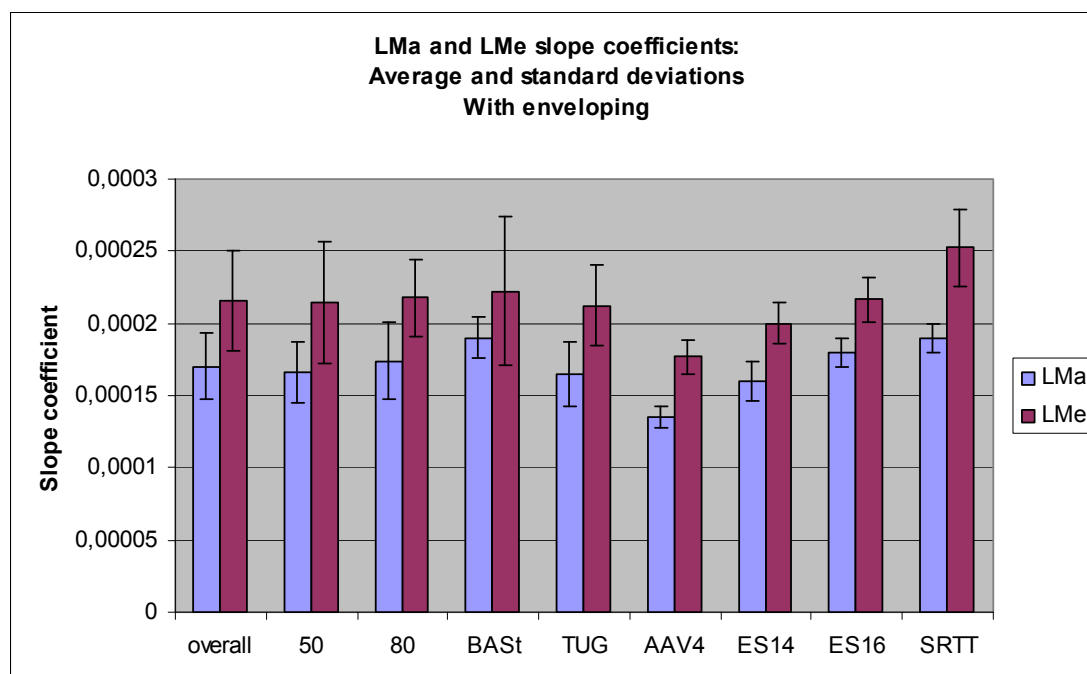


Figure 11.28: Slope coefficients LMa and LMe for various tyres and speeds – with enveloping

Based on Figure 11.29 and Figure 11.30 one can conclude that the slope coefficients with enveloping are independent of speed or institute, but dependent of tyre type. MPD, LMa and LMe have an overall average slope coefficient of 0.00223, 0.00017 and 0.00022 respectively, which is higher than without enveloping.



**Figure 11.29: Average values and standard deviations MPD per category (overall, speed, institute, tyre) – with enveloping**



**Figure 11.30: Average values and standard deviations LMa, LMe per category (overall, speed, institute, tyre) – with enveloping**

## 11.6 IRI

Table 11.13 shows IRI values measured on the test track on 100 m long sections<sup>3</sup>. Two runs direction west to east (each run for left and right wheel track) are averaged for each test section, except for M2 and N which are only based on one run.

**Table 11.13: IRI values measured on test track on 100 m long sections**

Test section	IRI [mm/m]
M1	1.59
F	1.49
L1	-
L2	-
E1	1.35
E2	1.55
M2	1.99
A	1.07
CC	-
A'	-
N	2.24
C	1.79

Figure 11.31 to Figure 11.33 show the correlations between IRI and  $C_r$ . While measurements performed by BAST and TUG do not reveal any correlation, the measurements performed by BRRC show some correlation, but which is still very low. This is partly caused by an outlier for M2. When discarding this outlier, a correlation of 0.27 and 0.29 remains. This dependency may also be due to the trailer. Perhaps the trailer of BRRC is more sensitive to IRI because of the suspension that is used. Follow-up will be made. Other graphs that are not shown in this section can be found in Annex H.

---

<sup>3</sup> IRI data were provided by IFSTTAR.

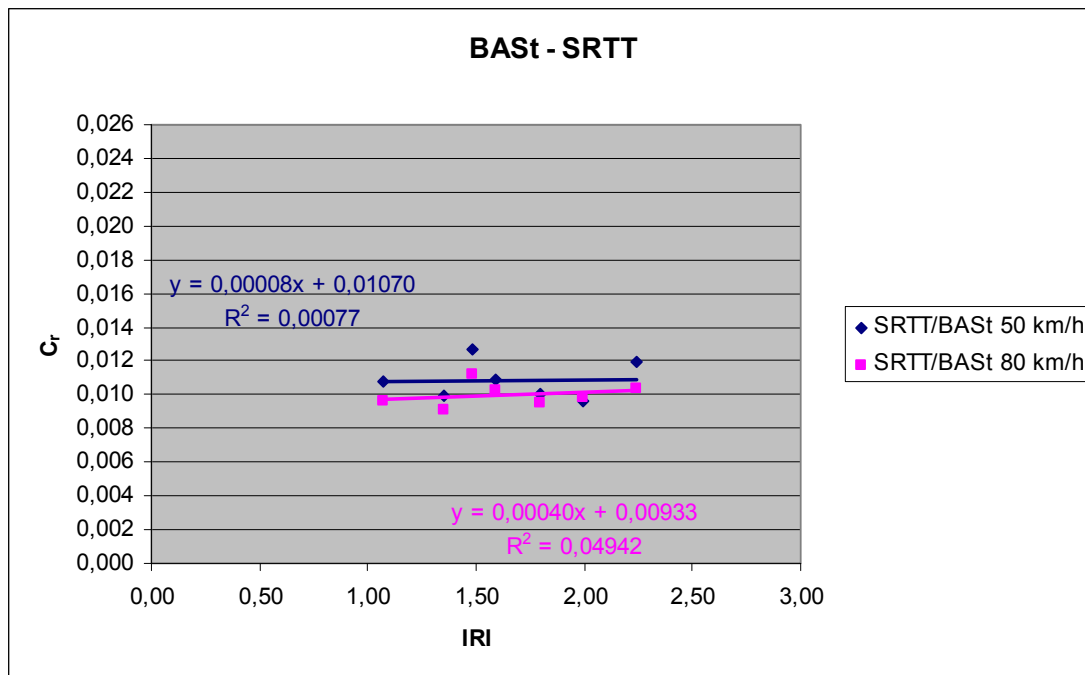


**Figure 11.31: Correlation between IRI and  $C_r$  for SRTT/BAST tyre (based on measurements performed by BAST)**

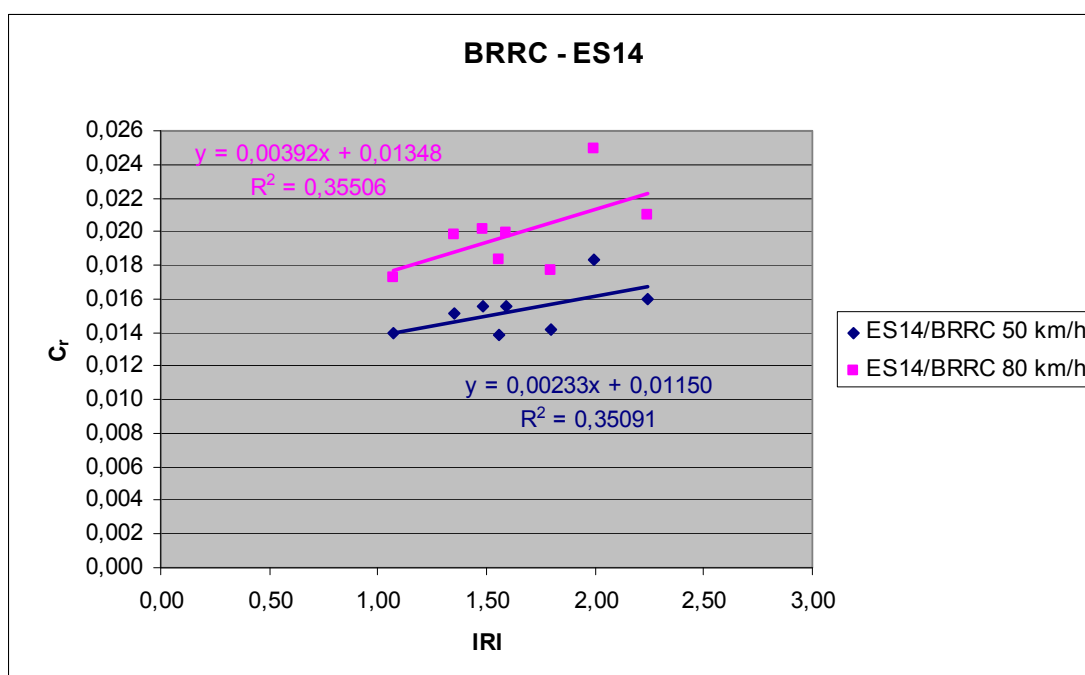


**Figure 11.32: Correlation between IRI and  $C_r$  for ES14/BRRC tyre (based on measurements performed by BRRC)**

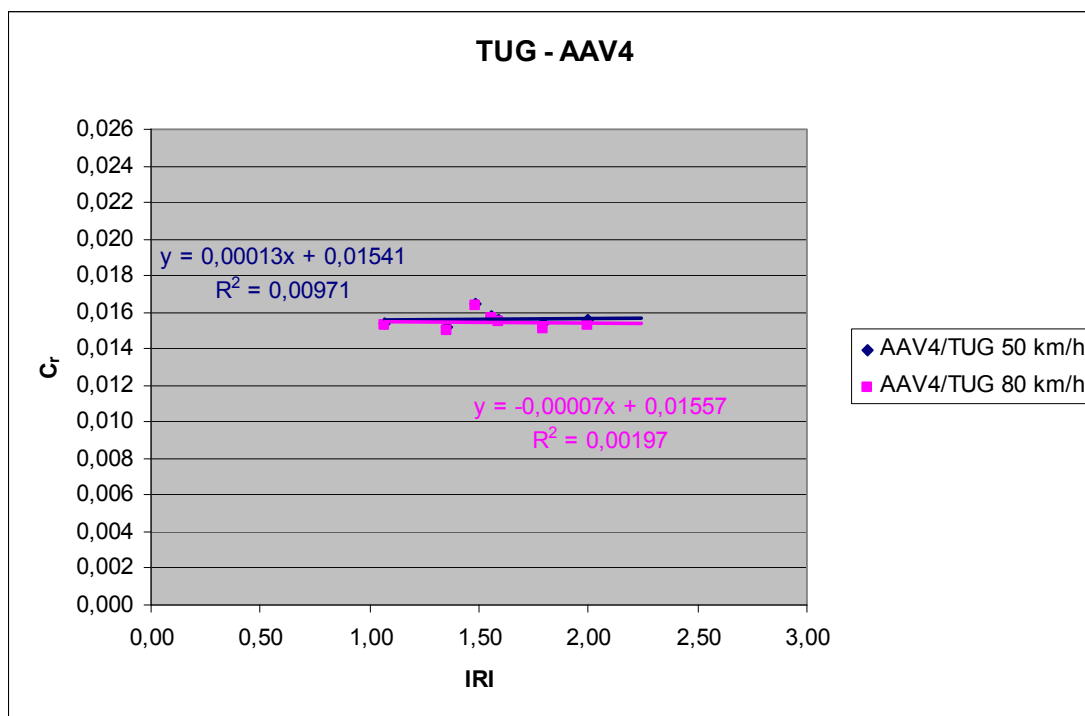


**Figure 11.33: Correlation between IRI and  $C_r$  for AAV4/TUG tyre (based on measurements performed by TUG)**

## 12 Conclusions

The following conclusions are made:

The short term repeatability of the BRRC and BAST measurements are in the order of 3 % of the average  $C_r$  values, which one can consider as just acceptable. The short term repeatability of the TUG trailer measurements is as low as 1 %, which is excellent.

The variability of the measurements from day to day is for BAST in the order of 7 %, which was considered as not acceptable as it is as high as differences one wishes to detect between pavements. For the BRRC trailer it is higher, indicating that there is a calibration problem, which needs a follow up. For the TUG trailer it could not be determined.

The correlation of the values of  $C_r$  measured with different samples of tyres of the same tyre type on the trailers of BAST and TUG are generally very good, except for the Avon AV4 tyre at 80 km/h (probably due to some temporary disturbing effect). In general reproducibility is rather poor; following what is written in the previous paragraph.

Reproducibility and day-to-day variation are the major problems of these rolling resistance measurement devices and needs to be studied much more in the near future. No device so far has demonstrated fully acceptable day-to-day variations.

Measurements have been done with different Michelin Energy Saver 14" tyre samples on the BRRC and TUG trailers. The correlation between the BRRC and TUG measurements over the test sections is rather poor at 50 km/h and almost non-existent at 80 km/h. The poor correlation at 50 km/h is due to one outlying value measured with the BRRC trailer, which is probably erroneous due to an acceleration effect. When discarding this outlier, a very good correlation is found. Also some differences between the two tyres were revealed by TUG drum measurements, which might have influenced the measurements on the test track. The lack of correlation at 80 km/h is most likely due to the lack of a wind shielding of the test tyre on the BRRC trailer, allowing air drag to play a significant.

Measurements with different samples of tyres of the same type on the TUG trailer revealed that the  $C_r$  values measured with the two Avon AV4 tyres are rather close to each other. Also an Avon AV4 tyre with corrupted tread was measured. These measurements showed differences in  $C_r$  of up to 17 % compared to the Avon AV4 tyres with normal tread. Two samples of the SRTT tyres, on the other hand, show differences in  $C_r$  of up to 40 %, probably due to the fact that the SRTT tyres were from different batches and one of them had rubber hardness outside the accepted range.

The  $C_r$  values measured with the Michelin Energy Saver 14" tyre are almost twice as high as those measured with the 16" version, mostly due to the tyre size.

For the TUG trailer measurements, the rolling resistance coefficient  $C_r$  is constant with speed or increases slightly with increasing speed over the range 50-110 km/h, despite they have wind shields over the test tyres. However, this increase is small and may be due to other mechanisms than air drag.

Temperature measured at the tyre shoulder is less stable than the temperature inside the tyre, probably due to varying sun radiation exposure and a higher sensitivity to



wind and heating mechanisms while rolling. Moreover, the tyre temperature seems to be more stable when the tyre is inflated with nitrogen: the interior temperature drops less quickly at standstill with nitrogen than with air. Driving at 80 km/h, a constant tyre inflation and interior temperature is reached after about 10 minutes or 13 km.

Michelin Energy Saver tyres show the highest correlations of the tested tyres between rolling resistance and texture for most texture wavelengths. The correlations are better when applying a special procedure called enveloping to the road texture profile curve before processing it into frequency spectra or calculating MPD. The highest correlations are found in the megatexture range.

The  $C_r$  values measured by BAST and TUG show good to excellent correlations with the considered texture parameters, especially with macrotexture expressed as MPD and with the megatexture level (LMe). Only the BAST measurements with the Avon AV4 tyre at 80 km/h show poor correlations with all texture parameters, and this might be an indication that this data set is erroneous. All TUG results, on the other hand, correlate extremely well with both MPD and LMe. The best results are obtained with the Michelin Energy Saver tyre and the application of enveloping on the texture profile further improves the correlations. The BRRC results show moderate correlation at 50 km/h, which would improve drastically if one "suspect" data point would be removed as an "outlier", but poor correlation at 80 km/h. The latter is most probably due to a bias by air drag on the non-shielded test tyre.

Correlations between  $C_r$  and MPD, LMa and LMe without enveloping give an overall average slope coefficient of 0.00174, 0.00013 and 0.00019, respectively. Correlations between  $C_r$  and MPD, LMa and LMe when applying enveloping have an overall average slope coefficient of 0.00223, 0.00017 and 0.00022 respectively. The slope increase when enveloping is applied, is probably due to the increasing correlation.

No correlation is found between  $C_r$  and the road evenness measure IRI, for the IRI range of 1.07 - 2.24 mm/m for the TUG trailer in this study. However, the BRRC trailer seems to have some weak correlation with IRI, and the BAST trailer too in one case. However, the influence may also be due to other circumstances. Nevertheless, this does not mean that unevenness does not affect rolling resistance; it may well be that these trailer systems are relatively insensitive to unevenness.

For the range of surfaces on the test track (MPD from 0.08 to 2.77 mm) the  $C_r$  for the test tyres increased from the smoothest to the roughest of the surfaces by 21 - 55 %, depending on the tyre type. Such rolling resistance differences correspond to roughly 7 - 18 % in fuel consumption differences, using calculations made in SP 2 of MIRIAM for light vehicles driving on a typical two-lane highway at 90 km/h (to be published in January 2012).

## 13 References

- [1] ISO 13473-5:2009, Characterization of pavement texture by use of surface profiles - Part 5: Determination of megatexture
- [2] Sandberg. U. (ed), Rolling Resistance – Basic information and State-of-the-Art on Measurement methods, Deliverable No. 1 in MIRIAM SP1, version 1 June 2011, downloadable from <http://miriam-co2.net> and from [www.transguide.org](http://www.transguide.org)
- [3] Von Meier. A.; van Blokland. G.J.; Descornet. G.; The influence of texture and sound absorption on the noise of porous road surfaces, PIARC 2nd International Symposium on Road Surface Characteristics, 1992
- [4] Sandberg, Ulf; Ejsmont, Jerzy A.; Bergiers, Anneleen; Goubert, Luc; Zöller, Marek, Rolling Resistance – Measurement Methods for Studies of Road Surface Effects, Deliverable No. 2 in MIRIAM SP1, 2011, downloadable from <http://miriam-co2.net> and from [www.transguide.org](http://www.transguide.org)
- [5] De Bie, H., Hofmans, C., Masterproef: Rolweerstand van Belgische wegdekken, Artesis Antwerp, Belgium, 2010-2011
- [6] ISO 28580:2009, Passenger car, truck and bus tyres – Methods of measuring rolling resistance – Single point test and correlation of measurement results
- [7] Descornet, G., Road-Surface Influence on Tire Rolling Resistance, Surface Characteristics of Roadways: International Research and Technologies, ASTM STP 1031, W.E. Meyer and J. Reichert, Eds., American Society for Testing and Materials, Philadelphia, USA, 1990
- [8] Sandberg, U.; Ejsmont, Jerzy A., Tyre/Road Noise Reference Book, Informex, SE-59039 Kisa, Sweden ([www.informex.info](http://www.informex.info))

## Annexes

### A. Texture spectra measured in middle, right and left wheel track direction east

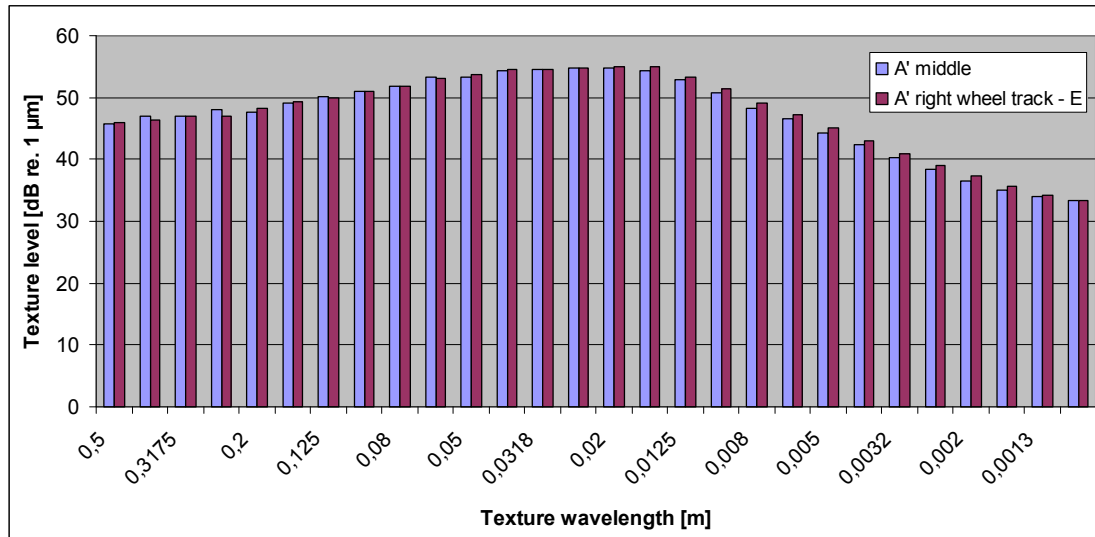


Figure A.1: Texture spectra test section A'

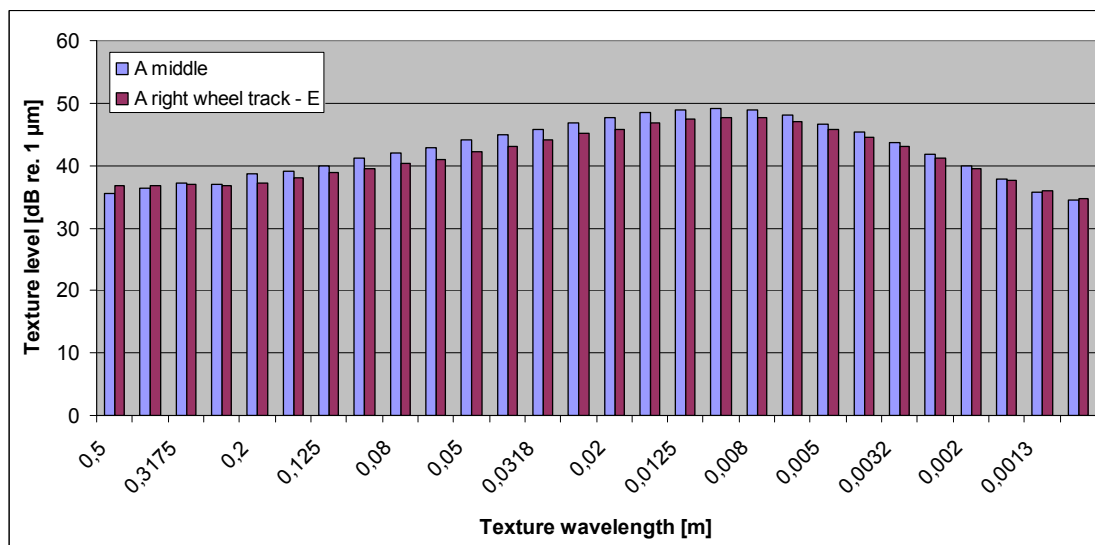


Figure A.2: Texture spectra test section A

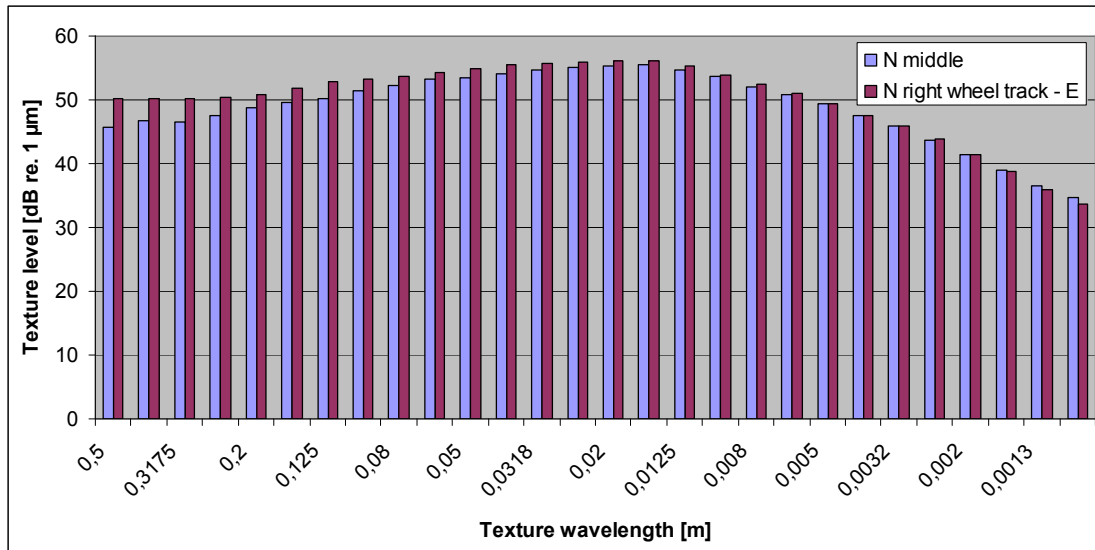


Figure A.3: Texture spectra test section N (ground in middle)

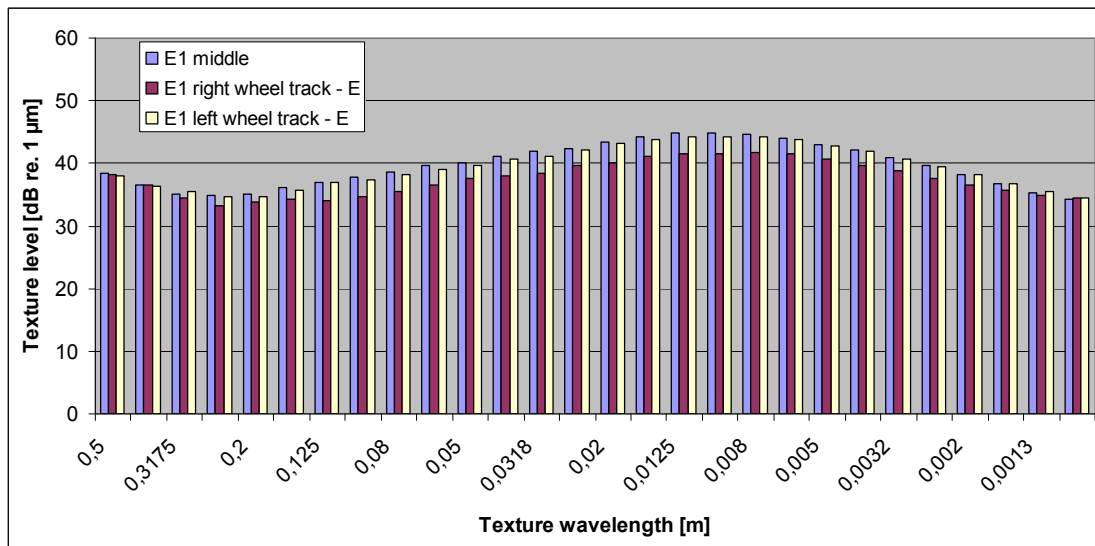


Figure A.4: Texture spectra test section E1 (road marking in middle)

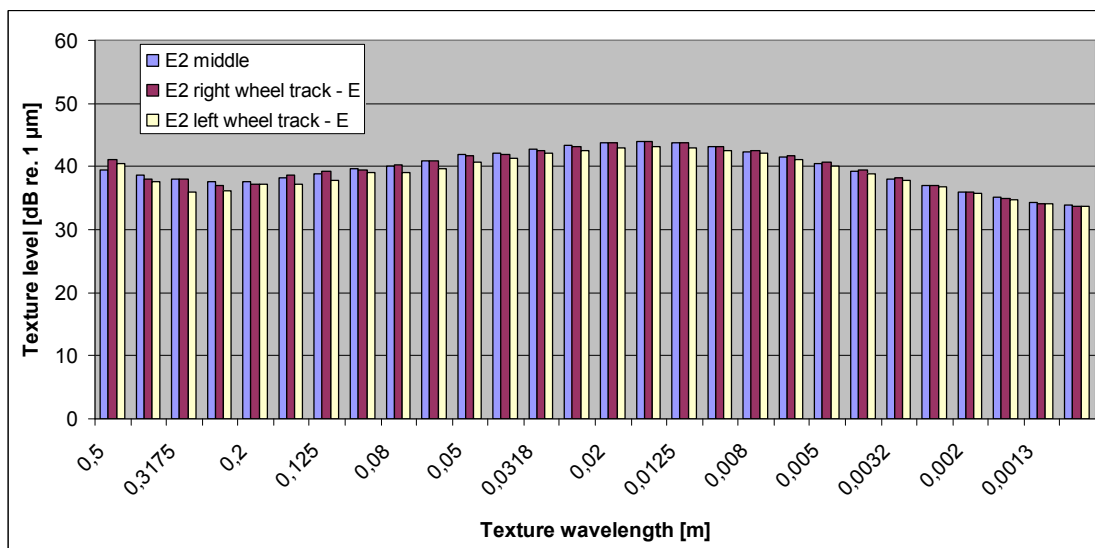


Figure A.5: Texture spectra test section E2 (road marking in middle)

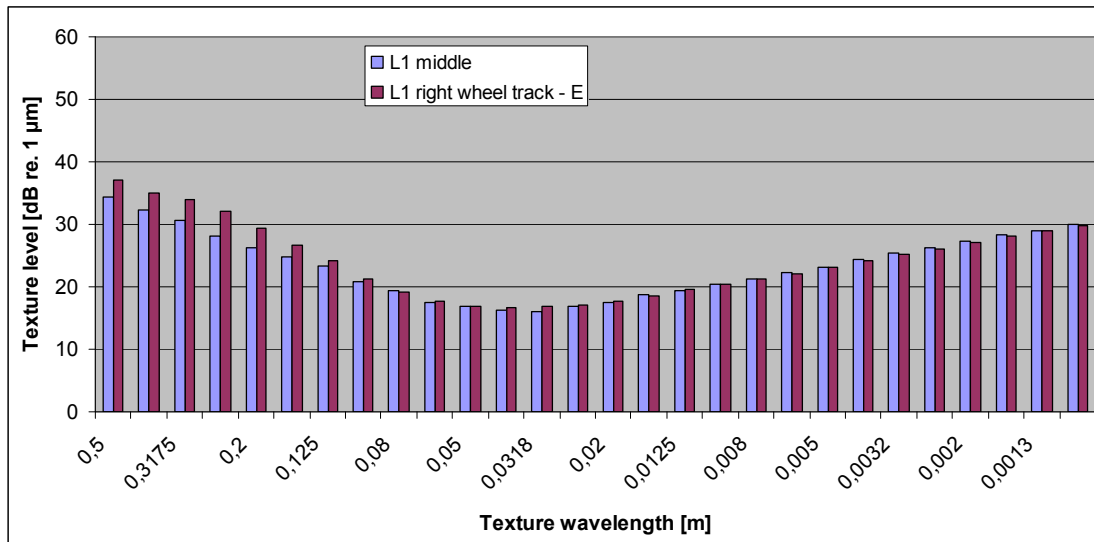


Figure A.6: Texture spectra test section L1

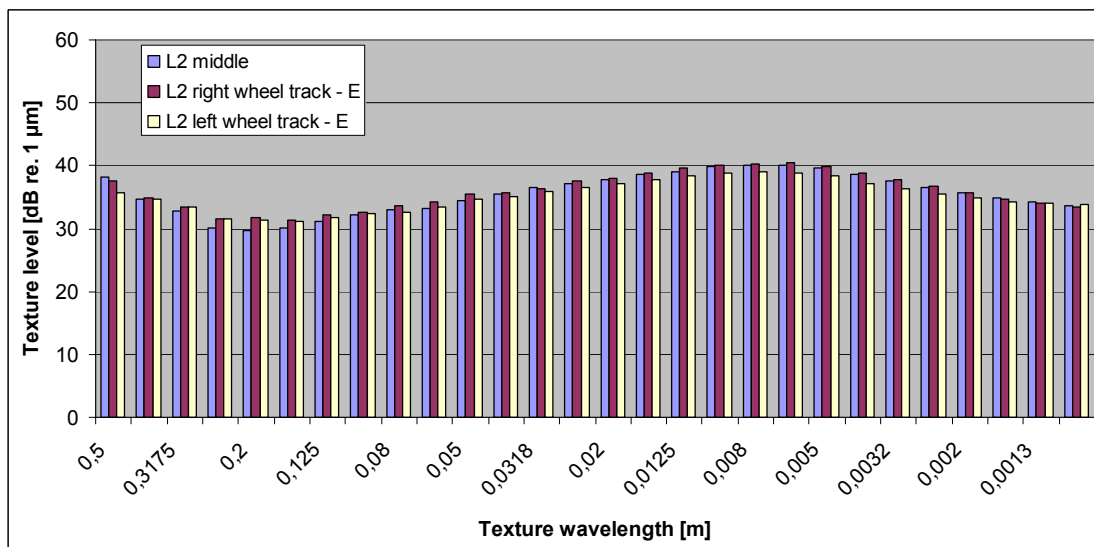


Figure A.7: Texture spectra test section L2

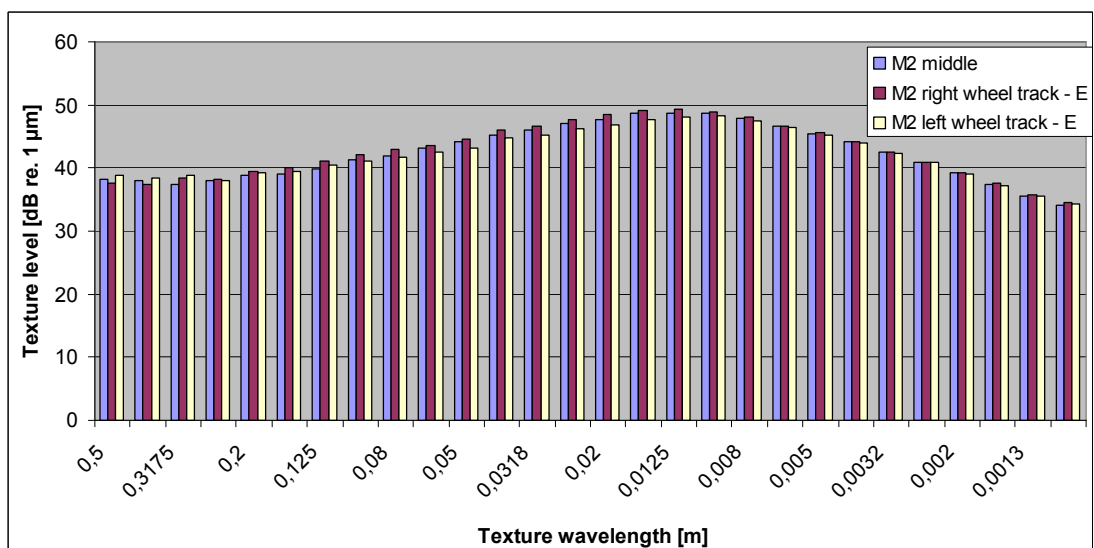
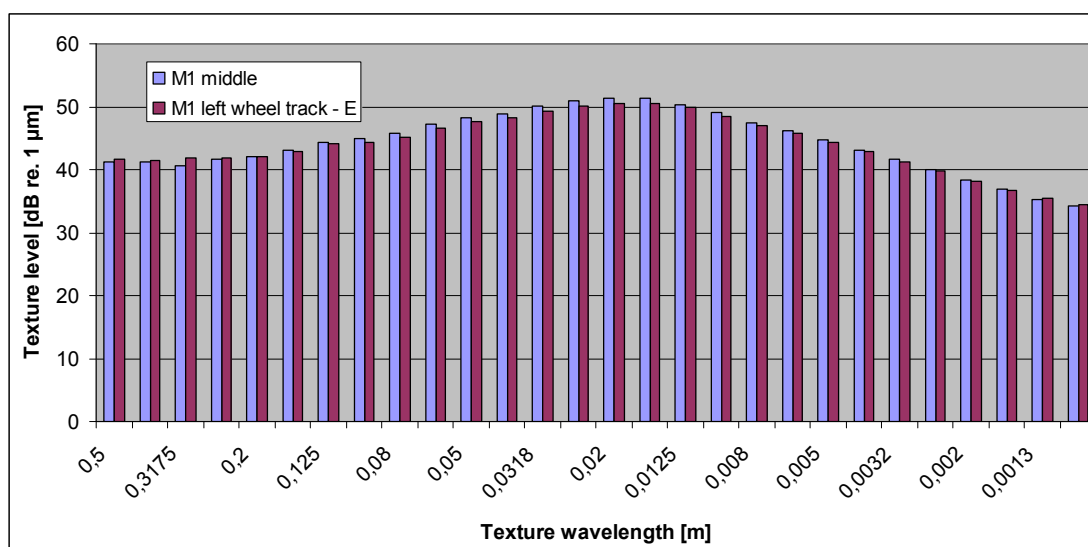
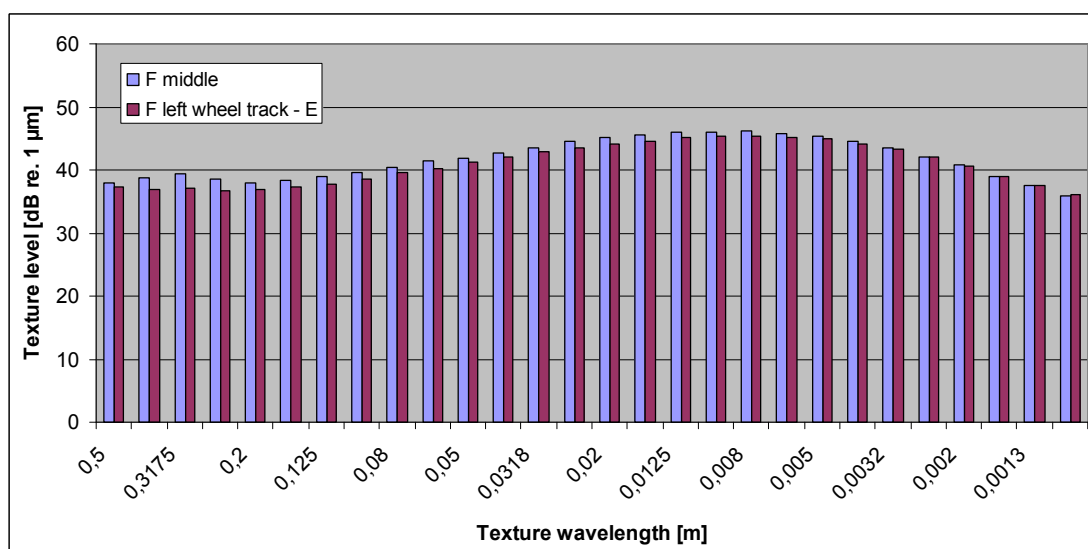


Figure A.8: Texture spectra test section M2



**Figure A.9: Texture spectra test section M1**



**Figure A.10: Texture spectra test section F**

## B. Correlation between MPD and $C_r$ for various tyres measured by different participants – without enveloping

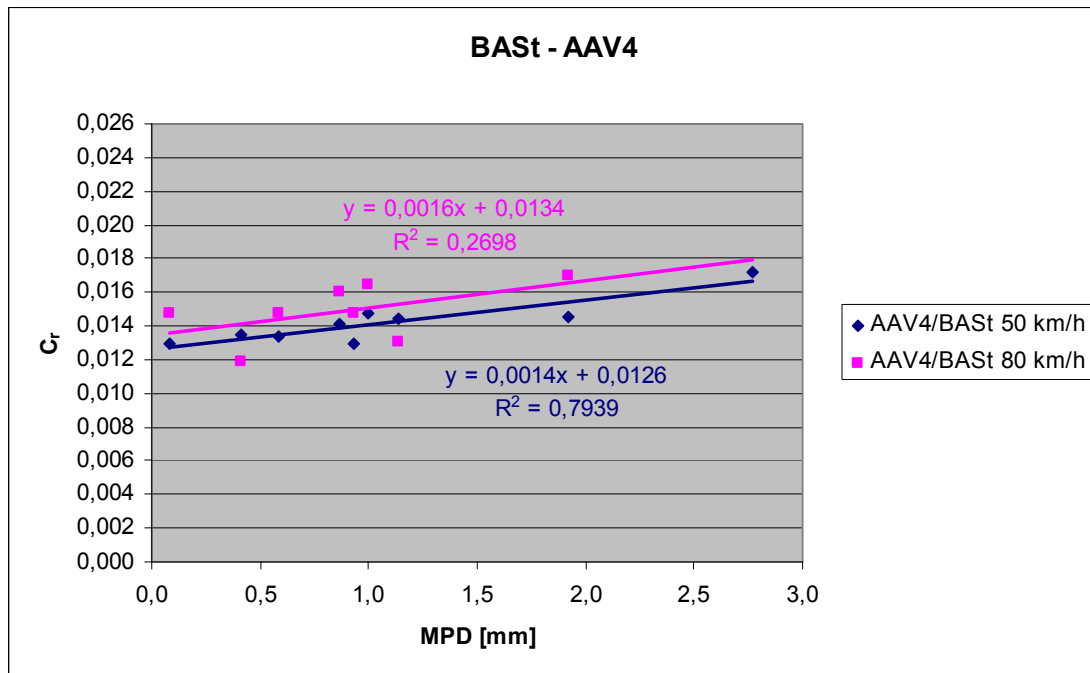


Figure B.1: Correlation between MPD and  $C_r$  for AAV4/BASSt tyre (based on measurements performed by BASSt)

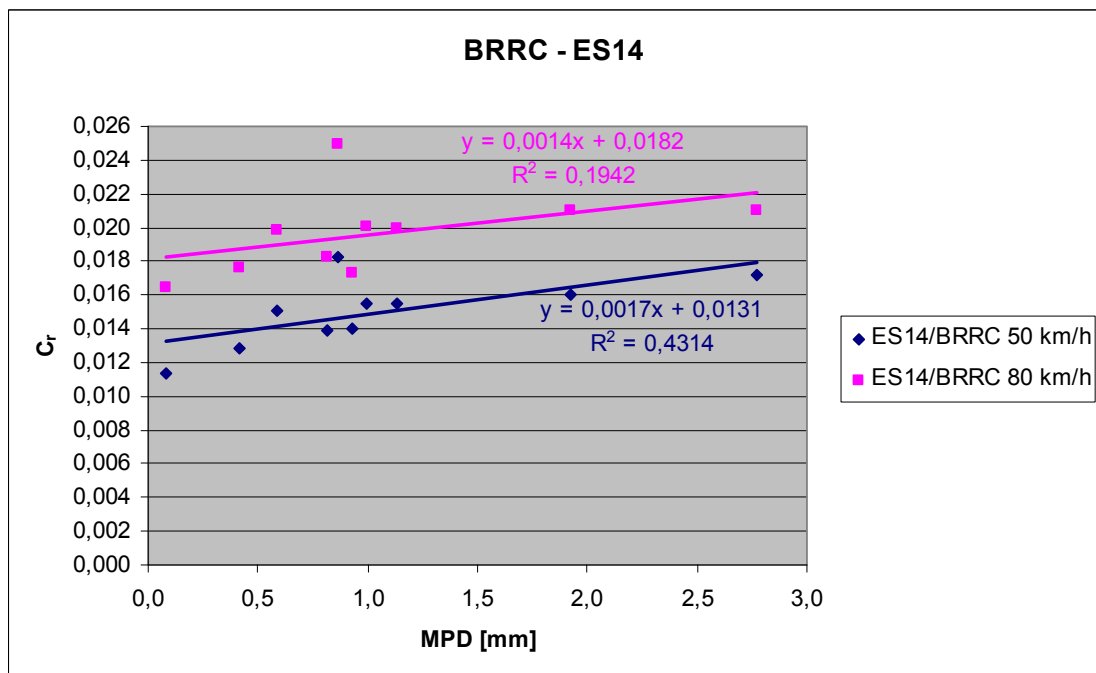
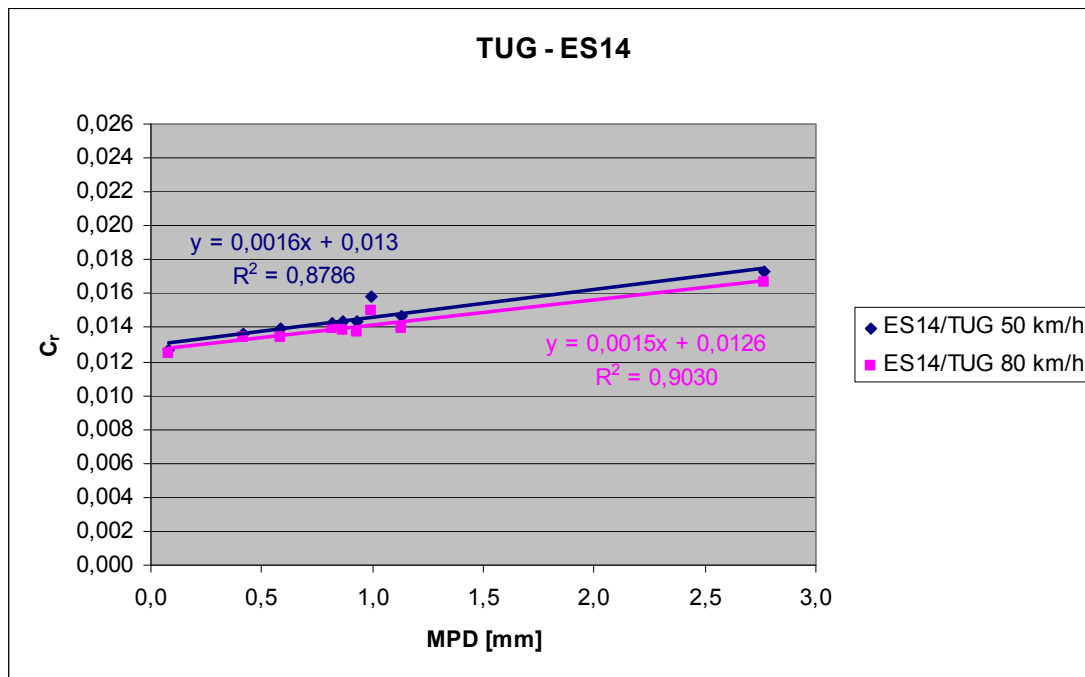
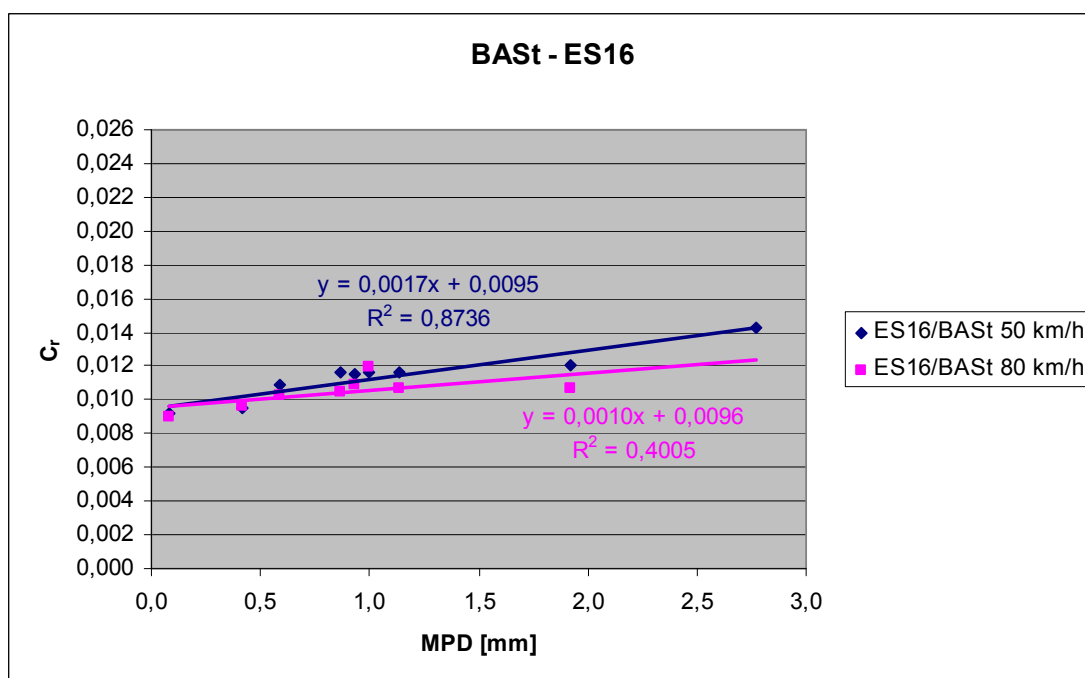


Figure B.2: Correlation between MPD and  $C_r$  for ES14/BRRC tyre (based on measurements performed by BRRC)



**Figure B.3: Correlation between MPD and  $C_r$  for ES14/TUG tyre (based on measurements performed by TUG)**



**Figure B.4: Correlation between MPD and  $C_r$  for ES16/BASSt tyre (based on measurements performed by BASSt)**



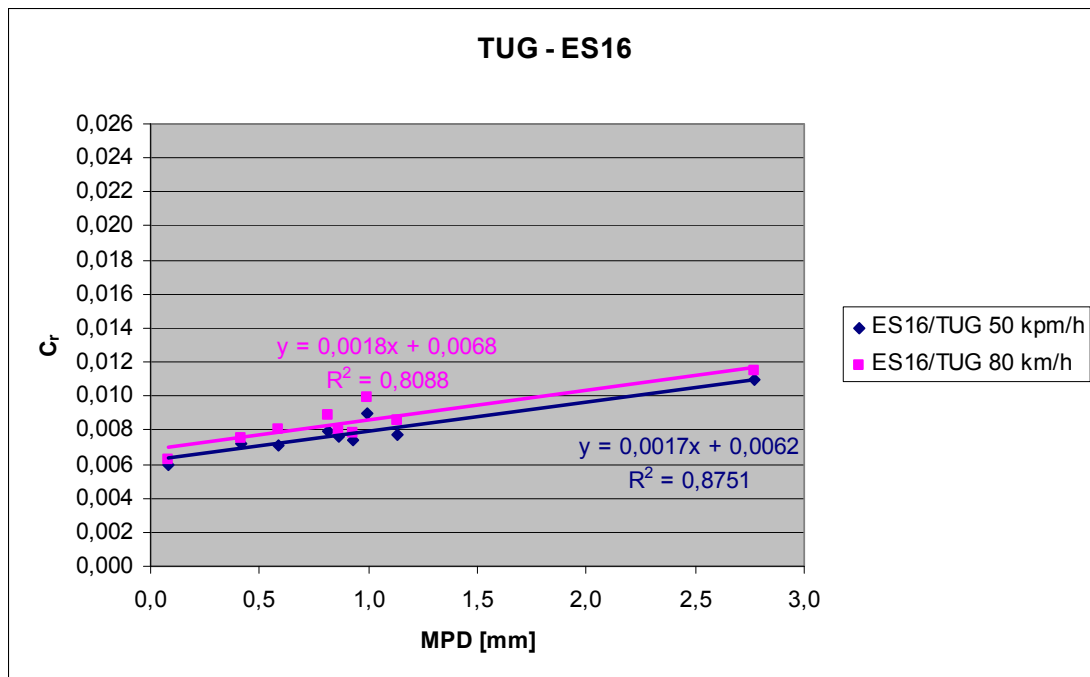


**Figure B.5: Correlation between MPD and  $C_r$  for ES16/TUG tyre (based on measurements performed by TUG)**

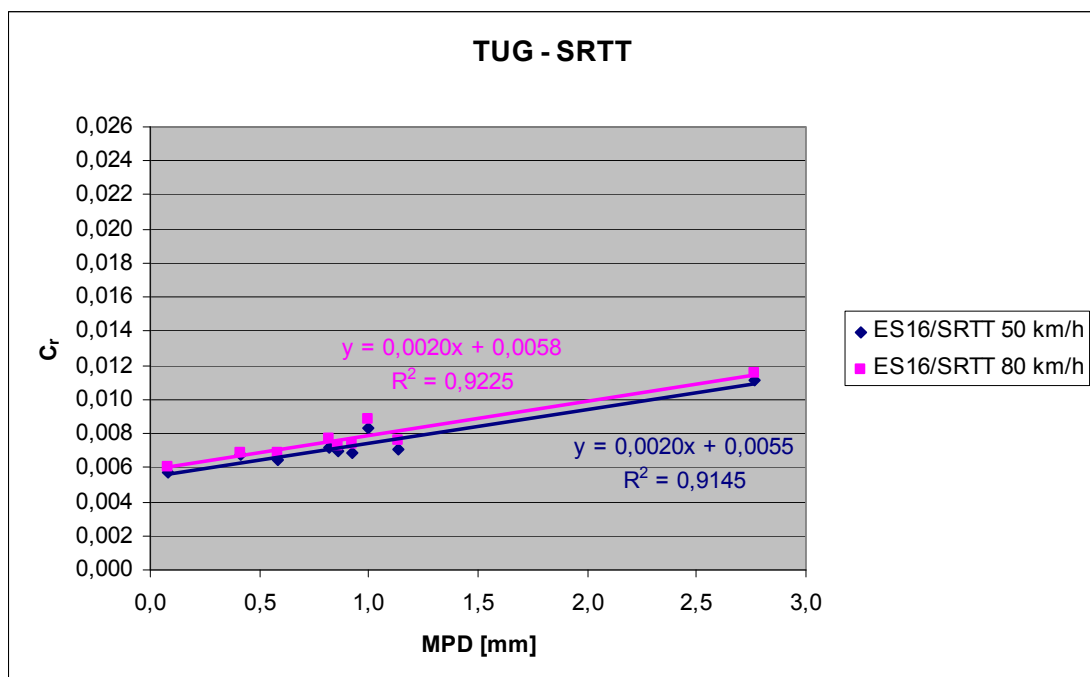


**Figure B.6: Correlation between MPD and  $C_r$  for SRTT/TUG tyre (based on measurements performed by TUG)**

### C. Correlation between MPD and $C_r$ for various tyres measured by different participants – with enveloping

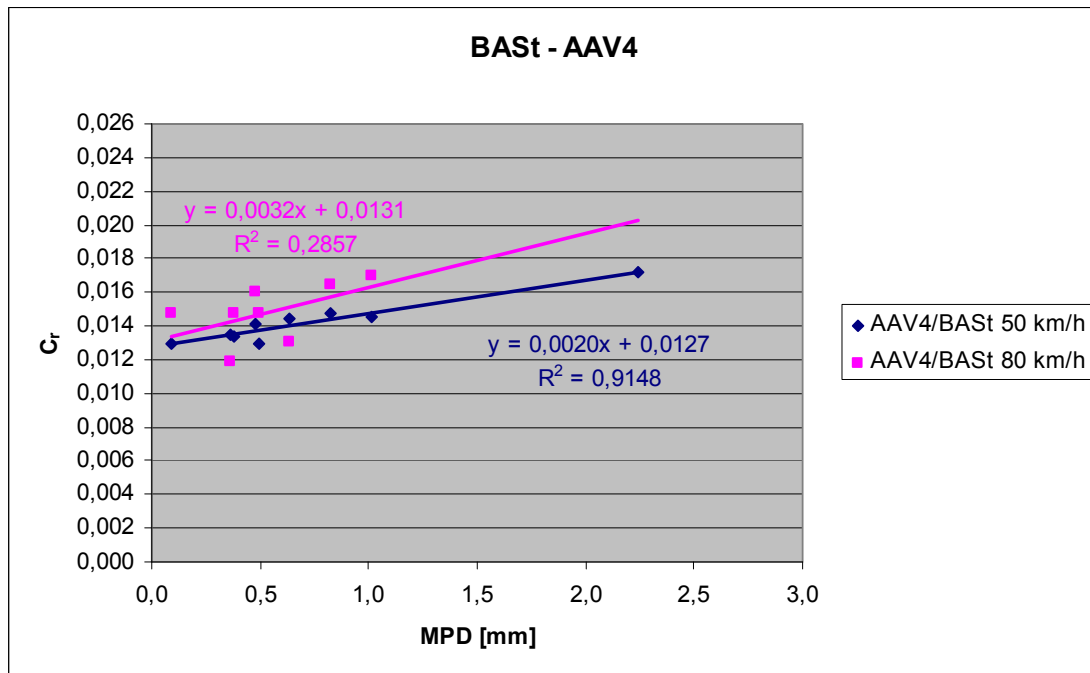


Figure C.1: Correlation between MPD and  $C_r$  for AAV4/BASSt tyre (based on measurements performed by BASSt) – with enveloping

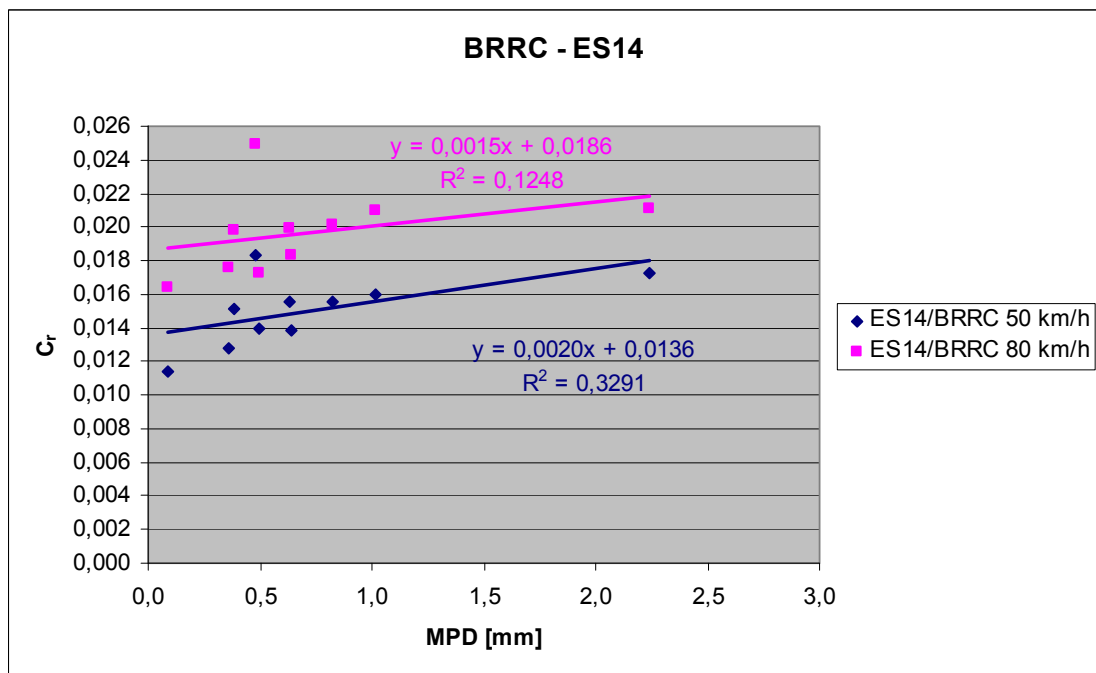
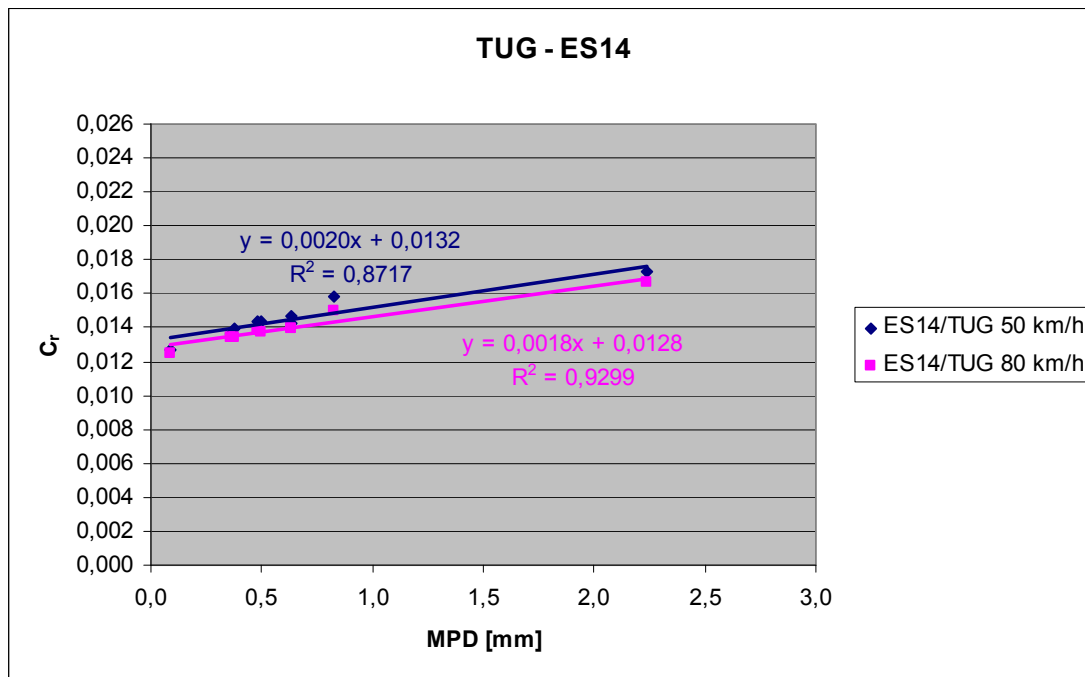
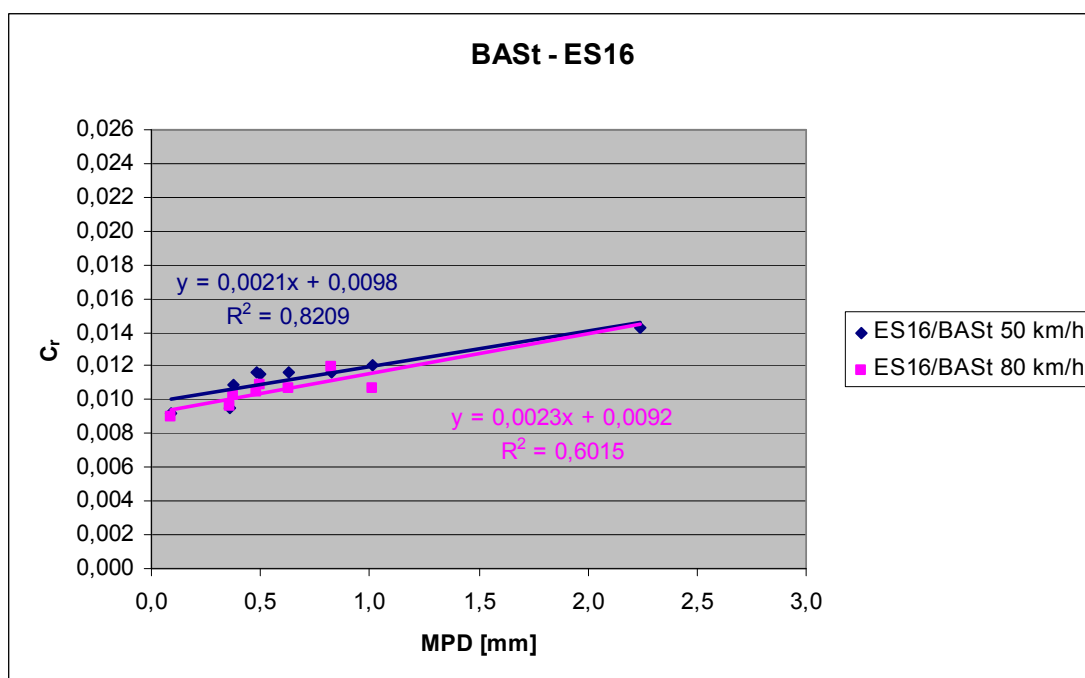


Figure C.2: Correlation between MPD and  $C_r$  for ES14/BRRC tyre (based on measurements performed by BRRC) – with enveloping



**Figure C.3: Correlation between MPD and  $C_r$  for ES14/TUG tyre (based on measurements performed by TUG) – with enveloping**



**Figure C.4: Correlation between MPD and  $C_r$  for ES16/BASt tyre (based on measurements performed by BASt) – with enveloping**

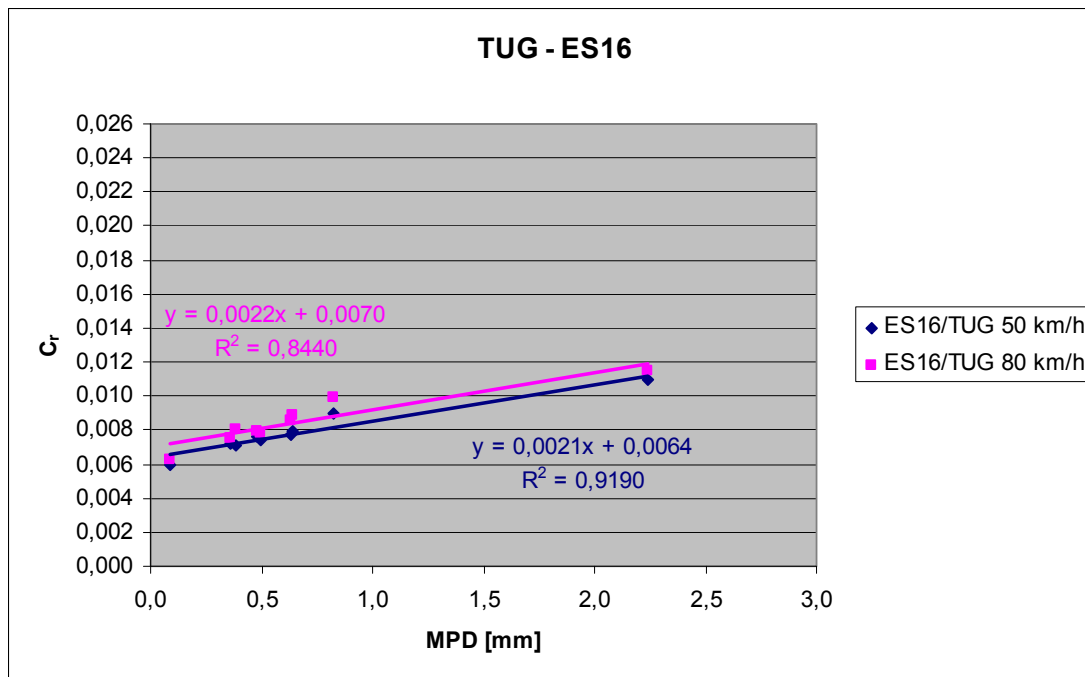


**Figure C.5: Correlation between MPD and  $C_r$  for ES16/TUG tyre (based on measurements performed by TUG) – with enveloping**

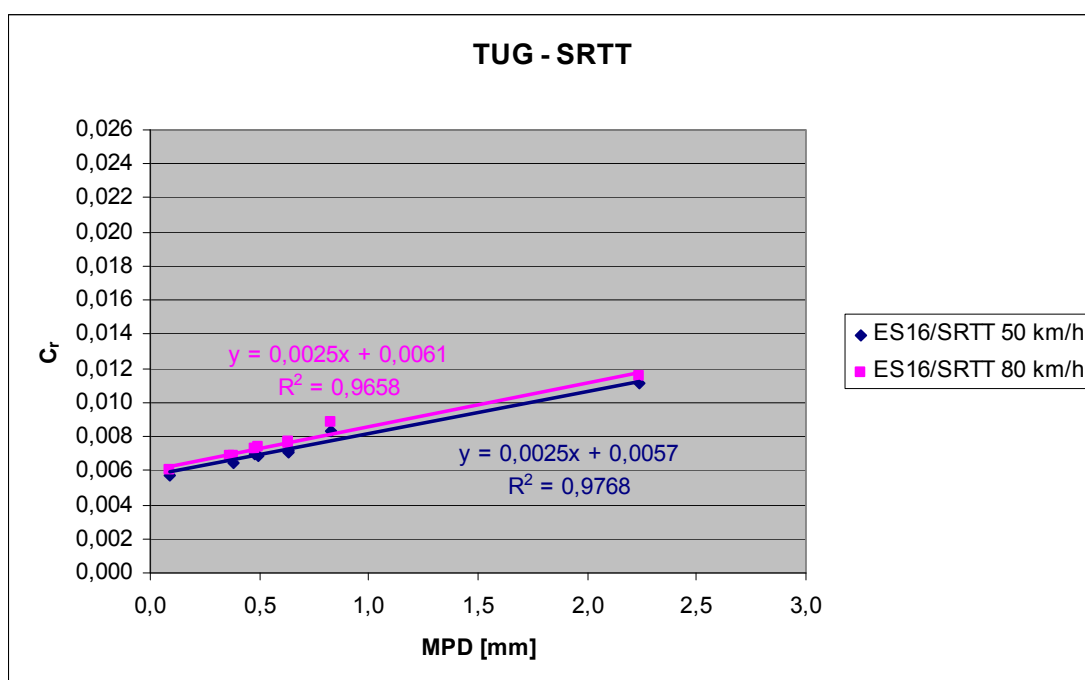


**Figure C.6: Correlation between MPD and  $C_r$  for SRTT/TUG tyre (based on measurements performed by TUG) – with enveloping**

## D. Correlation between macrotexture and $C_r$ for various tyres measured by different participants – without enveloping

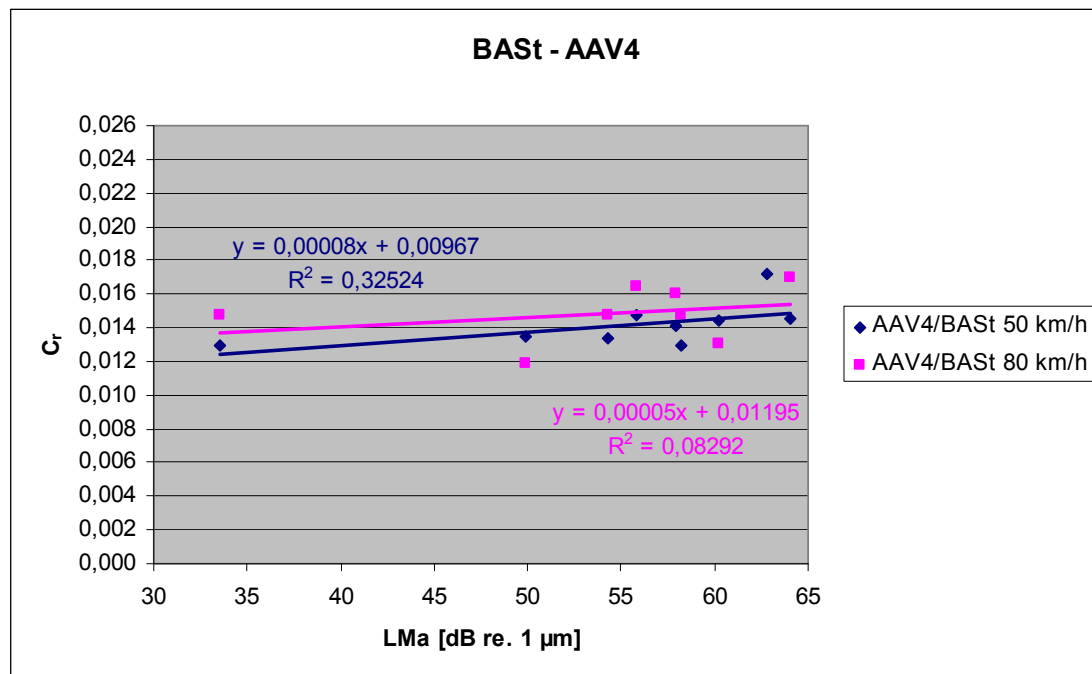


Figure D.1: Correlation between macrotexture and  $C_r$  for AAV4/BASSt tyre (based on measurements performed by BASSt)

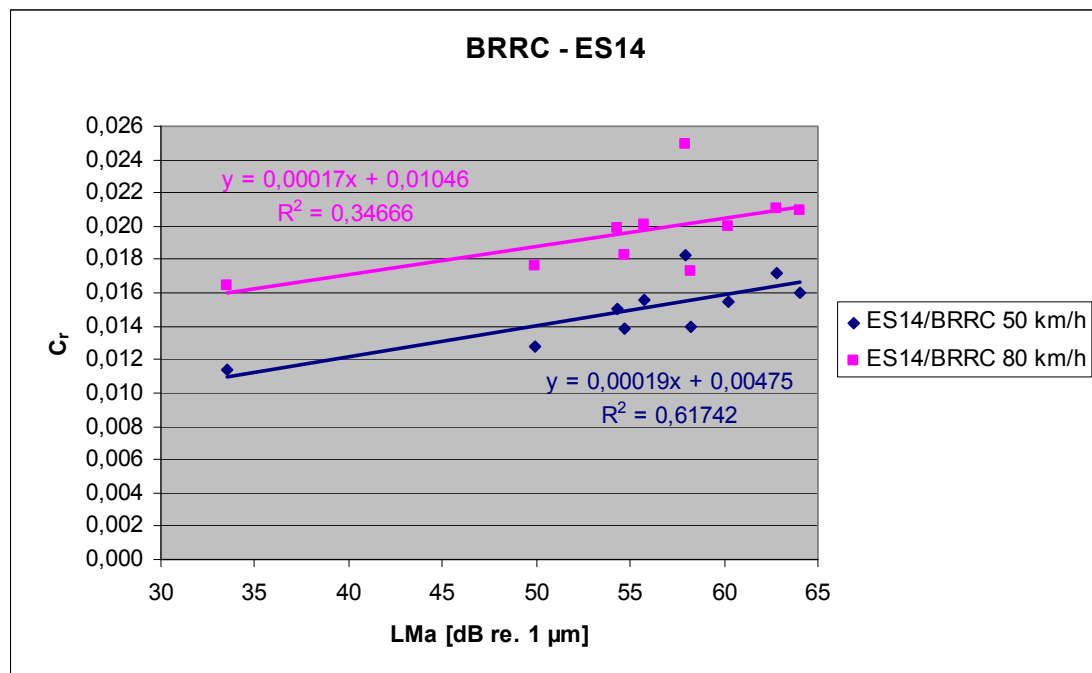
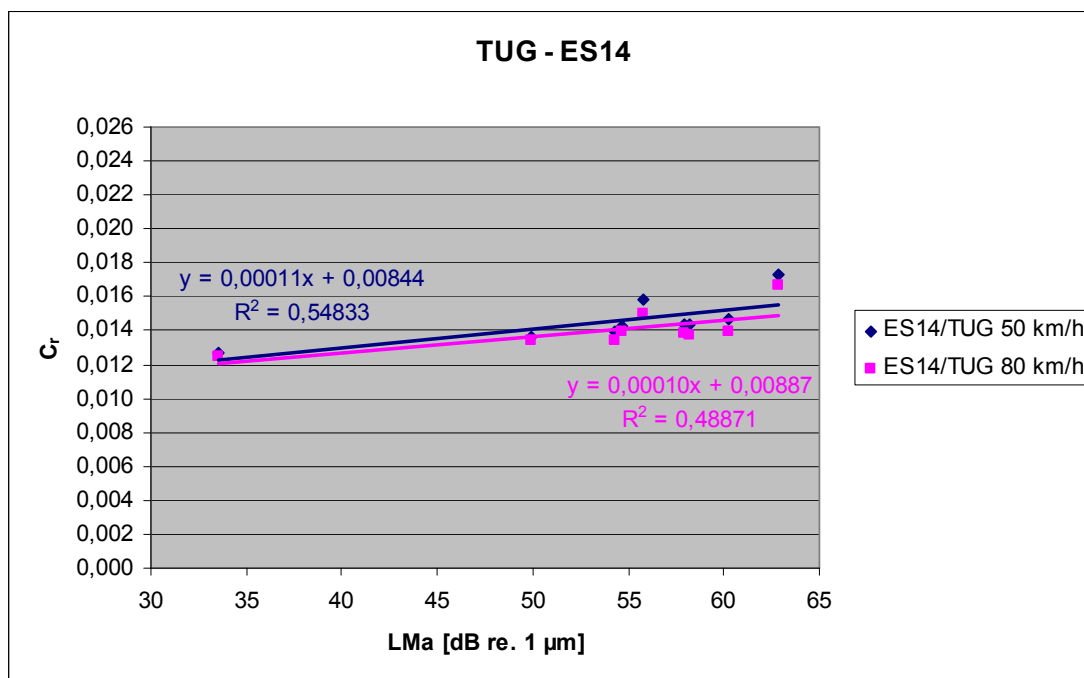
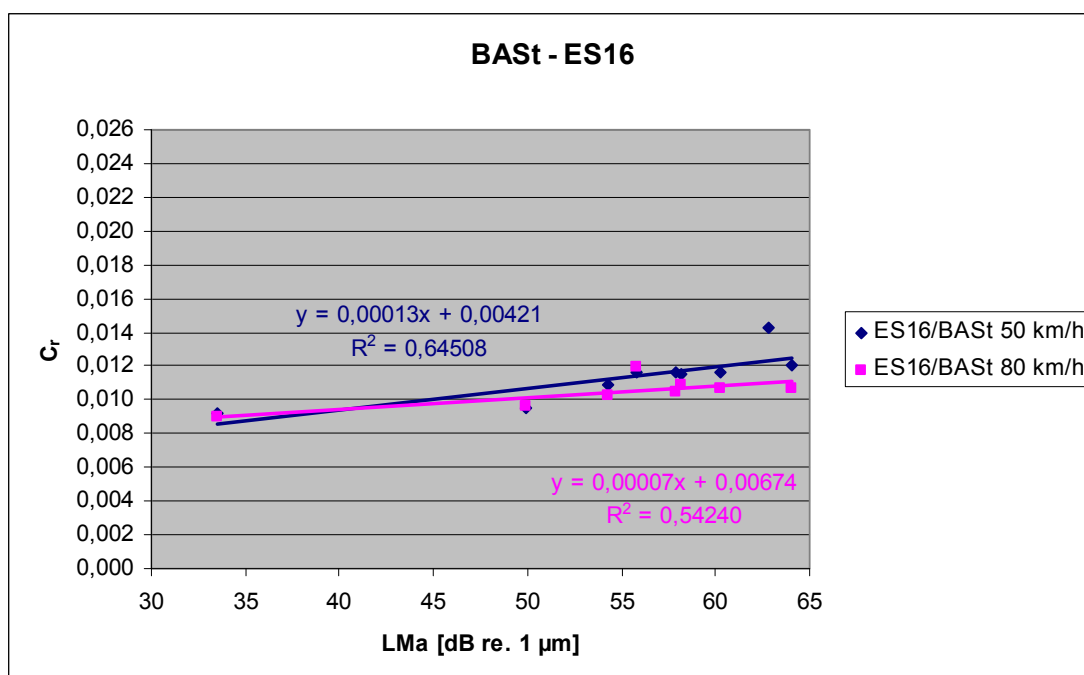


Figure D.2: Correlation between macrotexture and  $C_r$  for ES14/BRRC tyre (based on measurements performed by BRRC)



**Figure D.3: Correlation between macrotexture and  $C_r$  for ES14/TUG tyre (based on measurements performed by TUG)**



**Figure D.4: Correlation between macrotexture and  $C_r$  for ES16/BASt tyre (based on measurements performed by BASt)**

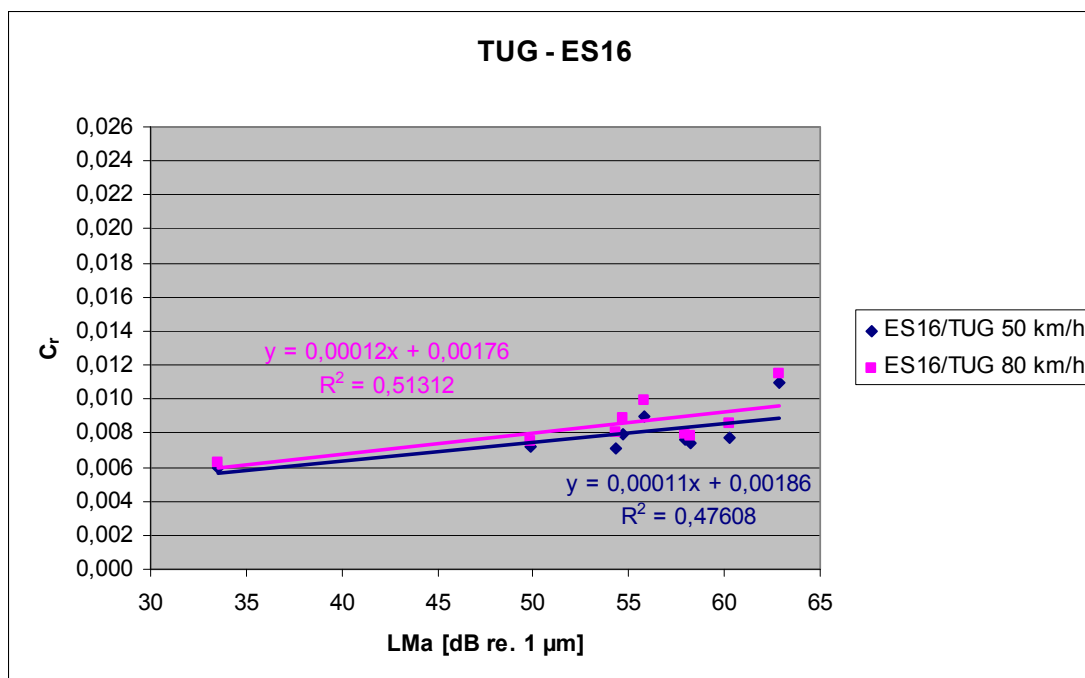


**Figure D.5: Correlation between macrotexture and  $C_r$  for ES16/TUG tyre (based on measurements performed by TUG)**

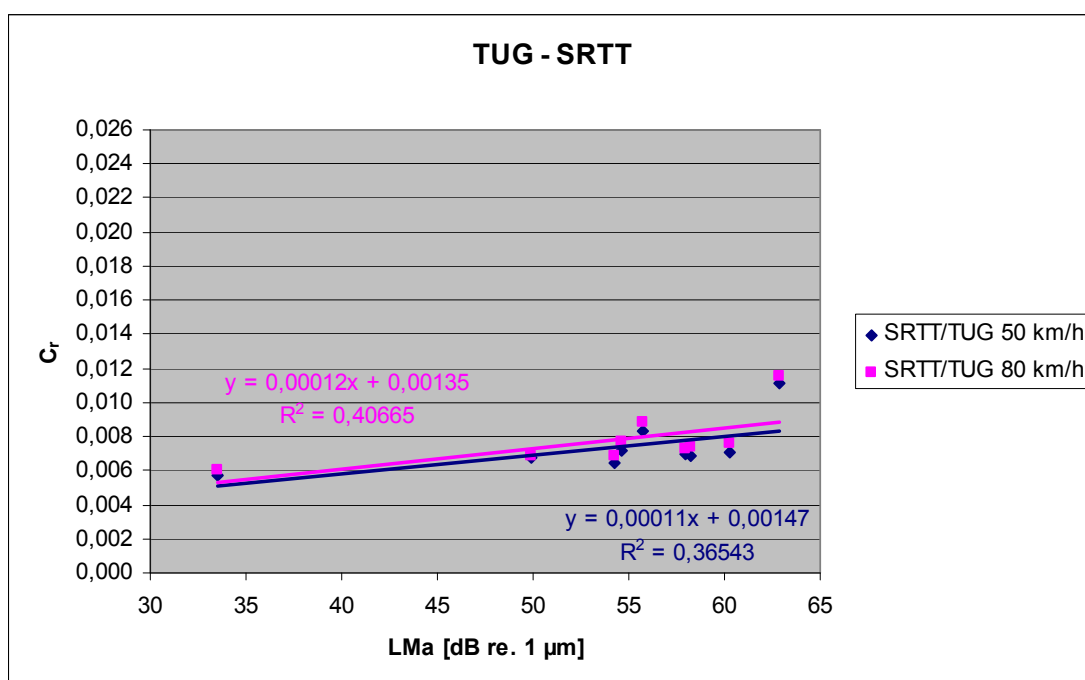


**Figure D.6: Correlation between macrotexture and  $C_r$  for SRTT/TUG tyre (based on measurements performed by TUG)**

## E. Correlation between macrotexture and $C_r$ for various tyres measured by different participants – with enveloping

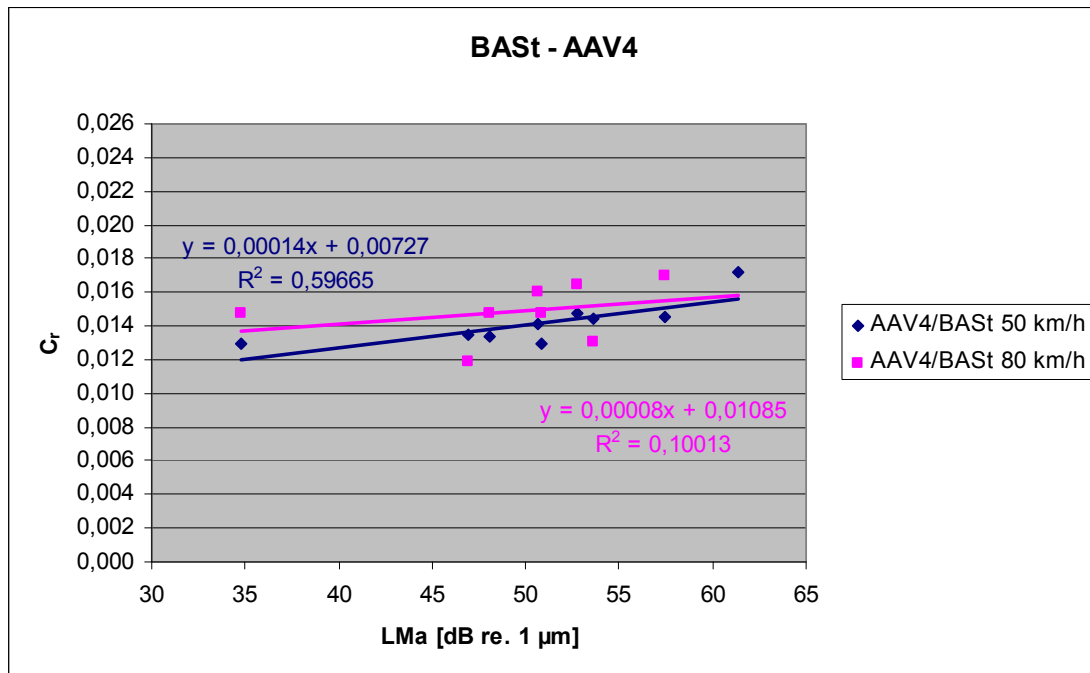


Figure E.1: Correlation between macrotexture and  $C_r$  for AAV4/BASSt tyre (based on measurements performed by BASSt) – with enveloping

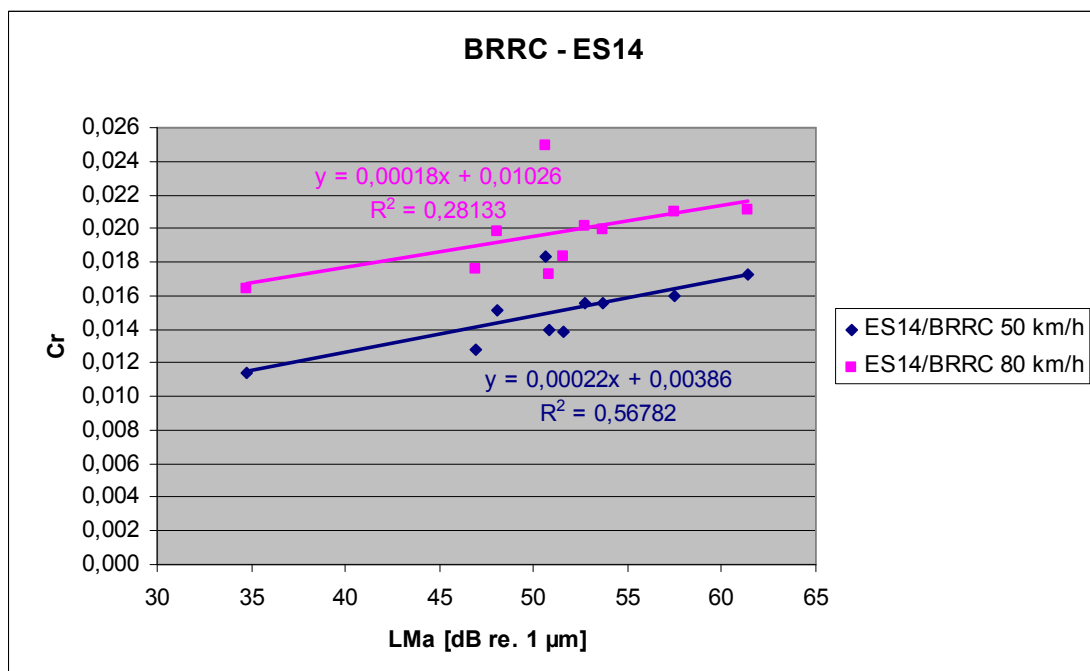
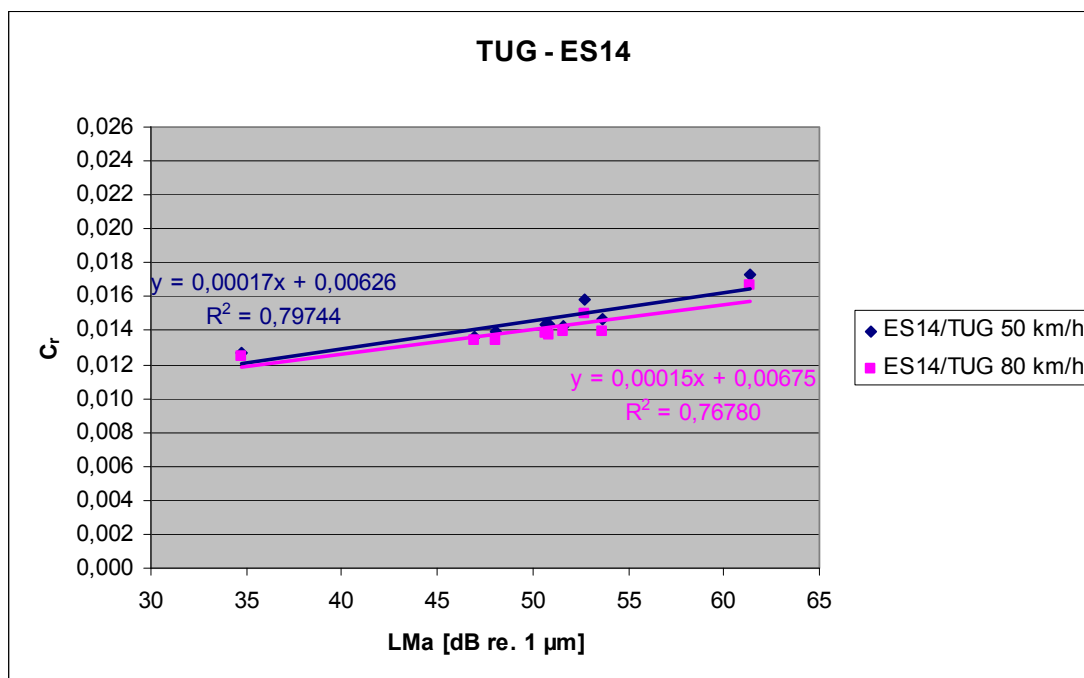
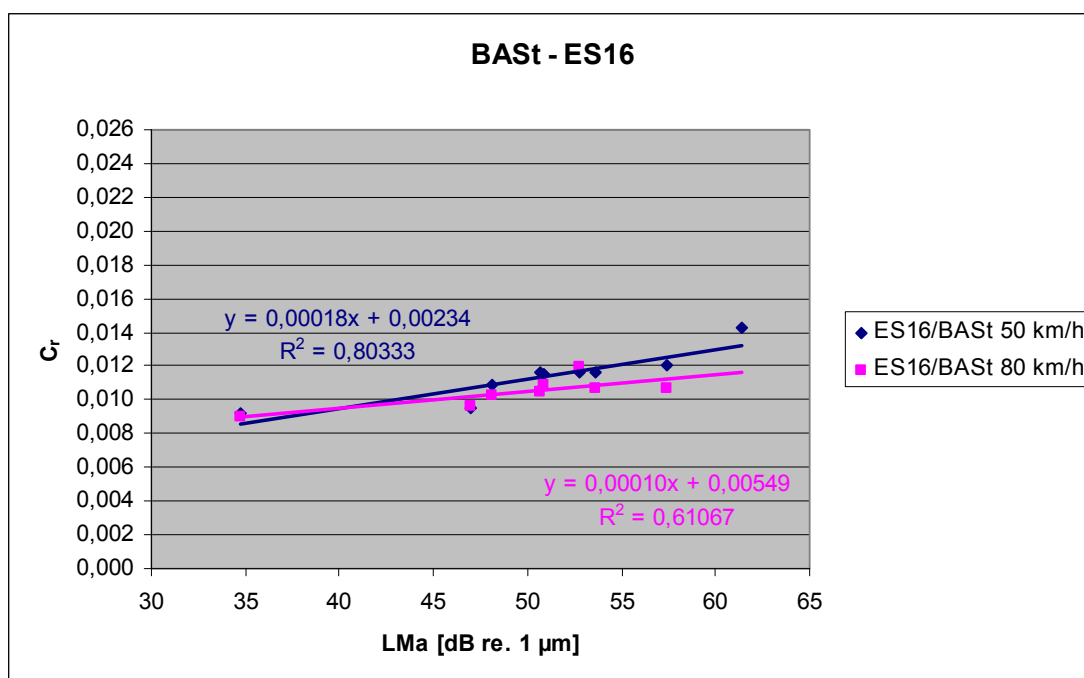


Figure E.2: Correlation between macrotexture and  $C_r$  for ES14/BRRRC tyre (based on measurements performed by BRRRC) – with enveloping





**Figure E.3: Correlation between macrotexture and  $C_r$  for ES14/TUG tyre (based on measurements performed by TUG) – with enveloping**



**Figure E.4: Correlation between macrotexture and  $C_r$  for ES16/BASt tyre (based on measurements performed by BASt) – with enveloping**

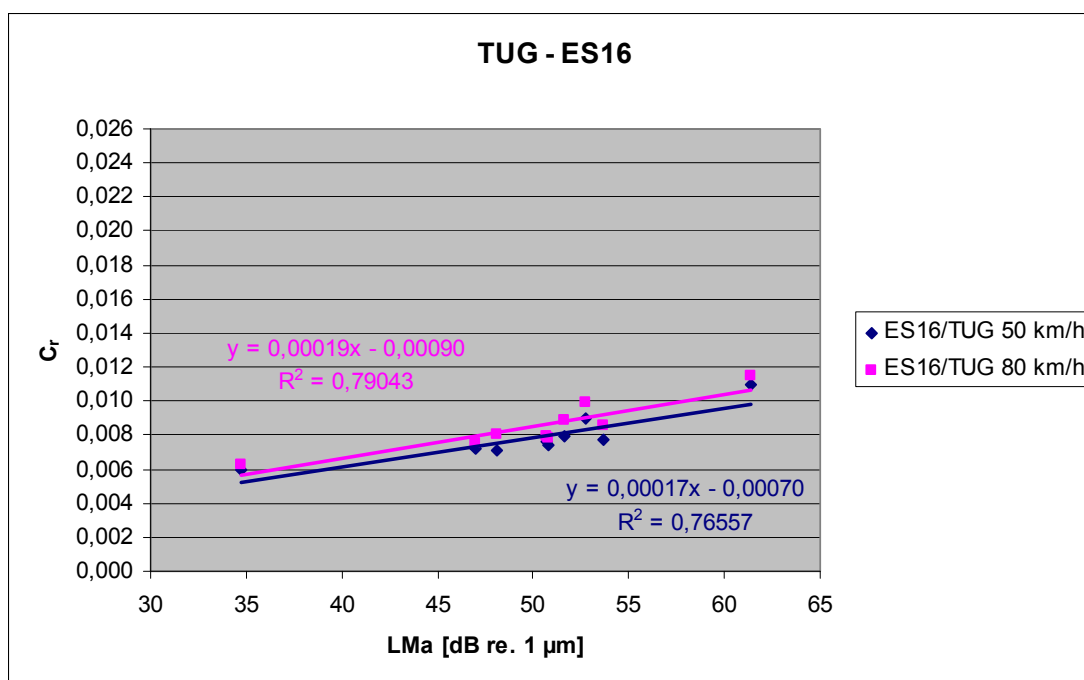


**Figure E.5: Correlation between macrotexture and  $C_r$  for ES16/TUG tyre (based on measurements performed by TUG) – with enveloping**

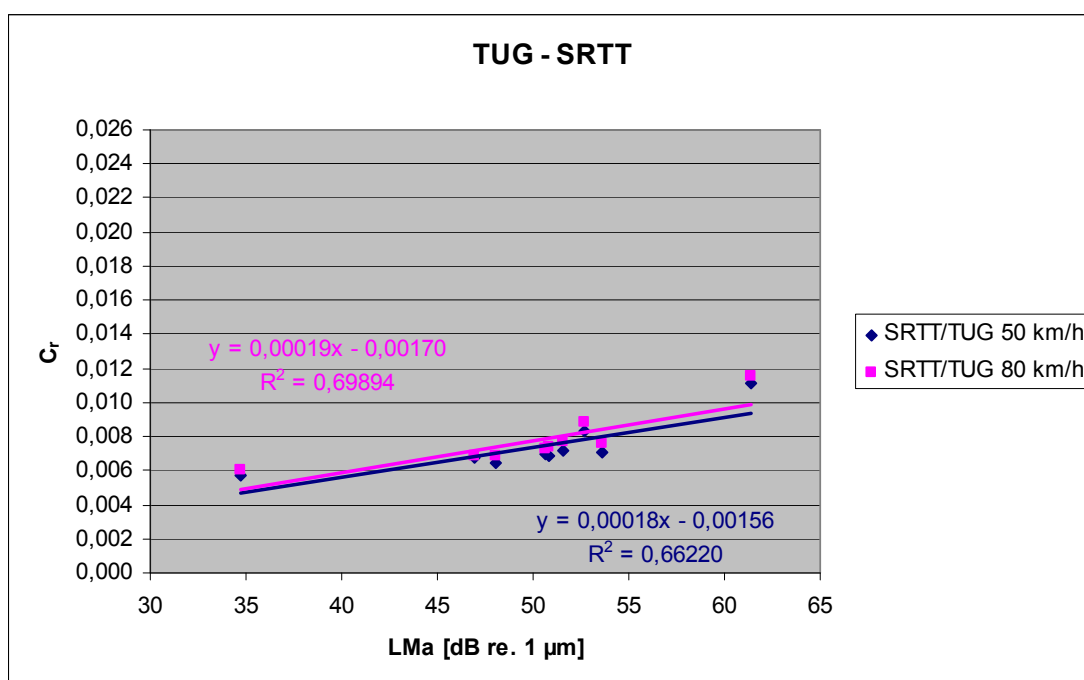


**Figure E.6: Correlation between macrotexture and  $C_r$  for SRTT/TUG tyre (based on measurements performed by TUG) – with enveloping**

## F. Correlation between megatexture and $C_r$ for various tyres measured by different participants – without enveloping

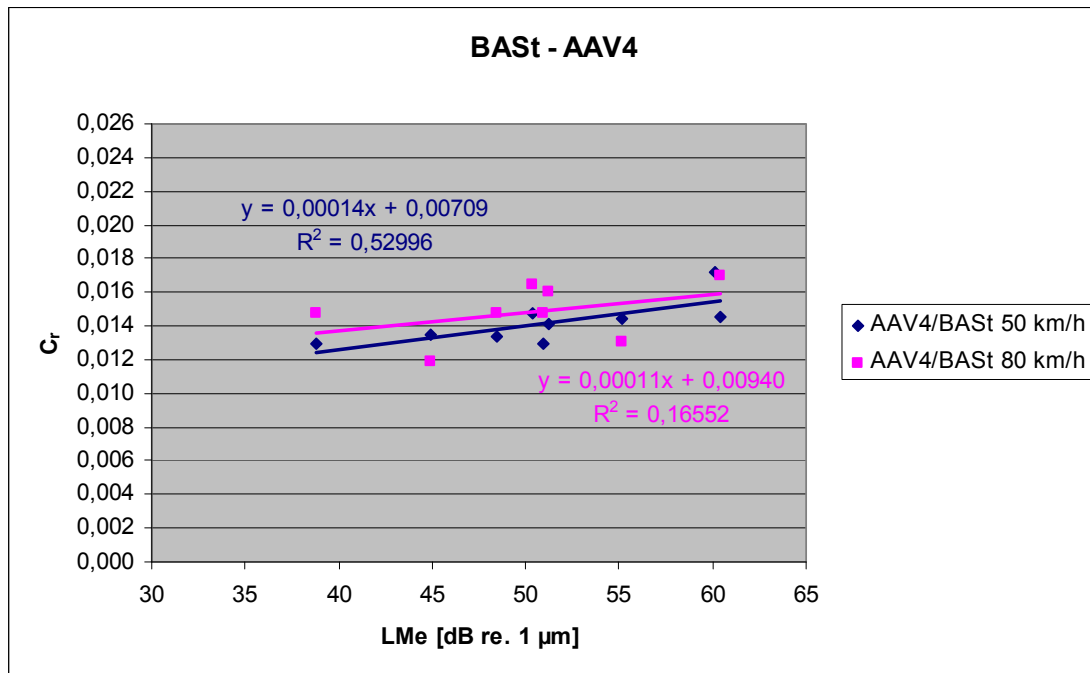


Figure F.1: Correlation between megatexture and  $C_r$  for AAV4/BASSt tyre (based on measurements performed by BASSt)

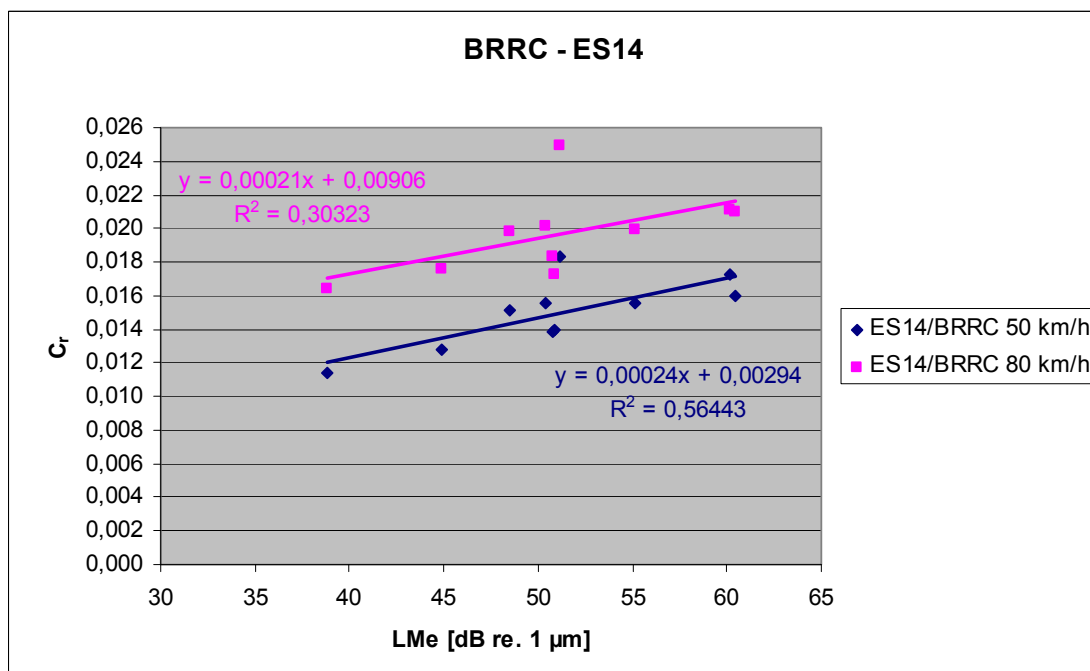
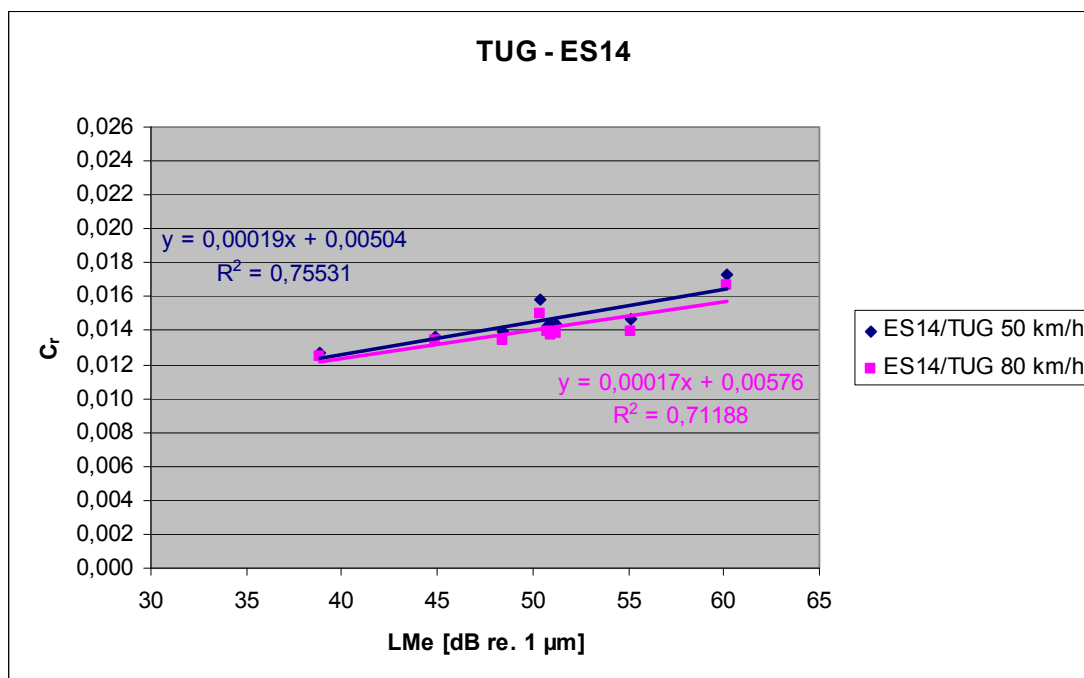
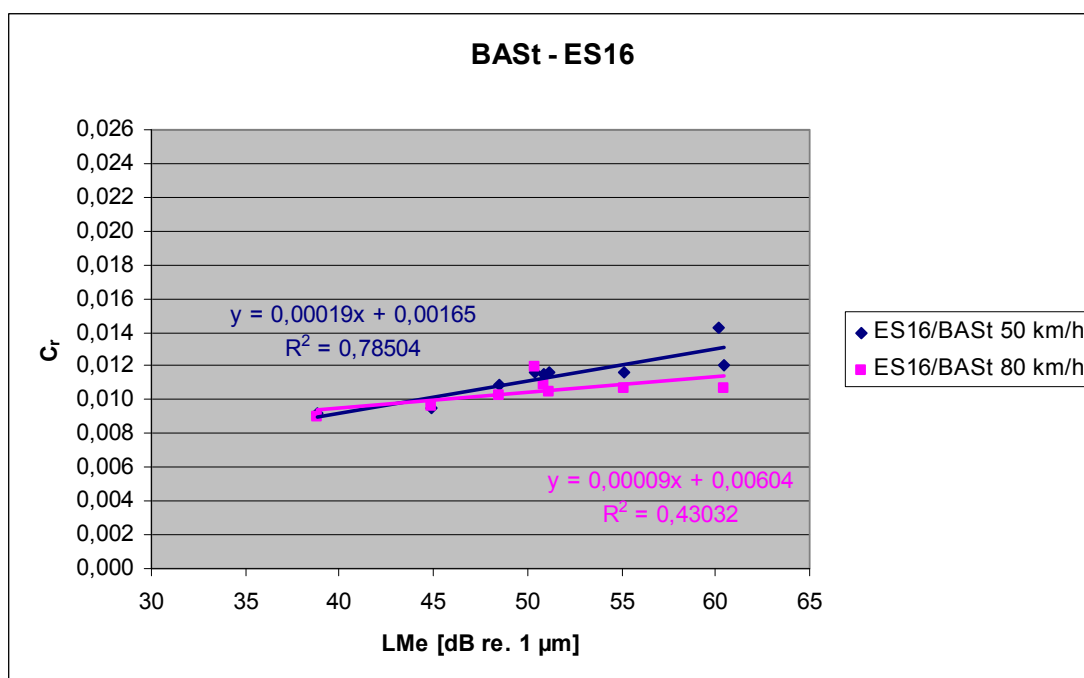


Figure F.2: Correlation between megatexture and  $C_r$  for ES14/BRRRC tyre (based on measurements performed by BRRRC)



**Figure F.3: Correlation between megatexture and  $C_r$  for ES14/TUG tyre (based on measurements performed by TUG)**



**Figure F.4: Correlation between megatexture and  $C_r$  for ES16/BASt tyre (based on measurements performed by BASt)**

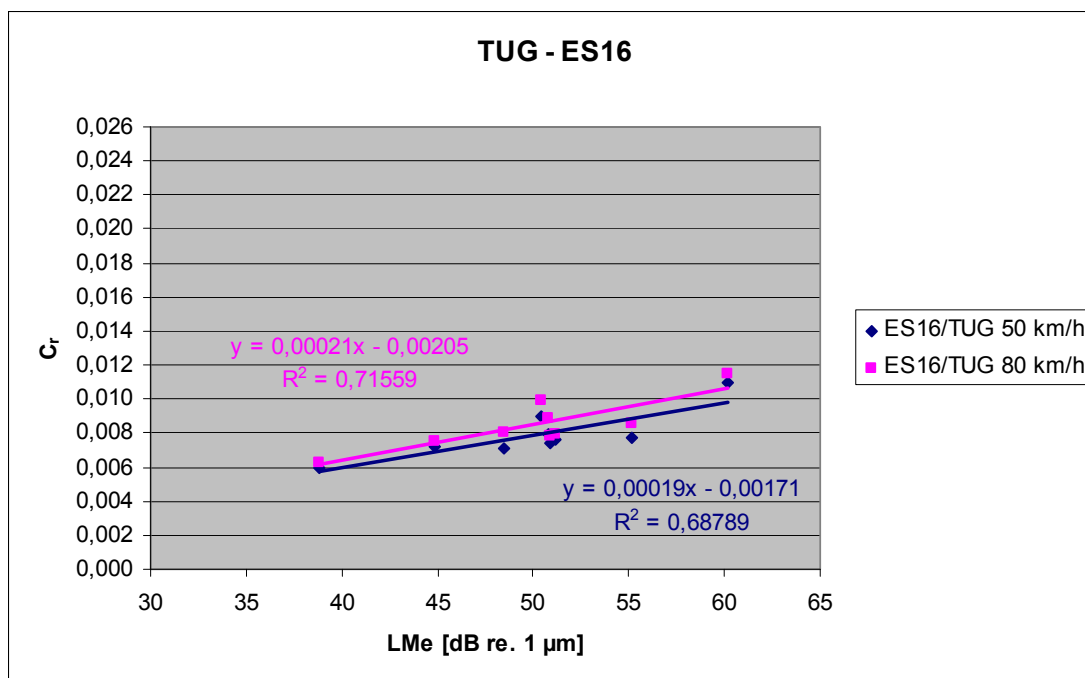


**Figure F.5: Correlation between megatexture and  $C_r$  for ES16/TUG tyre (based on measurements performed by TUG)**

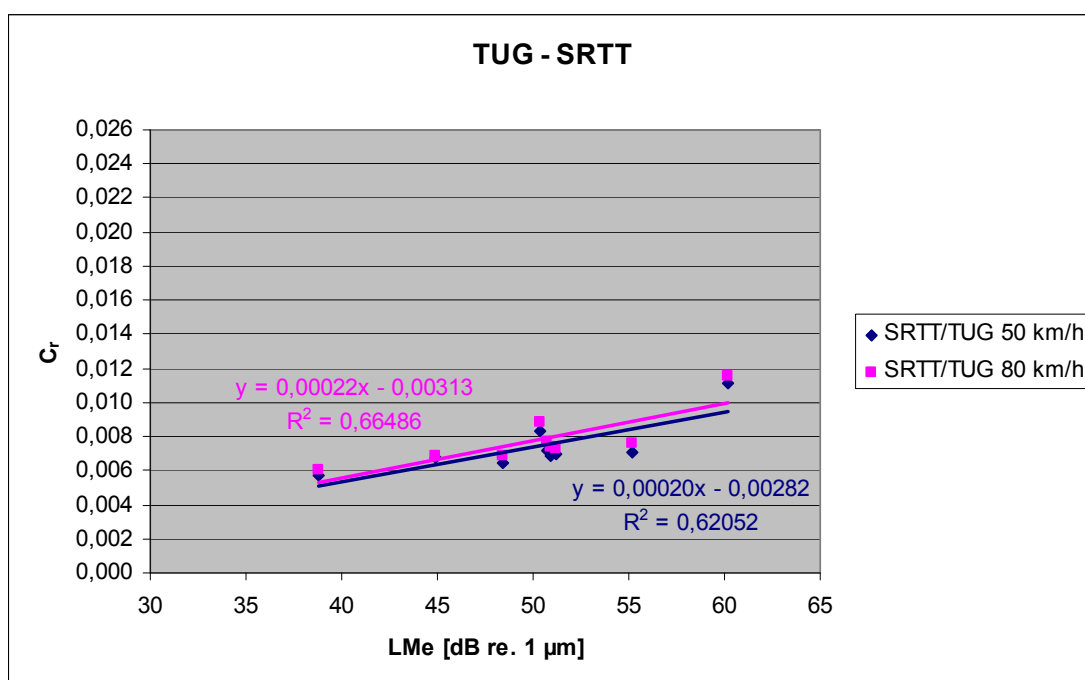


**Figure F.6: Correlation between megatexture and  $C_r$  for SRTT/TUG tyre (based on measurements performed by TUG)**

## G. Correlation between megatexture and $C_r$ for various tyres measured by different participants – with enveloping

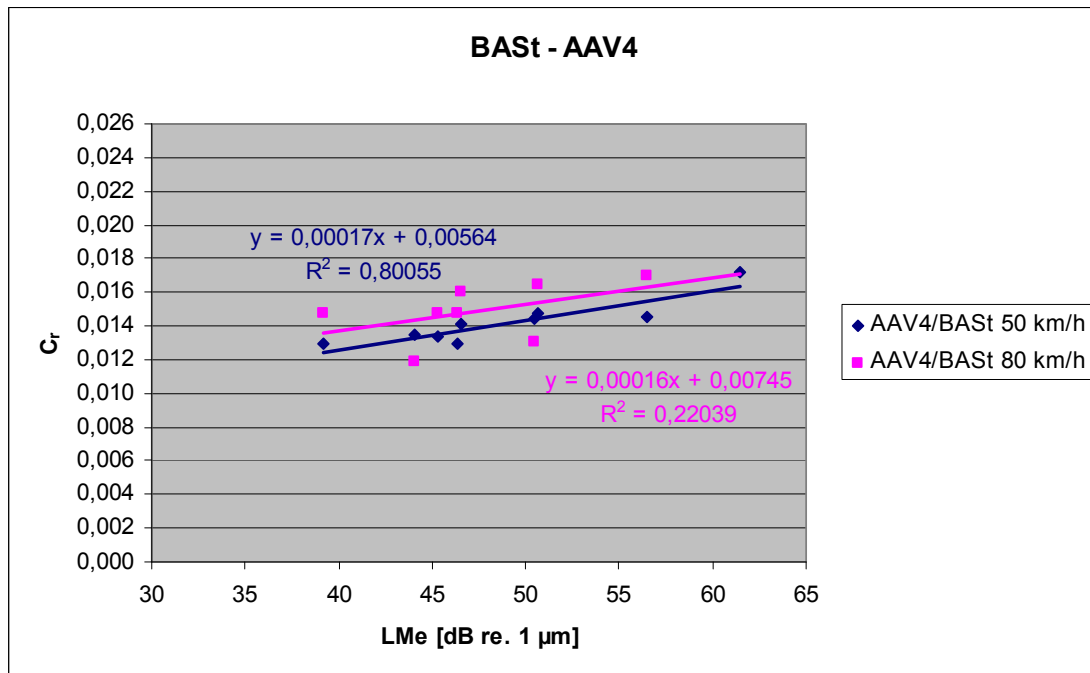


Figure G.1: Correlation between megatexture and  $C_r$  for AAV4/BASSt tyre (based on measurements performed by BASSt) – with enveloping

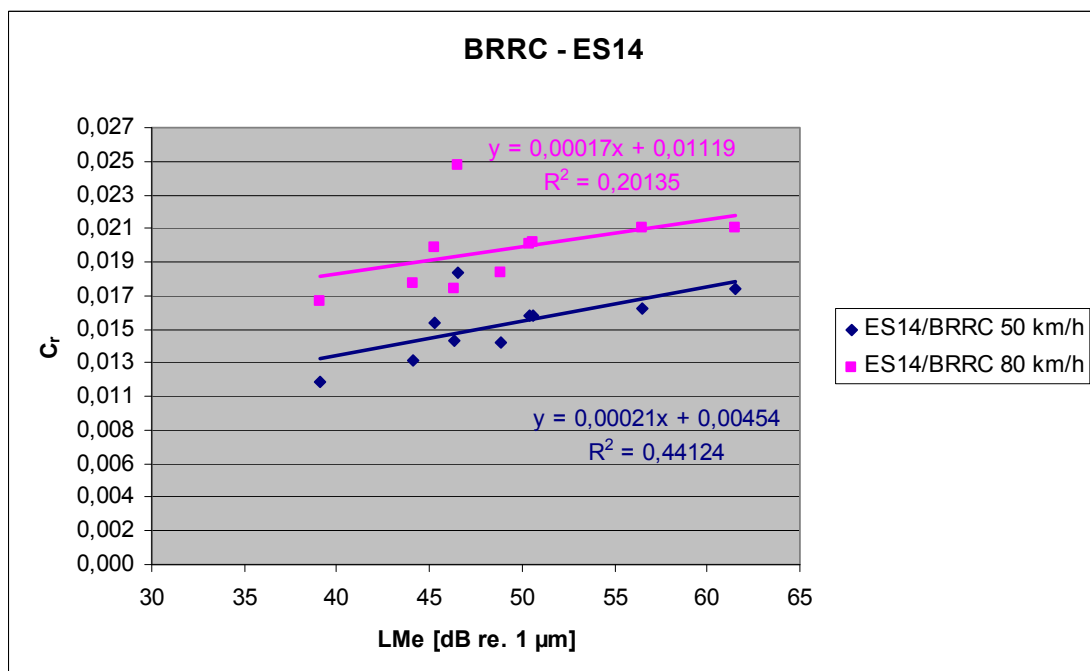
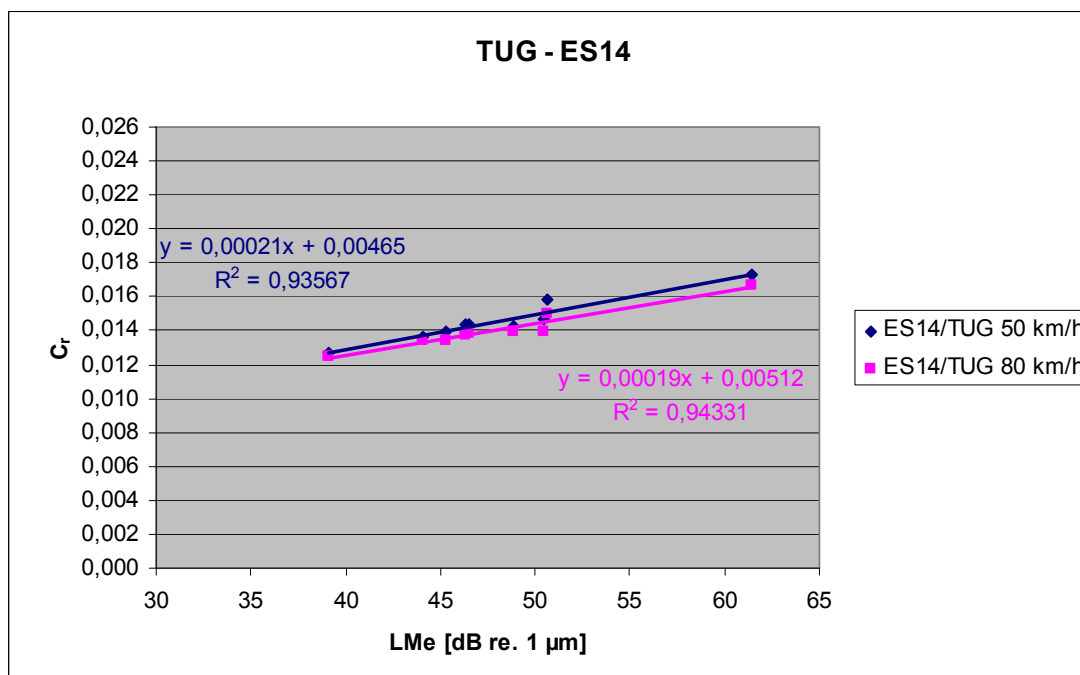
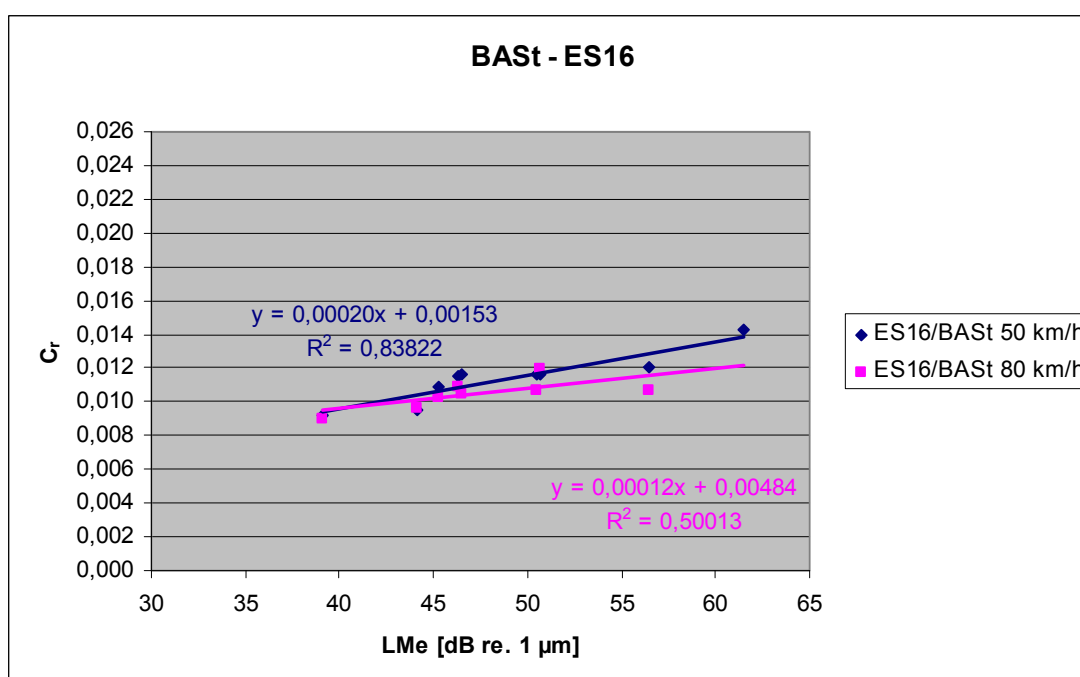


Figure G.2: Correlation between megatexture and  $C_r$  for ES14/BRRRC tyre (based on measurements performed by BRRRC) – with enveloping



**Figure G.3: Correlation between megatexture and  $C_r$  for ES14/TUG tyre (based on measurements performed by TUG) – with enveloping**



**Figure G.4: Correlation between megatexture and  $C_r$  for ES16/BASt tyre (based on measurements performed by BASt) – with enveloping**

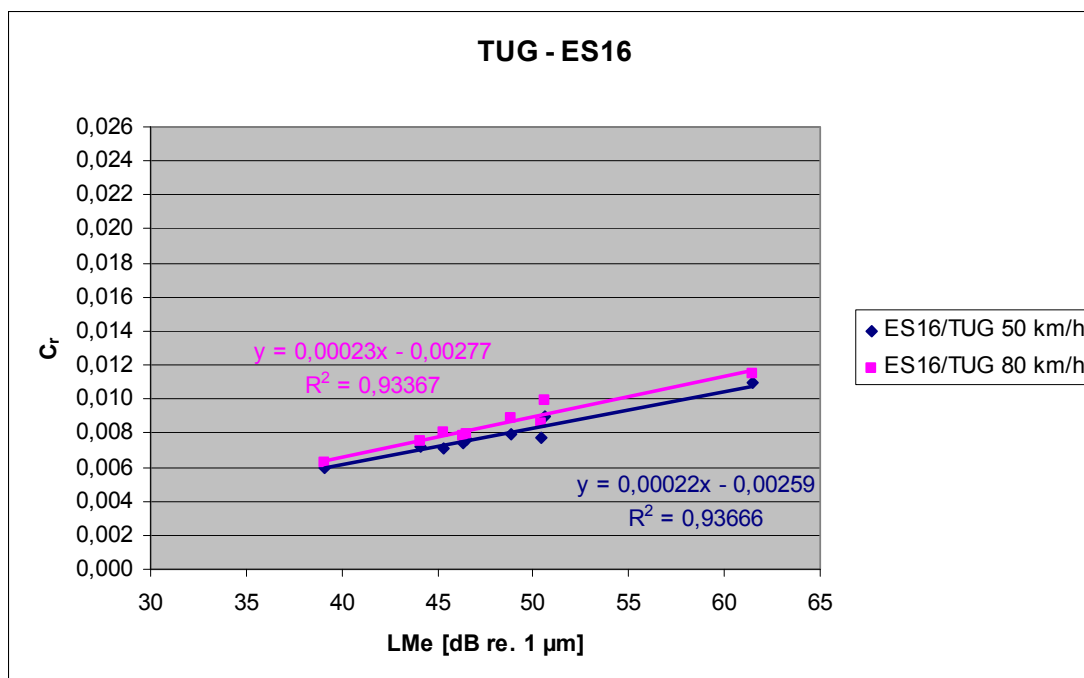


**Figure G.5: Correlation between megatexture and  $C_r$  for ES16/TUG tyre (based on measurements performed by TUG) – with enveloping**

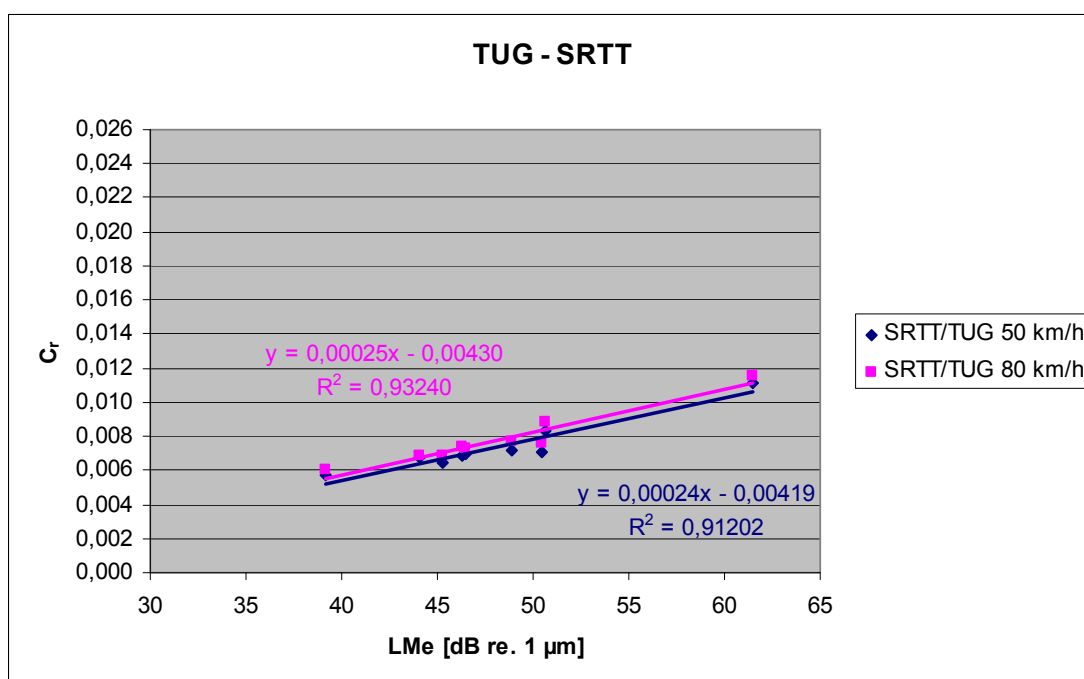


**Figure G.6: Correlation between megatexture and  $C_r$  for SRTT/TUG tyre (based on measurements performed by TUG) – with enveloping**



## H. Correlation between IRI and $C_r$ for various tyres and different participants

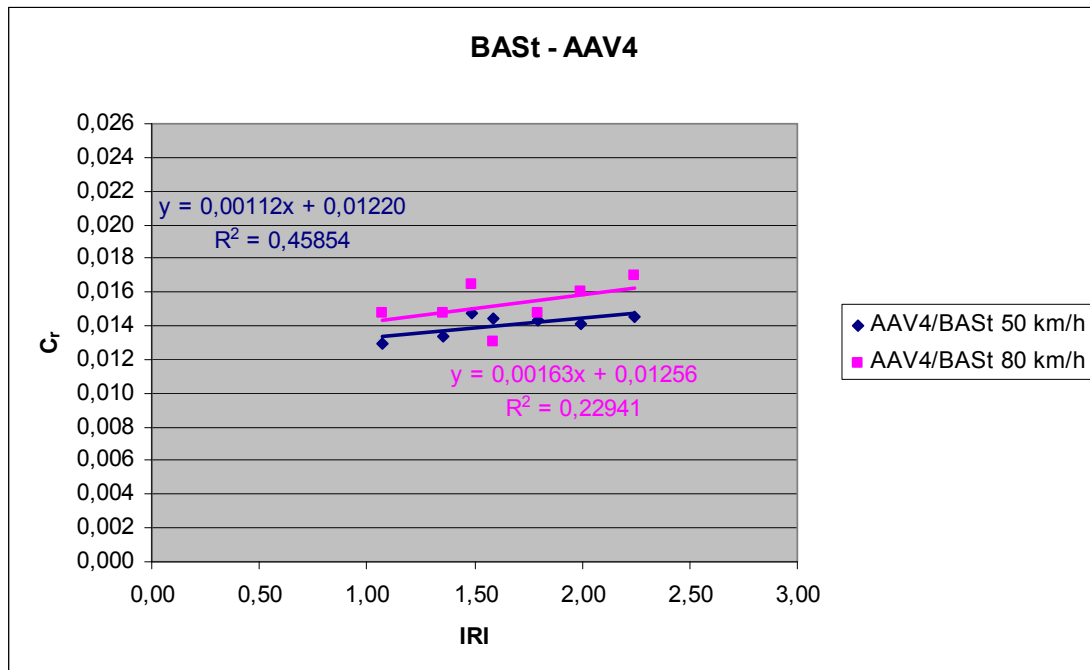


**Figure H.1: Correlation between IRI and  $C_r$  for AAV4/BASSt tyre (based on measurements performed by BASSt)**

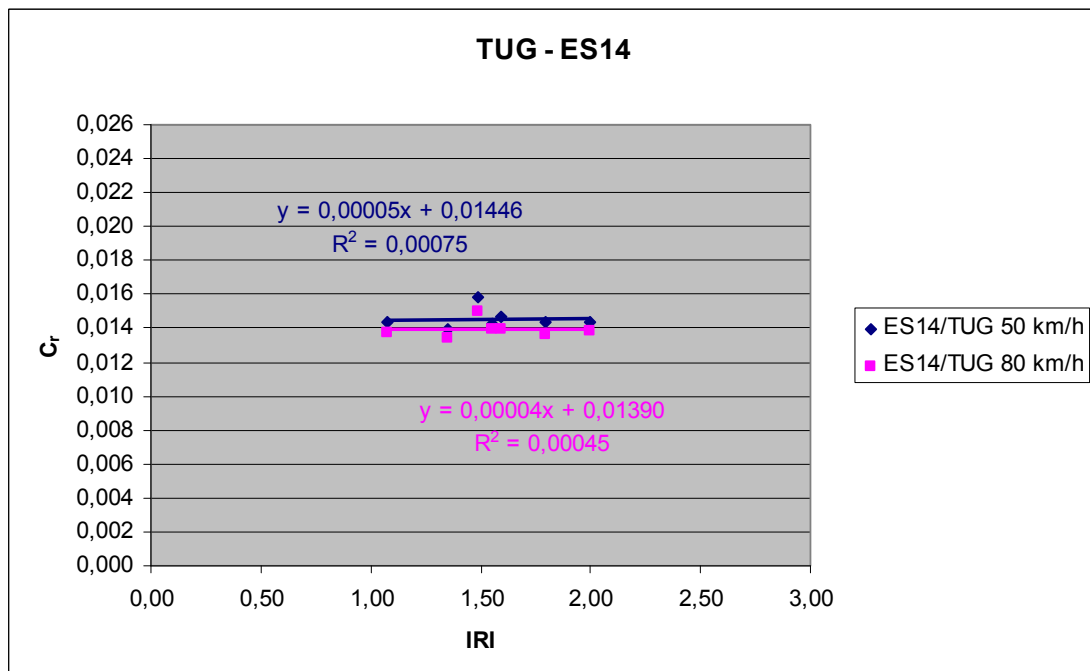


**Figure H.2: Correlation between IRI and  $C_r$  for ES14/TUG tyre (based on measurements performed by TUG)**

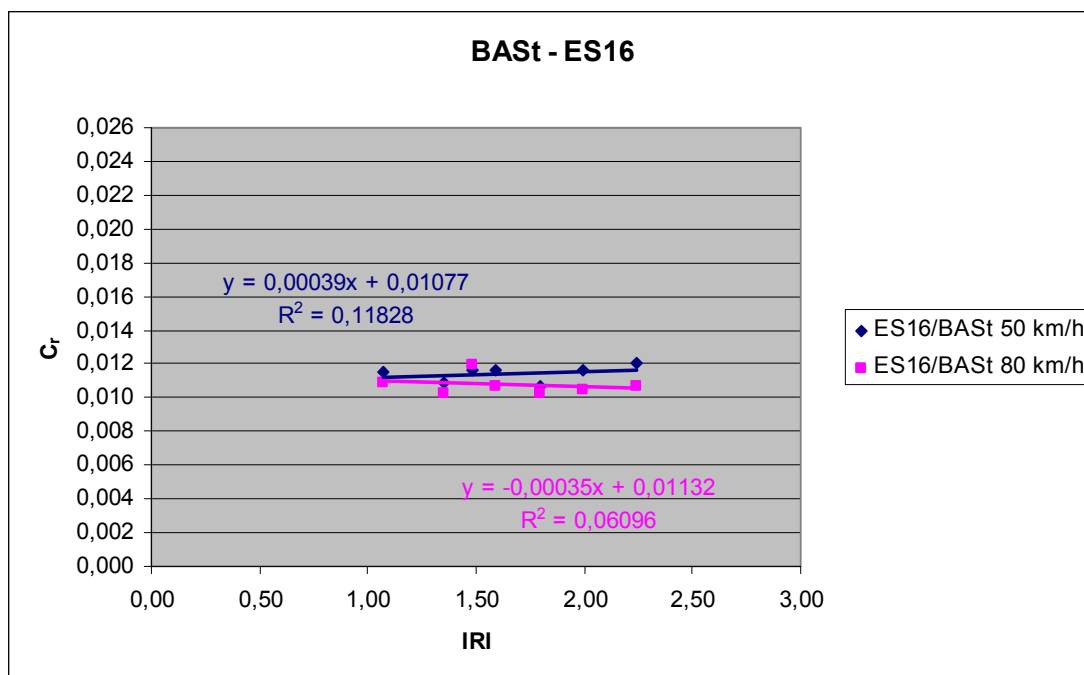


**Figure H.3: Correlation between IRI and  $C_r$  for ES16/BASt tyre (based on measurements performed by BASt)**

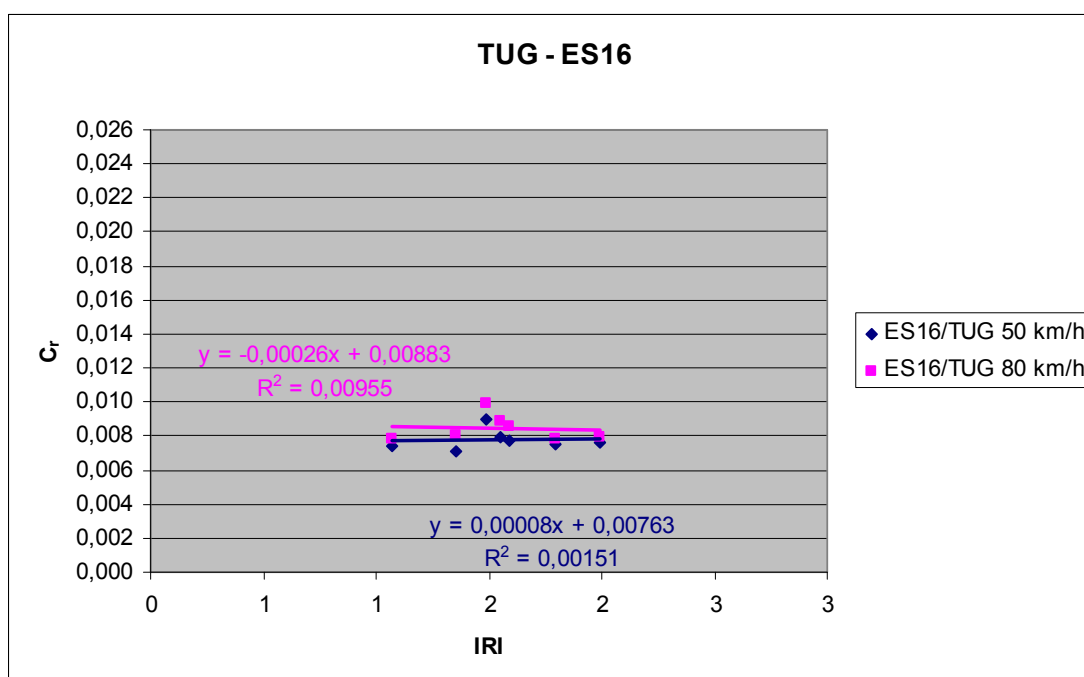


**Figure H.4: Correlation between IRI and  $C_r$  for ES16/TUG tyre (based on measurements performed by TUG)**

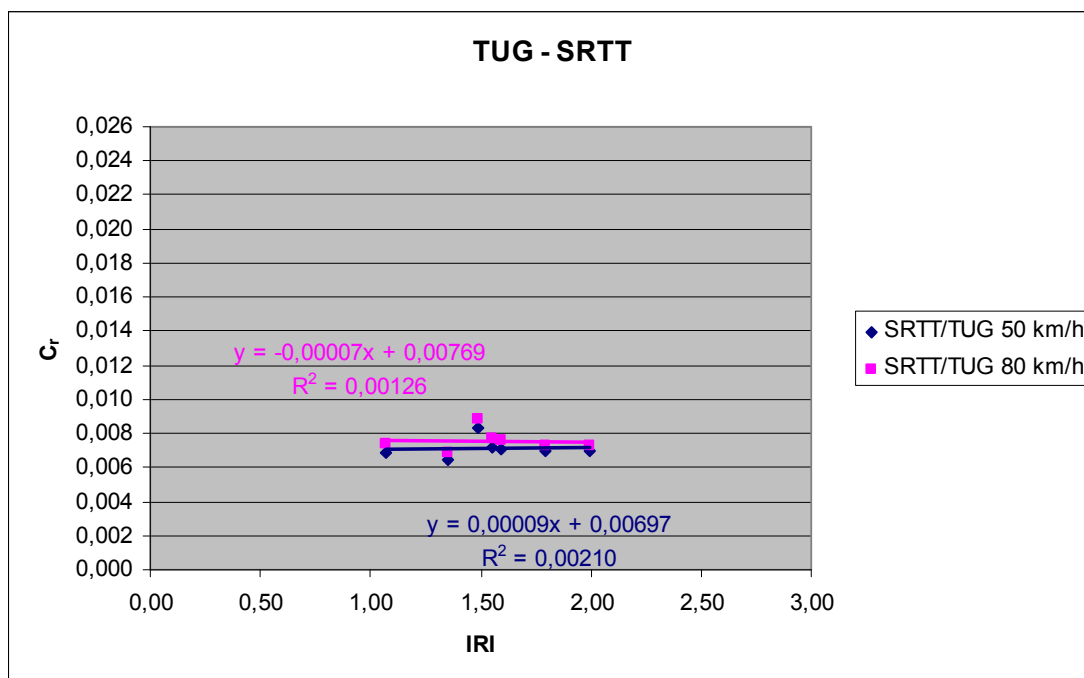


**Figure H.5: Correlation between IRI and C<sub>r</sub> for TUG/SRTT tyre (based on measurements performed by TUG)**